THE UNIVERSITY *of* EDINBURGH

Robust Spectrum Sensing Techniques for Cognitive Radio Networks

Qi Huang

A thesis submitted for the degree of Doctor of Philosophy.
The University of Edinburgh.
October 2015

Abstract

Cognitive radio is a promising technology that improves the spectral utilisation by allowing unlicensed secondary users to access underutilised frequency bands in an opportunistic manner. This task can be carried out through spectrum sensing: the secondary user monitors the presence of primary users over the radio spectrum periodically to avoid harmful interference to the licensed service.

Traditional energy based sensing methods assume the value of noise power as *prior* knowledge. They suffer from the noise uncertainty problem as even a mild noise level mismatch will lead to significant performance loss. Hence, developing an efficient robust detection method is important. In this thesis, a novel sensing technique using the F-test is proposed. By assuming a multiple antenna assisted receiver, this detector uses the F-statistic as the test statistic which offers absolute robustness against the noise variance uncertainty. In addition, since the channel state information (CSI) is required to be known, the impact of CSI uncertainty is also discussed. Results show the F-test based sensing method performs better than the energy detector and has a constant false alarm probability, independent of the accuracy of the CSI estimate.

Another main topic of this thesis is to address the sensing problem for non-Gaussian noise. Most of the current sensing techniques consider Gaussian noise as implied by the central limit theorem (CLT) and it offers mathematical tractability. However, it sometimes fails to model the noise in practical wireless communication systems, which often shows a non-Gaussian heavy-tailed behaviour.

In this thesis, several sensing algorithms are proposed for non-Gaussian noise. Firstly, a non-parametric eigenvalue based detector is developed by exploiting the eigenstructure of the sample covariance matrix. This detector is *blind* as no information about the noise, signal and channel is required. In addition, the conventional energy detector and the aforementioned F-test based detector are generalised to non-Gaussian noise, which require the noise power and CSI to be known, respectively. A major concern of these detection methods is to control the false alarm probability. Although the test statistics are easy to evaluate, the corresponding null distributions are difficult to obtain as they depend on the noise type which may be unknown and non-Gaussian. In this thesis, we apply the powerful bootstrap technique to overcome this difficulty. The key idea is to reuse the data through resampling instead of repeating the experiment a large number of times. By using the nonparametric bootstrap approach to estimate the null distribution of the test statistic, the assumptions on the data model are minimised and no large sample assumption is invoked. In addition, for the F-statistic based method, we also propose a degrees-of-freedom modification approach for null distribution approximation. This method assumes a known noise kurtosis and yields closed form solutions. Simulation results show that in non-Gaussian noise, all the three detectors maintain the desired false alarm probability by using the proposed algorithms. The F-statistic based detector performs the best, e.g., to obtain a 90% detection probability in Laplacian noise, it provides a 2.5 dB and 4 dB signal-to-noise ratio (SNR) gain compared with the eigenvalue based detector and the energy based detector, respectively.

Declaration of originality

I hereby declare that the research recorded in this thesis and the thesis itself was composed and originated entirely by myself in the School of Engineering at The University of Edinburgh.

Qi Huang

Acknowledgements

Foremost, I would like to express my sincere thank to my supervisors Dr. Peijung. Chung and Prof. John.Thompson for their valuable guidance, warm encouragement and patient during my PhD. The PhD would not have been possible without their knowledge and support. Thanks also go to Prof. Peter M. Grant for his constructive advice throughout my research work and thesis writing. I also wish to thank my examiners, Prof. Arumugam Nallanathan and Dr. Nick Polydorides, for their efforts in reviewing this thesis and valuable comments.

Further thanks go to the Institute for Digital Communications (IDCOM) for the funding support and providing a friendly and enthusiastic research environment. Thanks to all my friends and collogues I've met in IDCOM for helping and supporting me to complete my research work. They have given me wonderful memories of my school days in the University of Edinburgh.

Last but not least, I would like to thank my parents for their unconditional love and support over the past 26 years. Special thanks to my husband, Xiang Wang, for always being there for me during the good time and the bad. Their continuously support and encouragement help me become the person I am today.

Contents

Declaration of originality . . . iii
Acknowledgements . . . iv
Contents . . . v
List of figures . . . vii
List of tables . . . ix
Acronyms and abbreviations . . . x
Nomenclature . . . xii

1 Introduction **1**
1.1 Motivation . . . 1
1.1.1 Motivation for Cognitive Radio: Spectrum is Underutilised . . . 1
1.1.2 Motivation for Noise Robust Spectrum Sensing Techniques . . . 3
1.2 Thesis Objectives and Contributions . . . 5
1.2.1 Thesis Objectives . . . 5
1.2.2 Main Contributions . . . 5
1.3 Thesis Structure . . . 6

2 Background **9**
2.1 Cognitive Radio . . . 9
2.1.1 Cognitive Radio Technology . . . 10
2.1.2 Cognitive Radio Applications . . . 13
2.2 Spectrum Sensing Techniques . . . 15
2.2.1 Conventional Spectrum Sensing Techniques . . . 17
2.2.2 Spectrum Sensing for Non-Gaussian noise . . . 26
2.3 Conclusion . . . 30

3 F-test Based Spectrum Sensing **32**
3.1 Introduction . . . 32
3.2 System Model . . . 34
3.3 Preliminaries of F-test . . . 35
3.4 F-test Based Detector . . . 38
3.5 Impact of Imperfect CSI . . . 40
3.6 Simulation Results . . . 44
3.7 Conclusion . . . 53

4 Spectrum Sensing for Non-Gaussian Noise Using Bootstrap Techniques **54**
4.1 Introduction . . . 54
4.2 System Model . . . 56
4.3 Preliminaries of Bootstrap Techniques . . . 56
4.4 Nonparametric Eigenvalue Based Detector . . . 59
4.5 Energy Based Detector . . . 65
4.6 The Accuracy of Bootstrap . . . 66
4.7 Simulation Results . . . 69

4.8 Conclusion 76

5 F-statistic Based Spectrum Sensing for Non-Gaussian Noise 78
5.1 Introduction 78
5.2 System Model and Problem Statement 79
5.3 Degrees-of-Freedom Modification 81
5.4 The Bootstrap Approximation 84
5.5 Extensions 87
5.6 Simulation Results 89
5.7 Conclusion 95

6 Conclusions and Future Work 96
6.1 Conclusions 96
6.2 Limitations and Future Work 98
6.2.1 Limitations 98
6.2.2 Future Work 99

A Proof of Property 5.1 100

B Proof of Property 5.2 103

C Publications 105

References 124

List of figures

1.1 Measured spectrum occupancy by band over a 3-day period , in: (a) New York City, with an average spectrum utilisation 13.1%; and (b) Chicago, with an average spectrum utilisation 17.1%. 2

2.1 Functional cycle of cognitive radio 11
2.2 Illustration of coverage and protection area of primary transmission 12
2.3 The application of cognitive radio. 14
2.4 A schematic diagram of the hypothesis testing problem in (2.2). 16
2.5 Block diagram for the energy detector. 19
2.6 Comparison of detection algorithms using likelihood ratio principle. 20
2.7 OFDM signal structure. 23

3.1 SIMO network used for spectrum sensing. 34
3.2 Block diagram of the F-test with degrees of freedom n_1 and n_2 37
3.3 Probability of detection versus SNR. Target false alarm probability $P_f = 0.1$, $M = 4$ receiving antennas and $L = 100$ samples. 45
3.4 Probability of detection versus number of receiving antennas M. Target false alarm probability $P_f = 0.1$, $L = 100$ samples and SNR $= -10$ dB. 46
3.5 ROC curve, for $M = 4$ receiving antennas, $L = 100$ samples and SNR $= -10$ dB. 47
3.6 Performance v.s. noise uncertainty E. The performance for: (a) False Alarm Probability; and (b) Detection probability is plotted. Target false alarm probability $P_f = 0.1$, $M = 4$ receiving antennas, $L = 100$ samples and SNR $= -10$ dB. 48
3.7 Normalised histogram of the test statistic for F-test based method under channel uncertainty: (a) $T_F\left(\hat{\mathbf{h}}|\mathcal{H}_0\right)$; and (b) $T_F\left(\hat{\mathbf{h}}|\mathcal{H}_1\right)$. The uncertainty level is selected as σ_e^2 =0, 0.3, 0.6 and 0.9, respectively, for $M = 4$ receiving antennas, SNR $= 0$ dB and $L = 100$ samples. 49
3.8 False alarm probability v.s. channel uncertainty σ_e^2. Target false alarm probability $P_f = 0.1$, $M = 4$ receiving antennas, $L = 100$ samples and SNR $= -10$ dB. 50
3.9 Detection probability v.s. channel uncertainty σ_e^2. Target false alarm probability $P_f = 0.1$, $M = 4$ receiving antennas, $L = 100$ samples and SNR $= -10$ dB. 51
3.10 Detection probability v.s. channel uncertainty σ_e^2. Target false alarm probability $P_f = 0.1$, $M = 8$ receiving antennas, $L = 100$ samples and SNR $= -10$ dB. 52

4.1 A schematic diagram of the bootstrap principle 57
4.2 The: (a) mean; and (b) standard deviation of the test statistic $\hat{T}_{EV}$ versus the sample size L, for Laplacian distributed data with Identity covariance matrix and corresponding eigenvalues $[1,\ 1,\ 1,\ 1]^T$. Number of bootstrap replications $B_1 = 30$, $M = 4$ receiving antennas and $L = 100$ samples. 63

4.3 The: (a) mean; and (b) standard deviation of the test statistic $\hat{T}_{EV}$ versus the sample size L, for Gaussian Mixture distributed data with Identity covariance matrix and corresponding eigenvalues $[1,\ 1,\ 1,\ 1]^T$. Number of bootstrap replications $B_1 = 30$, $M = 4$ receiving antennas and $L = 100$ samples. 64
4.4 Normalised histogram of 500 bootstrap statistic for: (a) eigenvalue based approach; and (b) energy based approach. Laplacian data is applied. The solid line is the probability density function of their test statistic under null hypothesis, obtained from 1000 Monte Carlo simulations. $M = 4$ receiving antennas and $L = 100$ samples. 68
4.5 Normalised histogram of 500 bootstrap statistic for: (a) eigenvalue based approach; and (b) energy based approach. Gaussian Mixture data is applied. $M = 4$ receiving antennas and $L = 100$ samples. 69
4.6 Probability of false alarm versus sample size L, for: (a) Laplacian noise; (b) Gaussian Mixture noise. Target false alarm probability $P_f = 0.1$ and $M = 4$ receiving antennas are applied. 72
4.7 Probability of detection versus SNR under Gaussian noise. Target false alarm probability $P_f = 0.1$, $M = 4$ receiving antennas and $L = 100$ samples. 73
4.8 Probability of detection versus SNR under: (a) Laplacian noise; and (b) Gaussian Mixture noise. Target false alarm probability $P_f = 0.1$, $M = 4$ receiving antennas and $L = 100$ samples. 74
4.9 Probability of detection versus number of receiving antennas, M, under: (a) Laplacian noise; and (b) Gaussian Mixture noise. Target false alarm probability $P_f = 0.1$, SNR $= -8$ dB and $L = 100$ samples. 75

5.1 Normalised histogram of 500 bootstrap statistics, $\hat{Z}^*$, under: (a) Laplacian noise; and (b) Gaussian Mixture noise. The solid line is the empirical probability density function of $Z(\mathcal{H}_0)$, obtained from 1000 Monte Carlo simulations. $L = 500$ samples and $M = 4$ receiving antennas. 86
5.2 Probability of false alarm versus sample size, L, for three methods calculating the test threshold, under: (a) Laplacian noise; and (b) Gaussian Mixture noise. Target false alarm probability $P_f = 0.1$ and $M = 4$ receiving antennas. 90
5.3 Probability of detection versus sample size, L, for three methods calculating the test threshold,under: (a) Laplacian noise; and (b) Gaussian Mixture noise. Target false alarm probability $P_f = 0.1$, SNR $= -14$ dB and $M = 4$ receiving antennas. 91
5.4 Probability of detection versus SNR(dB) under: (a) Laplacian noise; and (b) Gaussian Mixture noise. Target false alarm probability $P_f = 0.1$, $M = 4$ receiving antennas and $L = 500$ samples. 93
5.5 Probability of detection versus number of receiving antennas, M, under: (a) Laplacian noise; and (b) Gaussian Mixture noise. Target false alarm probability $P_f = 0.1$, SNR $= -14$ dB and $L = 500$ samples. 94

List of tables

2.1 Summary of sensing algorithms that are robust against uncertain noise power . 25
2.2 Summary of sensing algorithms for Non-Gaussian noise 28

3.1 Summary of the simulated detection algorithms. M: number of receiving antennas. L: sample size. N: Number of Monte carol trails. 44

4.1 The bootstrap procedure for the eigenvalue based detection problem 62
4.2 The bootstrap procedure for the energy based detection problem 67
4.3 Summary of the simulated detection algorithms. M: number of receiving antennas. L: sample size. B and B_1 denote the number of bootstrap replications for distribution approximation and sample eigenvalue bias correction, respectively. 70

5.1 The bootstrap procedure for approximating the null distribution of Z 85
5.2 Summary of the simulated detection algorithms. M: number of receiving antennas. L: sample size. N: Number of Monte carol trails. B and B_1 denote the number of bootstrap replications for distribution approximation and sample eigenvalue bias correction, respectively. 92

Acronyms and abbreviations

ACF	Autocorrelation function
ADC	Analogue-to-digital converter
AGM	Arithmetic-to-geometric mean
BPF	Band pass fliter
CAC	Cyclic autocorrelation
CCAV	Covariation coefficient absolute value
CDF	Cumulative distribution function
CLT	Central Limit Theorem
CP	Cyclic Prefix
CRN	Cognitive radio network
CSD	Cyclic spectral density
CSI	Channel state information
DNF	Doubly noncentral F-distribution
ECC	Electronic Communications Committee
FCC	Federal Communications Commission
GGM	Generalized Gaussian model
GMM	Gaussian mixture model
GLRT	Generalised likelihood ratio test
i.i.d	Independent and identically distributed
ISM	Industrial, scientific and medical
KS	Kolmogorov-Smirnov
LO	Locally optimal
M2M	Machine-to-machine
MDOF	Modified degrees of freedom
MIMO	Multiple-input and Multiple-output
ML	Maximal likelihood
MLE	Maximal likelihood estimate
MME	Maximum-minimum eigenvalue
NP	Neyman-Pearson

Ofcom	Office of Communications
OFDM	Orthogonal frequency division multiplexing
RF	Radio frequency
RMT	Random Matrix Theory
ROC	Receiver operating characteristics
US	United States
UK	United Kingdom
UMP	Uniformly most powerful
SNR	Signal to noise ratio
SIMO	Single-input and multiple-output
PCA	Polarity-coincidence-array
PDF	Probability density function
RF	Ratio frequency
TV	Television
TVWS	TV white space

Nomenclature

B	The number of bootstrap replications
E	The bound of noise variance uncertainty
F	F-statistic
F_{n_1,n_2}	F-distribution with degrees of freedom n_1 and n_2
$F'_{n_1,n_2}(\delta^2)$	Noncentral F-distribution with noncentral parameter δ^2
$F''_{n_1,n_2}\left(\delta_1^2,\delta_2^2\right)$	Doubly noncentral F-distribution with noncentral parameters δ_1^2 and δ_2^2
$\mathbf{I}$	Identity matrix
$\mathbf{w}(l)$	Additive white noise vector at the receiver antenna array
$w_i(l)$	Additive white noise at i-th antenna
$\mathbf{h}$	CSI vector
$\triangle\mathbf{h}$	The difference between the true value of CSI and its estimate
h_i	CSI between the primary transmitter and i-th receiving antenna
$\mathcal{H}_0$	Null hypothesis
$\mathcal{H}_1$	Alternative hypothesis
j	Imaginary unit that $j^2=-1$
L	Sample size
l	lth sampling instant
L_c	Length of CP symbols
L_s	Length of OFDM symbols
M	Number of receiving antennas
n_1, n_2	Degrees of freedom
m_1, m_2	Modified degrees of freedom
$\mathbf{P}$	Projection matrix
$\mathbf{p}$	A column vector consisting of diagonal elements of $\mathbf{P}$
P_f	False alarm probability
P_d	Detection probability
p	Tunable parameter of the L_p-norm detector
$\mathbf{R}_x$	Covariance matrix of $\mathbf{x}(l)$
$\mathbf{R}_y$	Covariance matrix of $\mathbf{y}(l)$

$\hat{\mathbf{R}}_y$	Sample covariance matrix of $\mathbf{y}(l)$
$R(\xi, \tau)$	Cyclic autocorrelation function defined in eq. (2.20)
$r_y(l, \tau)$	Autocorrelation function defined in eq. (2.18)
r_k	Rank of a projection matrix $\mathbf{p}_k$
$S(\xi, \omega)$	Cyclic spectral density function defined in eq. (2.19)
$s(l)$	Transmitted primary signal
T	Test statistic
T_F	Test statistic of the F-statistic based detector
T_{EV}	Test statistic of the eigenvalue based detector
T_{EG}	Test statistic of the energy based detector
$\mathbf{x}(l)$	Faded primary signal
$x_i(l)$	Faded primary signal at i-th antenna
$\mathbf{Y}$	Collected sample set that contains all the vectorial observations
$\mathbf{y}$	Collected sample set that contains all the scalar observations
$\mathbf{y}(l)$	Observed baseband signal vector
$y_i(l)$	Observed baseband signal at i-th antenna
Z	Logarithm of F-statistic defined in eq. (5.11)
$\mathcal{Z}$	Complex random variable
α	Target false alarm probability
λ_i	i-th eigenvalue of a covariance matrix
β_i	i-th sample eigenvalue of a sample covariance matrix
γ	Test threshold
ξ	Cyclic frequency
τ	Time delay
$\mathcal{F}$	Distribution function
$\hat{\mathcal{F}}$	Empirical distribution function
χ	The observations generated by distribution $\mathcal{F}$
ρ	Shape parameter of GGM defined in eq. (4.24)
Θ_0	The set of unknown parameters under null hypothesis
Θ_1	The set of unknown parameters under alternative hypothesis
ϑ	The parameter of a data model in Chapter 4
$\mathcal{T}_p$	Pivotal bootstrap statistic
$\mathcal{T}_{np}$	Non-pivotal bootstrap statistic

$\hat{\mathcal{T}}$	Bootstrap statistic defined in eq. (4.2)
$\delta^2, \delta_1^2, \delta_2^2$	Noncentrality parameter of F-distribution
σ_w^2	Noise variance
σ_e^2	The variance of channel uncertainty used in Chapter 3
σ_s^2	The variance of transmitted primary signal
σ_x^2	The variance of faded primary signal
σ	Standard deviation
$\mathcal{CN}$	Complex Gaussian distribution
$\emptyset$	Empty set
$\exp(\cdot)$	Exponential function
$I[\cdot]$	Indicator function
$\ln(\cdot)$	Logarithmic function
$\mathscr{L}(\cdot)$	Log-likelihood function
$I_k(\frac{1}{2}n_1, \frac{1}{2}n_2)$	Regularized beta function defined in eq. (3.17)
κ	Normalised kurtosis of a complex random variable
$O(\cdot)$	Order notation: of the same order as
$\Pr(\cdot)$	The probability of event
$\mathrm{tr}[\cdot]$	Trace operator
$S(\cdot)$	Spatial sign function defined in eq. (2.23)
$\mathrm{E}[\cdot]$	Statistical expectation
$\mathrm{Var}[\cdot]$	Statistical variance
$W(\cdot)$	CDF
$\hat{W}(\cdot)$	Empirical CDF
$W_{c,n1,n2}(\cdot)$	CDF of F-distribution
$W_{nc,n1,n2}(\cdot \mid \delta^2)$	CDF of noncentral F-distribution
$W_{dnc,n_1,n_2}(\cdot \mid \delta_1^2, \delta_2^2)$	CDF of doubly noncentral F-distribution
$\Phi(\cdot)$	CDF of Gaussian distribution
$f(\cdot)$	PDF function
$\Re(\cdot)$	The real parts of a complex-valued number
$\Im(\cdot)$	The imaginary parts of a complex-valued number
$\lvert\cdot\rvert$	Euclidean norm of a scalar
$\lVert\cdot\rVert$	Euclidean norm of a vector
$(\cdot)^*$	The bootstrap version of a statistic or parameter

$\hat{[\cdot]}$	The estimate of a statistic or parameter
$(\cdot)^{-1}$	Inverse operation
$[\cdot]^{T}$	Transpose operation
$[\cdot]^{H}$	Conjugate transpose operation
$[\cdot]^{-1}$	Inverse operation
$[\cdot]^{\dagger}$	Pseudo-inverse of a vector

Chapter 1
Introduction

Cognitive radio is a promising technology that improves the spectrum efficiency by allowing the unlicensed secondary user to dynamically utilise the licensed radio bands. The ability to detect the presence of licensed user is called spectrum sensing, which is an essential function of cognitive radio as it gives an awareness of the surrounding radio environment that prevents harmful interference to the licensed primary service. Traditional sensing techniques generally consider the detection of primary signals in additive Gaussian noise with a known power. However, their test performance might be limited to the sensitivity to the uncertain noise model. To cope with this problem, this thesis focuses on the noise robust sensing techniques, where the cases of unknown noise power and non-Gaussian noise are taken into considerations.

In this chapter, the origin and motivations of this work are introduced in Section 1.1. Then Section 1.2 summarises the objectives and key contributions of this thesis. Section 1.3 gives an overview of the remaining chapters.

1.1 Motivation

1.1.1 Motivation for Cognitive Radio: Spectrum is Underutilised

Radio spectrum is a nature and important resource required for wireless communications. Throughout the world, the utilisation of spectrum bands is regulated by government or world-wide agencies such as the Federal Communications Commission (FCC) in United States (US) and the Office of Communications (Ofcom) in United Kingdom (UK) etc. Traditionally, they allocate the spectrum bands to specific uses on a long-term basis, and grant licenses for these bands to protect the services.

Recently, there is a rapid growth in wireless communications with the users' expectation of being always wireless connected to a variety of services. Such ubiquitous and seamless connectivity requires huge demand on new wireless services, but is challenged by the radio scarcity

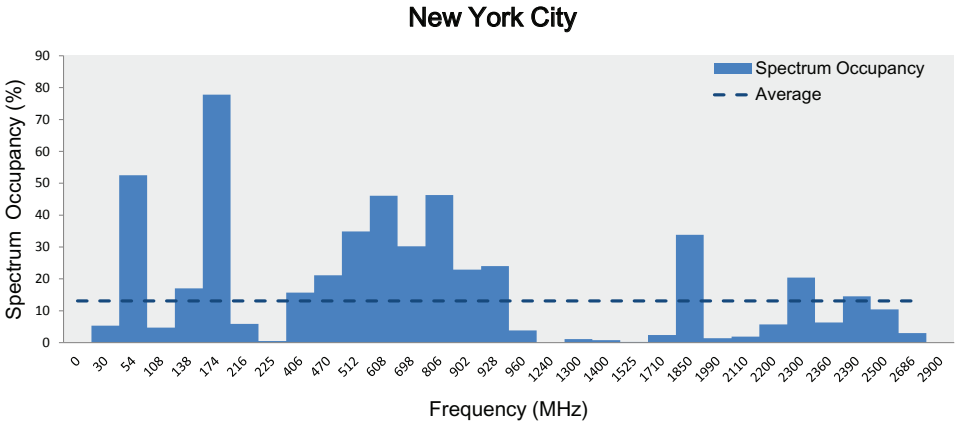

(a)

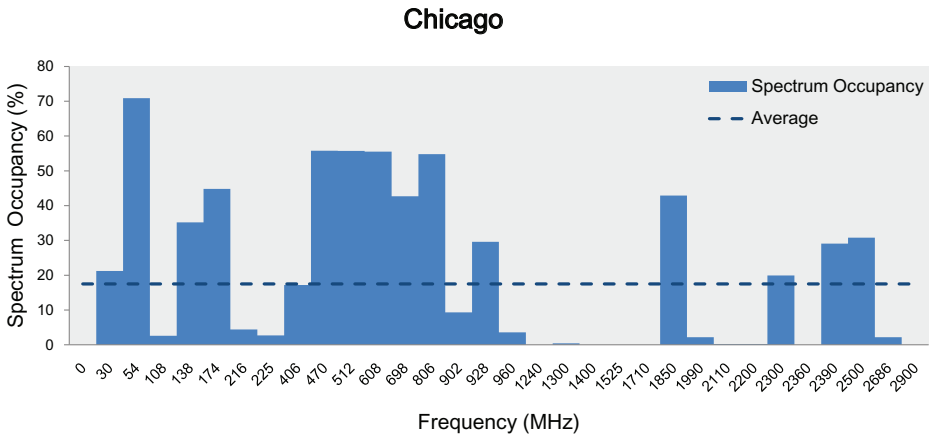

(b)

Figure 1.1: *Measured spectrum occupancy by band over a 3-day period [1], in: (a) New York City, with an average spectrum utilisation 13.1%; and (b) Chicago, with an average spectrum utilisation 17.1%.*

as most of the available spectrum bands have been assigned over the past decades [2]. There is limited or no spectrum left for the emerging wireless services.

On the other hand, many studies and reports have shown that the licensed spectrum bands are in fact underutilised. For example, Figure 1.1 plots the measurements of radio frequency (RF) utilisation from 30 MHz to 3 GHz, collected in New York City and Chicago rural areas over a 3-day period [3, 4]. The data reveal that their averaged spectrum utilisations are only 13.1% and 17.5%, respectively. Furthermore, as shown in the FCC report [5], depending on the geographic areas, a large portion licensed spectrum bands are with low occupancy, i.e., less than 15%, for significant periods of time. In addition, some certain bands, such as the cellular frequencies

and the industrial, scientific and medical (ISM) radio band (used in short-range and low power communications systems such as Bluetooth and wireless computer networks) have been very crowded in peak times, leading to a degraded quality of service and significant interference [1, 5, 6].

Such findings suggest that the traditional fixed spectrum allocation schemes are no longer efficient, which motivates the development of cognitive radio. By allowing the unlicensed users (secondary users) to dynamically operate at the underutilised radio spectrum assigned to the licensed users (primary users) [7], cognitive radio offers a solution to alleviate the spectrum congestion problem in some certain bands and yields more usable bandwidth to support the high data rates wireless services in next-generation communication systems.

1.1.2 Motivation for Noise Robust Spectrum Sensing Techniques

Since cognitive radio is designed to co-exist with the traditional radio systems, a key requirement is to enable the protection of licensed primary services. Such a task can be carried out through spectrum sensing which refers to the ability of a cognitive radio to detect the activities of licensed users over the frequency band of interest. In order to prevent harmful interference to the primary service, or keep the interference at a minimal level, sensing must be quick and robust to track the real-time variations of the surrounding radio environment.

Sensing techniques for unknown noise power

The energy detector [8–11] is the most widely used sensing scheme due to its low implementation complexity and good detection performance. It requires the exact value of noise power to be known and uses it to construct the test statistic and determine the test threshold. However, the central problem of the energy detector is its sensitivity to noise variance uncertainty. If the knowledge of noise power is not accurate, the energy detector will perform rather poorly or become invalid due to the high false alarm probability and significant performance loss in detection probability [12]. Hence, sensing methods that are invariant to the noise power are required to be considered.

Many efficient spectrum sensing techniques have been proposed to address this issue. One popular approach is to develop *blind* detectors [13–17], which refers to the detection without any *prior* knowledge of primary signal, fading channel and noise parameter. Or, feature based

detectors that do not make assumptions on known noise power [18–21] can be applied if some features of the primary signal, i.e., second-order statistic or cyclic frequencies, are known to the cognitive radio user.

However, as summarised in Table 2.1, Chapter 2, analytical solutions for the aforementioned detection methods are generally difficult to obtain. In addition, for the feature based detectors, commonly a long observation time is needed to exploit the signal features and high computational complexity is required for implementation.

Sensing techniques for non-Gaussian noise

The majority of current sensing methods consider the additive noise to be Gaussian distributed as implied by Central Limit Theorem (CLT) and it generates mathematically tractable models. However, another important noise source in practical wireless communication systems is man-made [22], i.e., typically caused by the automotive ignition, electromechanical switches and industrial thermal processes etc, which exhibits impulsive behaviour and makes the whole noise distribution heavy-tailed. For example, a measurement of impulsive noise in a digital television (TV) radio channel, i.e., at a central frequency of 762 MHz with 10 MHz bandwidth, has been reported in [23]. In addition, in [24], the indoor measurement in ISM band indicates the impulsive nature of noise. More experimental measurements of the man-made impulsive noise can be found in [23–26], and the references therein.

In the context of cognitive radio networks, non-Gaussian noise is a more reasonable setting as most of its applications, e.g., cellular networks [27] and public safety networks [28] etc, are in urban environments where man-made noise must be considered. Unfortunately, under non-Gaussian noise, standard sensing techniques tend to yield unacceptable high false alarm probability and degraded detection probability due to the uncertain distribution of the test statistic, requiring the design of robust sensing methods that considers the possible deviations of noise distribution from Gaussian model.

A review of current sensing techniques for non-Gaussian noise [29–35] is given in Chapter 2, Section 2.2.2. Again, the main issue of these detectors is the difficulty to obtain analytical solutions. Once the Gaussian noise assumption is removed, the test statistic and its distribution are generally complicated and depend on several unknowns. To deal with this problem, a conventional approach is to obtain the empirical solution using the Monte Carlo method [36],

which requires the sensing conditions to be reproducible, or assumptions on large data records are invoked so that asymptotic results can be applied [37].

1.2 Thesis Objectives and Contributions

1.2.1 Thesis Objectives

According to the aforementioned challenges for noise robust sensing schemes, this thesis has two main objectives:

• Develop a sensing method that is invariant to noise variance uncertainty and achieves good detection performance with relatively low computational complexity.

• Remove the assumption on Gaussian noise. Instead, a broad class of distributions are considered which includes Gaussian noise as a special case. Depending on different operation conditions, develop sensing algorithms that are valid in a variety of non-Gaussian noise without requirements on reproducible experiment conditions and large samples.

1.2.2 Main Contributions

The main contributions of this thesis are outlined as follows:

• An F-test based sensing method is developed by considering a multiple receiving antenna system. The proposed approach, in which channel state information (CSI) is required, offers absolute robustness against noise variance uncertainty and is relatively easy to implement. Based on the statistical properties of F-distribution, the accurate value for test threshold and detection probability are derived, respectively. Simulation results show that the proposed F-test based detector achieves a significant performance improvement compared with the energy detector. This work has been published in 2013 IEEE International Conference on Communications (ICC) [38].

• The impact of CSI uncertainty is investigated. Theoretical analysis indicates when the CSI estimate is imperfect, the F-test based detector suffers a mild performance loss in probability of detection and its false alarm probability remains unchanged. The detection probability can be evaluated using doubly noncentral F-distribution and a simple approximated value is also presented to avoid its computational complexity. This work has been published in IEEE

Transactions on Wireless Communications [39].

• Two sensing algorithms, the nonparametric eigenvalue based detector and the energy based detector, are developed for arbitrary noise types with finite power. The first one employs the eigenstructure of sample covariance matrix and the second is an extension of the conventional energy detector. For both detectors, the powerful bootstrap resampling techniques are applied to estimate the test statistic's null distribution and sufficiently accurate test thresholds are obtained for moderate sample size. The key idea is to reuse the data through resampling instead of repeating the experiment a large number of times. Results show the two detection methods maintain their false alarm probability in a variety of noise types and demonstrate superiority when the noise is non-Gaussian. Part of this work has been published in 2014 IEEE Global Communications Conference (GLOBECOM) [40].

• The F-test based detector is generalised to non-Gaussian noise. To maintain the pre-determined false alarm probability in non-Gaussian noise, two methods are developed to estimate the null distribution of the F-statistic by exploiting different *prior* knowledge of noise. The first modified degrees of freedom (MDOF) based approach assumes the value of noise kurtosis is known and the result is obtained in closed form. The second approach is based on the computational bootstrap procedure which results in minimal requirements on the noise model as only a sequence of noise samples is needed for training purpose. Theoretical analysis shows that both methods yield accurate statistical approximations with moderate sample size. From numerical results, it is observed that the F-statistic based detector maintains its target false alarm probability in various types of non-Gaussian noise, achieving performance gain compared with other robust detectors. Furthermore, this work has general validity which can be extended to other linear regression problems with complex number measurements. This work has been submitted to IEEE Transactions on Cognitive Communications and Networking.

1.3 Thesis Structure

The reminder of this thesis is structured as follows:

Chapter 2

This chapter provides background knowledge about the topic of thesis. It starts with an introduction to the cognitive radio technology, including its origins, key functionalities, applications

and related standard activities. Then a literature review of conventional spectrum sensing techniques for Gaussian noise is presented, in which the robust sensing algorithms for uncertain noise variance are highlighted. Finally, current sensing algorithms for non-Gaussian noise are reviewed and summarised.

Chapter 3

This chapter proposes an F-test based sensing technique by considering a multiple antenna assisted receiver. This method uses the F-statistic as the test statistic which offers absolute robustness against noise variance uncertainty. Statistical properties of F-distribution are applied to derive the test threshold and detection probability, respectively. In addition, since this approach requires *prior* knowledge of the fading channel, which may be imperfect in the context of cognitive radio, the impact of CSI uncertainty is described and the performance loss in detection probability is derived.

Chapter 4

This chapter removes the conventional Gaussian noise assumption and proposes two bootstrap based sensing techniques which can be applied to a variety of noise types. Firstly, a nonparametric eigenvalue based approach is proposed by exploiting the eigenstructure of sample covariance matrix. Next, the standard energy detector is generalised to non-Gaussian noise by studentizing its test statistic. For both detectors, bootstrap technique is used to non-parametrically estimate the test statistic's null distribution, leading to a test threshold that meets the target false alarm probability. The application of bootstrap is highlighted, and its advantages and accuracy are described.

Chapter 5

This chapter generalises the conventional F-test based detection method to non-Gaussian noise. Since the null distribution of the F-statistic is unknown in non-Gaussian noise, two approximation methods are proposed based on different *prior* knowledge of the noise. The first approach assumes a known noise kurtosis and approximates the null distribution by an F-distribution with modified degrees of freedom. Then a bootstrap based method is developed which relaxes the assumption on high order noise moments and only requires a sequence of noise samples for training purpose. The accuracy of both methods are described. Finally, the results are extended to a more general linear regression hypothesis testing problem.

Chapter 6

This chapter concludes the thesis, states the limitations and describes several interesting topics which are potentially worthy of further investigation.

Chapter 2

Background

Cognitive radio is a novel wireless communication approach that addresses the issues of spectrum inefficiency and spectrum scarcity. In order to improve the licensed band utilisation, it allows the unlicensed secondary users to exploit the frequency bands in an opportunistic manner [1, 2]. Since the licensed primary users have a higher priority, one key issue of cognitive radio is to check the spectrum availability periodically and keep the interference to the primary service at a minimal level [7]. This task requires the secondary user to have a cognition of the surrounding radio environment, or spectrum sensing. In this thesis, we focus on dealing with two challenges in spectrum sensing, namely the detection in unknown noise power and the detection in non-Gaussian noise. Such topics have attracted researchers' attentions recently as the traditional sensing methods are shown to suffer from the sensitivity to the noise model uncertainty, requiring the design of the noise robust detectors.

This chapter shall start with an overall introduction to cognitive radio technology in Section 2.1. Then a review of current spectrum sensing techniques is presented in Section 2.2 with particular emphasis on related works for noise robust sensing algorithms.

2.1 Cognitive Radio

As discussed in Chapter 1, cognitive radio is motivated by the fast growing demand for high data rates and the actual poor underutilisation of licensed bands coupled with heavy overutilisation of some certain spectrum. First proposed by Mitola in 2000 [41] , cognitive radio has emerged as a promising technology for improving spectrum efficiency in the past decade. In this section, some background information of cognitive radio technology will be provided, including its origins, key functionalities, applications and related standard activities.

2.1.1 Cognitive Radio Technology

Cognitive radio is initially described by Mitola [41] as *"a radio or system that senses, and is aware of, its operational environment and can dynamically and autonomously adjust its radio operating parameters accordingly "*. More precisely, S.Haykin gives a formal definition for cognitive ratio in [7]:

"*Cognitive radio is an intelligent wireless communication system that is aware of its surrounding environment (i.e., outside world), and uses the methodology of understanding-by-building to learn from the environment and adapt its internal states to statistical variations in the incoming RF stimuli by making corresponding changes in certain operating parameters (e.g., transmit-power, carrier-frequency, and modulation strategy) in real-time, with two primary objectives in mind:*

• *highly reliable communications whenever and wherever needed;*

• *efficient utilisation of the radio spectrum.*"

From these definitions, we can conclude that different from a traditional radio, the cognitive radio has two main features: the cognition capability and the reconfigurability [1]. That is, the cognitive radio should have an awareness of the surrounding spectrum usage and have the ability to interactively make real-time decisions about the communication plan to be used. The procedure of how these key features interact with the surrounding radio environment is illustrated by a cognition cycle in Figure 2.1 [1].

Cognition Capability of Cognitive Radio

The cognition capability refers to the ability of cognitive radio transceiver to capture the available spectrum band, analyse the information and make an action by transmitting signals. For more details, it corresponds to the three components in Figure 2.1:

• Spectrum sensing/Database access. A key issue of cognitive radio is to protect the primary users from interference as they have a higher priority for spectrum utilisation. The incumbent protection can be carried out through either spectrum sensing or database access. The former one is a conventional approach in which the secondary users are required to sense the spectrum periodically to keep the interference at a minimal level. As shown in Figure 2.2, the secondary users may cause interference to the primary user even if they are outside the coverage of primary transmitter. Hence, spectrum sensing is required to have a much higher detection sensitivity

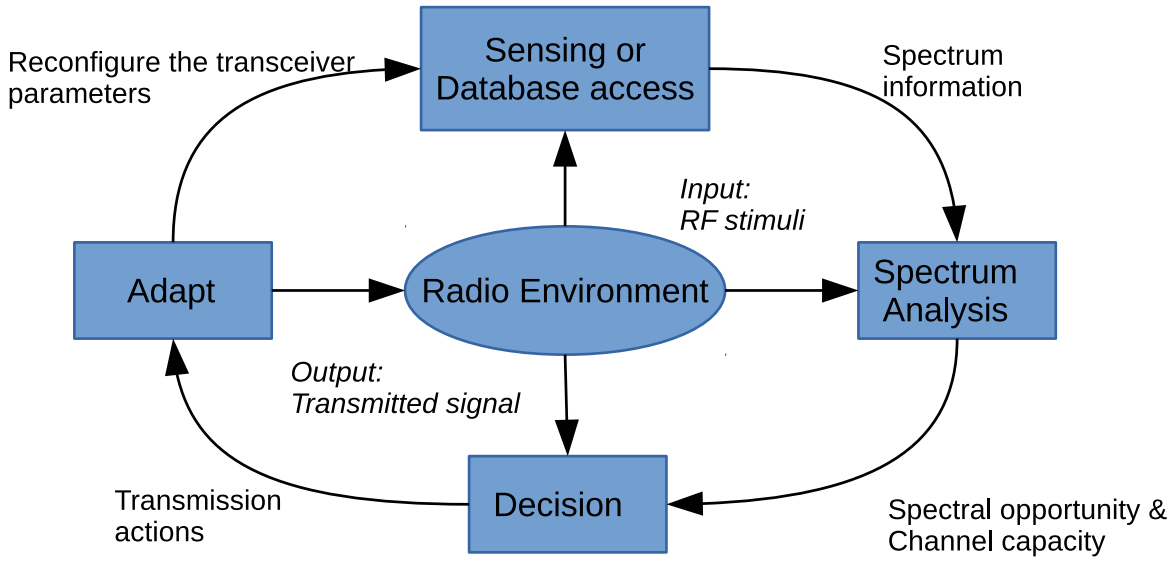

Figure 2.1: *Functional cycle of cognitive radio [1].*

than the conventional detectors. The database access is another way recommended in current rules for the opportunistic use of TV band [42, 43]. In such rules, the channel availability is determined by checking an authorised database, but the research on sensing is still encouraged for spectrum efficiency improvements and further dynamic access beyond TV bands.

• Spectrum analysis. Given the spectrum band of interest, spectrum analysis aims at providing a completed interpretation about the spectral opportunity and estimating the channel capacity for use by the secondary user. The former one intends to create the potential spectral opportunity by exploiting more dimensions. For example, in addition to the conventional spatial, time and frequency domains, the spectral opportunity can also be found in the angle dimension by using the beamforming technique, allowing the secondary user and primary user to simultaneously utilise a spectrum band [45]. Another task for spectrum analysis is to estimate the channel capacity through the feedback link between the cognitive radio transceiver and secondary user [7], i.e., as shown in Figure 2.2. These spectral characteristics, i.e., status and capacity, will be passed into the next decision step.

• Decision. According to the outcomes of the above procedures, a set of transmission actions will be taken, including the choice of appropriate spectrum band, modulation schemes, data rate and transmission power, etc. At the same time, all these parameters are gathered to be configured, preparing for the next upcoming transmission.

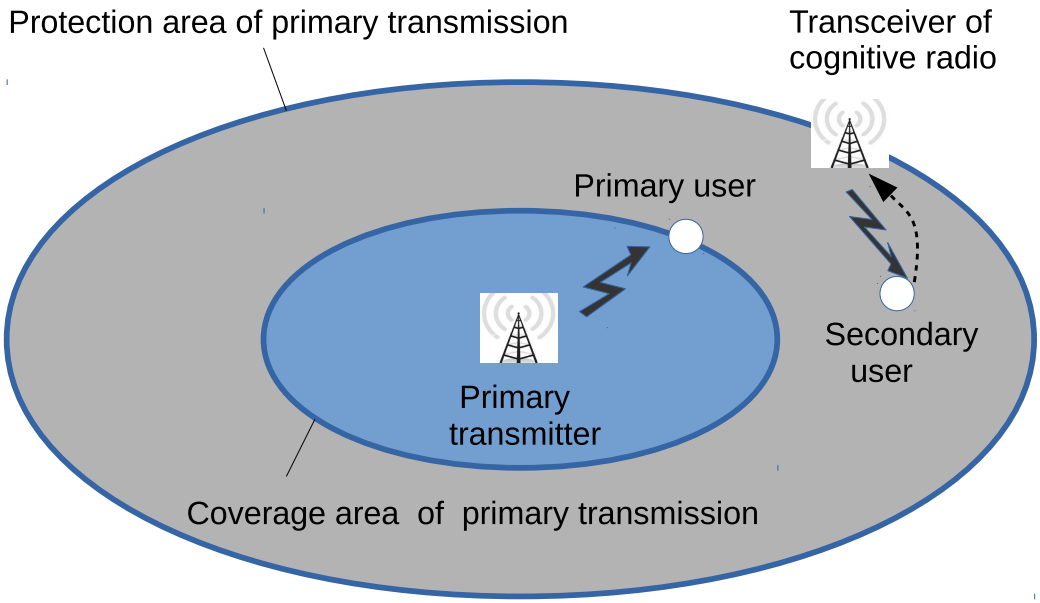

Figure 2.2: *Illustration of coverage and protection area of primary transmission [44].*

Reconfigurability of Cognitive Radio

Another key feature of cognitive radio that distinguishes itself from the conventional communication systems is the reconfigurability. That is, the cognitive radio should be able to adapt its transceiver parameters to the surrounding radio environment [7]. Traditional radio network, which uses fixed spectrum allocation schemes, is usually designed to operate at a specified spectrum band with respect to certain communication protocols. Such rules cannot be applied to cognitive radio network as the spectrum is only temporarily assigned to the secondary user and must be returned if the primary user becomes active. Hence, according to the spectral opportunity, a cognitive radio should have the mobility to be reprogrammed at various frequency bandwidths with different locations and sizes. Moreover, a certain communication protocol is no longer sufficient for the dynamic spectrum access. Instead, when a new spectral opportunity emerges, a cognitive radio terminal should be able to switch to an appropriate protocol by adjusting the modulation schemes etc. Furthermore, the transition of spectrum band and adjustment of communication technologies should be fast and smooth in order to guarantee a seamless wireless connectivity. Therefore, hardware devices that can provide continuous allocation of spectrum are required, which poses further challenges [46].

2.1.2 Cognitive Radio Applications

Due to the ability to adapt to the surrounding spectral environment, a cognitive radio can co-exist with a variety of wireless communication systems. Some of the major applications are listed as follows:

• Cellular networks. The use of cellular networks is undergoing a fast growth in recent years with the dramatical development of mobile internet requiring massive data connections, anywhere and anytime. This brings bandwidth challenges to the cellular network as it is easily to be overloaded. For example, the hotspot used in public places generates a large amount of data in a small area, which causes heavy data traffic in certain spectrum. Moreover, there also exist coverage issues for cellular network in some places, especially in rural areas. Facing those challenges, cognitive radio may offer solutions by opening the unlicensed spectrum opportunistically [27]. For instance, in certain urban area where the spectrum is overloaded, the data could be offloaded to the new available frequency bands from other licensed holders. In rural areas where the cellular network is not available for the cost issue, users can temporally operate at a leased band, such as the abundant TV channels, leading to a more efficient spectrum usage.

• Public safety network. Nowadays, the wireless communications are widely used by public safety users for a fast emergency service access, i.e., police and emergency medical aid. In order to ensure an efficient communication between the command centre and workers/users, the wireless services (voice, message, picture transfer and email etc.) are expected to be available at arbitrary time and location. Such requirements conflict with the current limited frequency resources allocated to the public safety [28]. In coping with this problem, cognitive radio technology can be applied with an appropriate spectrum coordination standard that allows the emergency workers to use additional spectrum if necessary. For example, the emergency responders could roam on an unoccupied TV spectrum or other potential bands in an area where more capacity is required to operate the public safety network.

• Machine-to-machine communications. Machine-to-machine (M2M) communications, characterised by the full automation among intelligent machines, is an emerging communication technology that offers ubiquitous connectivity between networked devices for exchanging informations without human intervention [47]. It is expected that a large amount of connected devices will exist in the near future, i.e., 50 billion networked devices are predicted to appear by 2020 [48]. With such a vast amount of connected devices, many issues such as spectrum

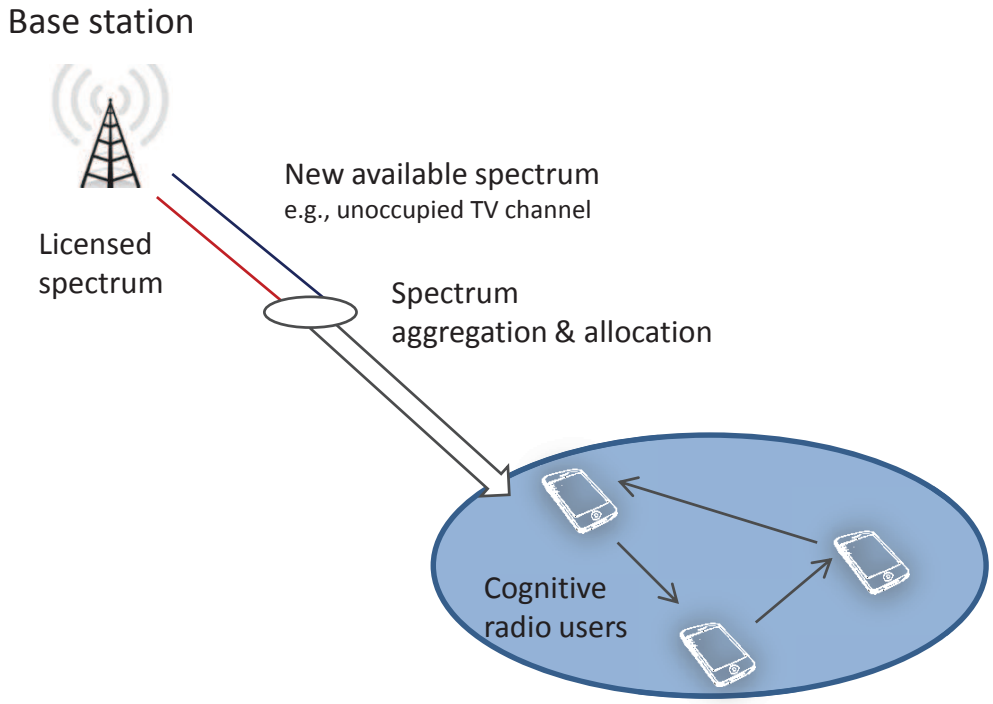

Figure 2.3: *The application of cognitive radio.*

congestion and interference will arise as the exchange of information could be between the sensor, the decision maker and the action executer. Cognitive radio technology can be applied to effectively overcome those challenges [49]. Through opportunistically exploiting the available spectrum across both the licensed and unlicensed bands, the M2M network can support the required data transmission for automatic inter-connectivity in a larger scale, and an improved quality of service can be expected as the cognitive radio technology enables the selection of better propagation bands.

In Figure 2.3, a typical cognitive radio application network is illustrated. This point-to-multipoint communication scheme is used in IEEE 802.22 standard [50], in which a base station configures the spectrum to operate and manages multiple cognitive radio users.

Standardisation activity in cognitive radio

Currently, the major applications of cognitive radio technology are in the unused TV spectrum, namely the TV white space (TVWP). The idea of opportunistic access of TV channel was first proposed by the US FCC in 2003 [51] and a number of standardisation activities have been developed over the past decade. For example, FCC has released the final rules for the dynamic access in 470-790 MHz TVWP [42] in 2010, and some related standards, i.e., IEEE 802.22

[50], IEEE 802.11af [52] and IEEE DySPAN [53] etc, have been published or are in development. Meanwhile, in 2012, the Ofcom in UK has released its decision to open the unused parts of TV spectrum, i.e., over the 470 to 790 MHz frequency band, and the corresponding implementation issues are planed to be completed by the end of 2015 [43]. In addition, the Electronic Communications Committee (ECC) in Europe has also published a number of reports regarding the technical principles for the operation of unlicensed wireless services in TVWP [54, 55].

2.2 Spectrum Sensing Techniques

As mentioned above, spectrum sensing is one of the most important tasks of cognitive radio technology as it provides an awareness of the surrounding radio environment and enables secondary user to occupy the spectrum holes without interfering with the primary transmission.

The problem of interest for spectrum sensing is to decide whether the primary users are active or not over a particular frequency band and geographical area. It can be formulated as a hypothesis testing problem, where the null hypothesis $\mathcal{H}_0$ and the alternative hypothesis $\mathcal{H}_1$ denote the absence and the presence of primary user, respectively. In the simplest form, we want to test the following binary hypothesis:

$$\begin{aligned} \mathcal{H}_0 &: \quad y(l) = w(l), \\ \mathcal{H}_1 &: \quad y(l) = x(l) + w(l),\ l = 0, 1, ..., L-1, \end{aligned} \tag{2.1}$$

where $y(l)$ is the observed baseband signal with sample size L. $x(l) = hs(l)$, i.e., one receiving antenna is considered, is the faded primary signal, where $s(l)$ denotes the signal transmitted by the primary user and h is the channel coefficient between the primary transmitter and sensing device. Generally, a block fading channel is considered which means that h is assumed to be constant during the sensing interval. The additive white noise $w(l)$ is assumed to be independent and identically distributed (i.i.d.), with zero-mean and variance σ_w^2. Note that σ_w^2 is also called noise power in this thesis. Moreover, it is worth mentioning that most of spectrum sensing schemes are designed for one primary signal source.

Note that the signal model in (2.1) is only an example and the observed signal may be vectorial, depending on the operation conditions. Throughout this thesis, lowercase and uppercase boldface letters are used to represent vectors and matrices, respectively. For instance, if a receiver

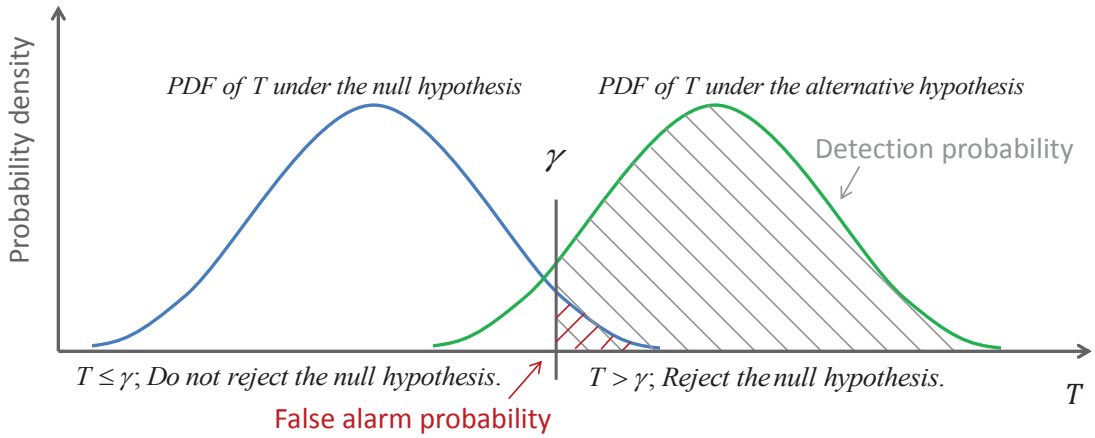

Figure 2.4: *A schematic diagram of the hypothesis testing problem in (2.2).*

antenna array with size M is applied, then $\mathbf{y}(l) = [y_1(l), y_2(l), \ldots, y_M(l)]^T$ will be used to represent the vectorial observation, where $y_i(l)$ ($i = 1, 2, ..., M$) stands for the scalar response at the ith receiver antenna and $[\cdot]^T$ represents transpose operation.

To test the null hypothesis $\mathcal{H}_0$ against the alternative hypothesis $\mathcal{H}_1$, generally it takes the form:

$$T \underset{\mathcal{H}_0}{\overset{\mathcal{H}_1}{\gtrless}} \gamma, \tag{2.2}$$

where T denotes the test statistic constructed from the observations and several known parameters. The scalar γ is the pre-determined test threshold to ensure a target significance value which is called false alarm probability in spectrum sensing. The performance of the binary test (2.2) is summarised by its false alarm probability (P_f) and detection probability (P_d), which are defined as follows:

$$P_f = \Pr(T > \gamma | \mathcal{H}_0), \tag{2.3}$$

$$P_d = \Pr(T > \gamma | \mathcal{H}_1). \tag{2.4}$$

A schematic diagram for the hypothesis testing problem (2.2) is shown in Figure 2.4, where the two distributions denote the probability density function (PDF) of the test statistic under $\mathcal{H}_0$ and $\mathcal{H}_1$, respectively. It can be observed that the detection probability depends on the value of the test threshold, which is related to the required false alarm probability, and the distance between the two PDFs.

In the context of cognitive radio, P_f denotes the probability that an idle spectrum is falsely ignored, which leads to a spectral loss. On the other hand, P_d determines the percentage of the occupied spectrum that is truly detected, which avoids harmful interference to the primary service. In the design of spectrum sensing techniques, we should keep P_f under a pre-specified level and choose the test statistic T to make P_d as large as possible.

2.2.1 Conventional Spectrum Sensing Techniques

Gaussian noise is a conventional noise model applied in current spectrum sensing literature. Implied by CLT, it provides a good model for noise caused by natural sources [7], such as thermal noise. In addition, the Gaussian noise assumption generally leads to mathematical tractable solutions. The detection of signal in Gaussian noise, such as the hypothesis testing problem in (2.1), is a traditional topic that has been discussed in detail in statistical books [56, 57]. The design of spectrum sensing algorithms is related to those long established detection theories, more than that, the background of wireless communications and cognitive radio network should be considered. For example, the observations are generally complex-valued due to the modern modulation schemes used in the primary transmission and the information of the primary signal is usually limited. In this section, some state-of-the-art spectrum sensing schemes will be introduced and explained. Particularly, the robust sensing algorithms for unknown noise power will be highlighted and a simple summary of them will be given in Table 2.1.

Likelihood Ratio Test/Matched Filter

The likelihood ratio test is a very general approach for testing hypothesis and it is the uniformly most powerful (UMP) test in the Neyman-Pearson (NP) sense [56], i.e., the detection probability is maximised for a fixed false alarm probability. Define $\mathbf{y} \triangleq [y(0), y(1), \ldots, y(L-1)]^T$ be the set of collected samples. Given the hypothesis testing problem (2.1), it uses the likelihood ratio as the test statistic:

$$T = \frac{f\left(\mathbf{y}\,|\mathcal{H}_1\right)}{f\left(\mathbf{y}\,|\mathcal{H}_0\right)}, \tag{2.5}$$

where $f\left(\mathbf{y}\,|\mathcal{H}_0\right)$ and $f\left(\mathbf{y}\,|\mathcal{H}_1\right)$ denote the PDFs of $\mathbf{y}$ under the null hypothesis $\mathcal{H}_0$ and the alternative hypothesis $\mathcal{H}_1$, respectively. Note that T in (2.5) measures how much more likely the observations $\mathbf{y}$ are generated from $\mathcal{H}_1$ than $\mathcal{H}_0$. Clearly, T will be relatively large if the alternative hypothesis $\mathcal{H}_1$ fits the observations better than the null hypothesis $\mathcal{H}_0$. We shall

pick $\mathcal{H}_1$, or declare the detection of primary signals, when the ratio T is large enough to exceed a given threshold. The likelihood ratio in (2.5) consists of the PDFs of the measurements $\mathbf{y}$ under both assumption models. This means that to evaluate T, all the data parameters should be known. Recall the spectrum sensing problem in (2.1). When both the signal, $x(l)$, and the noise power, σ_w^2, are perfectly known, we obtain the likelihood ratio test as a form of matched filter [58]:

$$T = \Re\left(\sum_l x(l)^H y(l)\right) \underset{\mathcal{H}_0}{\overset{\mathcal{H}_1}{\gtrless}} \gamma, \tag{2.6}$$

where $\Re(\cdot)$ denotes the real part of a complex-valued number.

The matched filter in (2.6) is a coherent detection, and thus less sensing time, i.e., $O(1/\text{SNR})$ samples where $O(\cdot)$ denotes the order notation, is needed to satisfy a given detection probability [9]. However, in the context of cognitive radio, it is difficult for secondary user to know all the signal and noise parameters. A more reasonable assumption is that these parameters are partially known, or even totally unknown. More precisely, let Θ_k be the set that contains unknown parameters, where the subscript, $k = 1, 2$, stands for $\mathcal{H}_0$ and $\mathcal{H}_1$, respectively. In such cases, a standard method is to use maximal likelihood (ML) to estimate Θ_k. Although the optimality may not be guaranteed, it turns out that the ML technique usually works well in many spectrum sensing schemes.

Energy Detector

The energy detector [8, 9] is the most widely used spectrum sensing scheme due to its simplicity. It needs to know the noise power σ_w^2, but no information of the primary signal is required. To derive the energy detector using the likelihood ratio criteria, assume that the exact value of σ_w^2 is known as a *prior* and $x(l)$ in (2.1) is zero-mean circularly symmetric complex Gaussian distributed with unknown variance σ_x^2. Hence, we have $\Theta_0 = \emptyset$, where $\emptyset$ denotes the empty set, and $\Theta_1 = \sigma_x^2$.

Based on the above assumptions, the distribution of $y(l)$ can be written in case by:

$$\begin{aligned} \mathcal{H}_0 &: \quad y(l) \sim \mathcal{CN}\left(0, \sigma_w^2\right), \\ \mathcal{H}_1 &: \quad y(l) \sim \mathcal{CN}\left(0, \sigma_x^2 + \sigma_w^2\right). \end{aligned} \tag{2.7}$$

Using ML method to estimate $\Theta_1 = \sigma_x^2$ under the alternative hypothesis and after eliminating

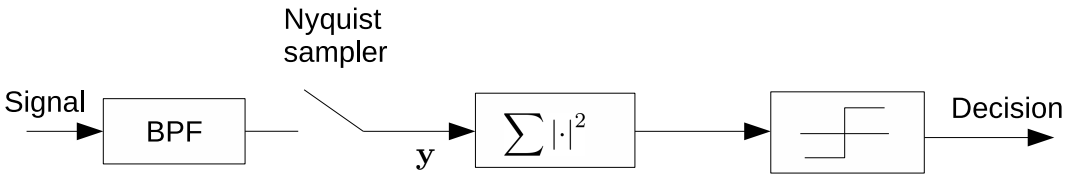

Figure 2.5: *Block diagram for the energy detector.*

the constant terms, the maximal likelihood ratio test takes the form:

$$T = \frac{\max\limits_{\Theta_1} f\left(\mathbf{y}\,|\mathcal{H}_1, \Theta_1\right)}{f\left(\mathbf{y}\,|\mathcal{H}_0\right)} = \sum_{l=0}^{L-1} \left|y\left(l\right)\right|^2 \underset{\mathcal{H}_0}{\overset{\mathcal{H}_1}{\gtrless}} \gamma, \tag{2.8}$$

where $|\cdot|$ denotes the standard scalar norm. The test (2.8) is also called the energy detector as it compares the energy of received samples with a pre-determined threshold.

A block diagram for the energy detector is shown in Figure 2.5, where the band pass filter (BPF) is applied to select the frequency band of interest. As shown in the Figure, the energy detector is easy to implement as it works in a non-coherent manner that no further knowledge of the primary signal is required. In addition, it offers a good performance, i.e., $O\left(1/\text{SNR}^2\right)$ samples are required to meet a target detection probability [9]. Due to these advantages, the energy detector becomes a popular choice for spectrum sensing and often acts as a benchmark for comparison.

A major drawback of the energy detector is its sensitivity to noise variance uncertainty [59], which refers to the mismatch between the exact value of noise power σ_w^2 and its estimate. Note that we need σ_w^2 to set the threshold of the energy detector as its test statistic's null distribution depends on it. The real value of σ_w^2 is usually unknown and the threshold in (2.8) is obtained by replacing the noise power with its estimate. However, even a small amount of estimation error will lead to a significant performance loss and make the energy detector become invalid [12]. An example can be found in Figure 3.6, Chapter 3. It can be observed that under noise variance uncertainty, the detection probability of the energy detector degrades severely and the false alarm probability far exceeds the target value.

This drawback of the energy detector motivates the research for robust detection methods. One solution is to find a detector setting the test threshold independent of the noise power, such as the Generalised Likelihood Ratio Test (GLRT) based detector and eigenvalue based detector,

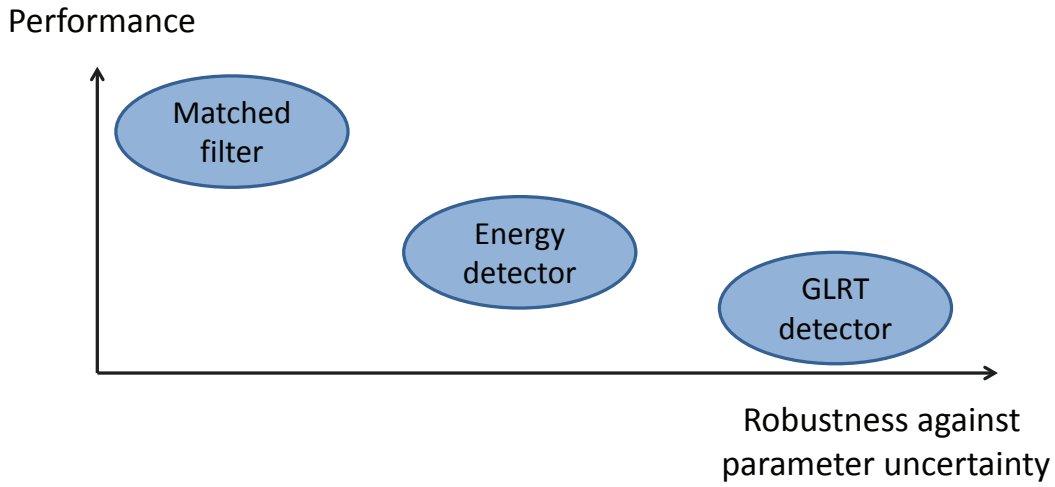

Figure 2.6: *Comparison of detection algorithms using likelihood ratio principle.*

which will be discussed later.

Generalised Likelihood Ratio Test (GLRT) based Detector

A GLRT based detection is usually considered when all the parameters are unknown. Hence, it offers absolute robustness against noise variance uncertainty. In the context of spectrum sensing, the GLRT based detection generally requires multiple receiving antennas as the ML estimates of Θ_1 for data model (2.1) need to exploit the inherent structure of sample covariance matrix [15–17]. Suppose a sensing device comprises M receiving antennas. Let $\mathbf{y}(l) = [y_1(l), y_2(l), \ldots, y_M(l)]^T$ be the baseband signal vector at the receiver antenna array, which can be written as:

$$\begin{aligned} \mathcal{H}_0 \quad &: \quad \mathbf{y}\left(l\right) = \mathbf{w}\left(l\right), \\ \mathcal{H}_1 \quad &: \quad \mathbf{y}\left(l\right) = \mathbf{x}\left(l\right) + \mathbf{w}\left(l\right),\ l = 0, 1, ..., L-1. \end{aligned} \tag{2.9}$$

Define $\mathbf{Y} \triangleq [\mathbf{y}(0), \mathbf{y}(1), \ldots, \mathbf{y}(L-1)]$ be the collected sample set. By using the ML method to estimate all the unknowns, the GLRT based detector takes the form:

$$T = \frac{\max\limits_{\Theta_1} f\left(\mathbf{Y}\left|\mathcal{H}_1, \Theta_1\right.\right)}{\max\limits_{\Theta_0} f\left(\mathbf{Y}\left|\mathcal{H}_0, \Theta_0\right.\right)} \underset{\mathcal{H}_0}{\overset{\mathcal{H}_1}{\gtrless}} \gamma. \tag{2.10}$$

In [17], the signal part of the observation $\mathbf{x}(l)$ was considered as a Gaussian distributed variate with zero-mean and unknown covariance, i.e., $\mathbf{x}(l) \sim \mathcal{CN}(0, \mathbf{R}_x)$ where $\mathbf{R}_x \triangleq \mathrm{E}\left[\mathbf{x}(l)\,\mathbf{x}(l)^H\right]$. Then the hypothesis testing problem in (2.9) can be converted to:

$$\begin{aligned} \mathcal{H}_0 &: \quad \mathbf{y}(l) \sim \mathcal{CN}\left(0, \sigma_w^2 \mathbf{I}\right) \\ \mathcal{H}_1 &: \quad \mathbf{y}(l) \sim \mathcal{CN}\left(0, \mathbf{R}_x + \sigma_w^2 \mathbf{I}\right). \end{aligned} \tag{2.11}$$

By using ML to estimate $\Theta_0 = \sigma_w^2$ and $\Theta_1 = [\mathbf{R}_x, \sigma_w^2]$ under both hypothesis, the GLRT based detector for (2.11) (i.e., [17]) is given by:

$$T = \frac{\frac{1}{M}\sum_{i=1}^{M}\beta_i}{\left(\prod_{i=1}^{M}\beta_i\right)^{\frac{1}{M}}} \underset{\mathcal{H}_0}{\overset{\mathcal{H}_1}{\gtrless}} \gamma, \tag{2.12}$$

where $\beta_1 > \beta_2 > \ldots > \beta_M$ denote the eigenvalues of the sample covariance matrix:

$$\hat{\mathbf{R}}_y = \frac{1}{L-1}\sum_{l=0}^{L-1}\mathbf{y}(l)\mathbf{y}(l)^H. \tag{2.13}$$

The test in (2.12) is also called the AGM detector as its test statistic computes the arithmetic-to-geometric mean of sample eigenvalues. Although the AGM detector is *blind*, results in [17] show that it achieves a better detection performance compared with the energy detector with noise variance uncertainty.

Note that the AGM detector treats the $\mathbf{R}_x$ in an unstructured manner. A more specified signal structure was considered in [15, 16], where the data model under $\mathcal{H}_1$ is expressed as:

$$\mathcal{H}_1 : \mathbf{y}(l) = \mathbf{h}s(l) + \mathbf{w}(l),\ l = 0, 1, ..., L-1. \tag{2.14}$$

Here, the primary signal $s(l)$ is characterised by an i.i.d Gaussian random variate with zero-mean and variance σ_s^2, i.e., $s(l) \sim \mathcal{CN}\left(0, \sigma_s^2\right)$. Then the covariance of $\mathbf{x}(l) = \mathbf{h}s(l)$ can be written as $\mathbf{R}_x = \mathbf{h}\mathbf{h}^H\sigma_s^2$, and we have $\Theta_0 = \sigma_w^2$ and $\Theta_1 = [\mathbf{h}, \sigma_s^2, \sigma_w^2]$. The consequent GLRT detector for testing:

$$\begin{aligned} \mathcal{H}_0 &: \quad \mathbf{y}(l) \sim \mathcal{CN}\left(0, \sigma_w^2 \mathbf{I}\right) \\ \mathcal{H}_1 &: \quad \mathbf{y}(l) \sim \mathcal{CN}\left(0, \mathbf{h}\mathbf{h}^H\sigma_s^2 + \sigma_w^2 \mathbf{I}\right) \end{aligned} \tag{2.15}$$

is (i.e., [15, 16]):

$$T = \frac{\beta_1}{\sum_{i=1}^{M} \beta_i} \underset{\mathcal{H}_0}{\overset{\mathcal{H}_1}{\gtrless}} \gamma. \tag{2.16}$$

Compared with the AGM detector, the test in (2.16) has an improved detection performance as it exploits the rank one property of $\mathbf{R}_x$. Moreover, the GLRT can be further adapted to a multiple-input multiple-output (MIMO) system [60] and uncalibrated receivers [61].

For the aforementioned detection algorithms using likelihood ratio principle, i.e., based on data model (2.1), there exists a trade-off between the detection performance and robustness against parameter uncertainty. As shown in Figure 2.5, the matched filter performs the best, but has the lowest robustness as it needs all the parameters to be known. While the GLRT detector has a relatively lower detection performance but enjoys the highest robustness as no information of the signal, channel and noise power is required.

Eigenvalue based Detector

As shown in the GLRT based detector, sometimes the primary signal imparts a specified structure to the sample covariance matrix that can be utilised. This happens when a multiple antenna assisted receiver is applied, or if the signal is oversampled [13]. Unlike the GLRT based detector, the eigenvalue based detector treats the signal as if its structure is unknown. For example, without the knowledge of the rank of $\mathbf{R}_x$, we assume it is either rank-deficient or full rank but non-white. In such cases, when $L \to \infty$, the sample covariance matrix $\hat{\mathbf{R}}_y$ under $\mathcal{H}_0$ has equal eigenvalues as $\hat{\mathbf{R}}_y \to \sigma_w^2 \mathbf{I}$; but forms differently when $\mathcal{H}_1$ is true as $\hat{\mathbf{R}}_y \to \mathbf{R}_x + \sigma_w^2 \mathbf{I}$. By using this property, the well-known maximum-minimum eigenvalue (MME) detector proposed in [13] is:

$$T = \frac{\beta_1}{\beta_M} \underset{\mathcal{H}_0}{\overset{\mathcal{H}_1}{\gtrless}} \gamma. \tag{2.17}$$

Note that both the MME and the GLRT based detectors exploit the eigenvalue properties of sample covariance matrix. The difference is that the MME detector only uses the autocorrelation of primary signal, while the GLRT based detectors also take the potential signal structure into account. Clearly, the MME detector will have relatively poor performance if the signal structure is known. Moreover, for these eigenvalue based detectors, analytical solutions for the test thresholds are difficult to obtain or require high computational complexity [62]. Although the empirical results can be obtained using the Monte Carlo method [36], it requires the sensing

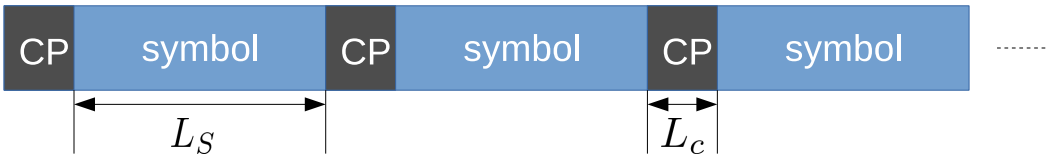

Figure 2.7: *OFDM signal structure.*

conditions to be reproducible. In addition, the simple asymptotic results derived from random matrix theory are shown to differ significantly from the exact value if the number of receiving antennas and the data samples are limited [63].

Feature based Detector

In the context of spectrum sensing, feature based methods refer to the detection of primary signal by exploiting its known statistical properties. The signal features, which are commonly seen in the man-made case, are a result of the adding of coding, the insertion of pilot or the modulation scheme used at the transmitter etc. For example, the orthogonal frequency-division multiplexing (OFDM) modulation contains cyclic prefix (CP), which refers to adding a sequence of symbol repetition at the end, for eliminating the inter-symbol interference. Moreover, most of communication systems add pilot to the transmitted signal for assisting the dedicated receivers. Doing these result in distinct signal features that can be used by detectors. In general, the feature based spectrum sensing schemes can be categorised into the second-order statistic based detector [19, 64, 65] and the cyclostationarity based detector [66–68].

• ***Second-order statistic based detector***

The second-order statistic based detector, as its name indicates, makes the decision based on the second-order statistic of the received signal. It relies on the fact that the transmitted signal has a correlated structure while the white noise does not. For example, consider an OFDM signal with a CP, as shown in Figure 2.7. Let L_s be the size of OFDM symbols, which is equivalent to the number of sub-carriers, and L_c be the length of CP symbols. Again, assume the transmitted primary symbols are i.i.d with zero-mean. In this case, the autocorrelation function (ACF) of the received signal in (2.1):

$$r_y(l,\tau) \triangleq \mathrm{E}\left[y(l)\, y(l+\tau)\right] \tag{2.18}$$

is time-varying and periodic in l as it is non-zero only at lag $\tau = L_s$ for some value of l. Assuming that L_s and L_c are known, this CP based non-stationary property of ACF can be

utilised by detectors for identifying primary signals [18, 19, 69].

In addition to the CP, another repetition structure we can used is the pilot [70], which is often inserted to signal at the transmitter for assisting the dedicated receivers, channel estimation and synchronisation purpose. Detectors based on the pilot induced structure have been proposed in [64, 65]. Interestingly, the results in [64] show that compared with the CP based method, the pilot based approach achieves a better detection performance and is more robust to the synchronisation error and frequency offset.

• ***Cyclostationarity based detector***:

A more popular approach of feature based sensing is to exploit the inherent cyclostationarity of the received signal. The cyclostationarity is caused by the periodic patterns in the signal statistic such as the aforementioned ACF.

For example, the cyclic spectral density (CSD) function of the received signal $y(l)$ can be written as [71]:

$$S_y(\xi,\,\omega) = \sum_{\tau} R_y(\xi,\tau)\exp(-j\omega\tau)\,, \tag{2.19}$$

where $R_y(\alpha,\tau)$ is the cyclic autocorrelation (CAC) at cyclic frequency ξ:

$$R_y(\xi,\tau) = \lim_{L\to\infty}\frac{1}{L}\sum_{l=0}^{L-1} r_y(l,\tau)\exp(-j\xi l)\,. \tag{2.20}$$

Both CSD and CAC functions output peak values if ξ is the fundamental frequencies of the primary signal. Hence, the cyclostationarity based detection can be constructed both in the frequency domain and time domain.

Typically, cyclic frequencies are related to symbol rate, carrier frequency or modulation scheme used in the transmitted primary signal. They can be assumed to be known [20, 21], or they can be estimated and used for signal detection [66, 68]. Since different modulated signals exhibit different inherent patterns, cyclostationarity based detection methods have the ability to differentiate the primary signal from the noise and interference, and thus more robust. However, large data records are required to fully exploit the cyclostationarity and generally a high computational complexity is needed for implementation as the evaluation of CSD/CAC is two-dimensional.

Note that the uncertain noise variance problem has been considered in some feature based

Detector	REF	Assumptions	Closed form solutions for test threshold
MME	[13]	Oversampling data model or multiple receiving antennas	Analytical/Asymptotic solutions
Zhang and Taherpour	[15, 17]	Multiple receiving antennas	Analytical/Asymptotic solutions
Chaudhari	[18]	OFDM primary signal with known L_s and low SNR scenario	Asymptotic solutions
Larsson	[19]	OFDM primary signal with known L_s and L_c	No
Urriza	[20]	Multiple receiving antennas and known cycle frequencies	Asymptotic solutions
Huang	[21]	At least one known cycle frequency and one known time delay	Asymptotic solutions

Table 2.1: *Summary of sensing algorithms that are robust against uncertain noise power*

detectors. For example, in [18, 19], the second-order property of the CP-OFDM primary signal is used to construct the test statistic using the likelihood ratio criteria and the ML method is applied to estimate the unknown noise power under both hypothesis. Moreover, one can benefit from the spectral correlation if some knowledge of the signal's cyclic characteristics is known. Examples can be found in [20] and [21], where the eigenstructure of cyclic covariance matrix and large sample statistics of CAC functions were exploited, respectively.

Other Topics

We have reviewed some of state-of-the-art spectrum sensing techniques, assuming narrowband signals and single sensing device. There are also other topics, which are beyond the scope of this thesis but worth mentioning.

- **Wideband spectrum sensing**

By contrast to the narrowband detection methods mentioned above, wideband sensing techniques aim to sense a band of spectrum that exceeds the coherence bandwidth of the channel. A standard way to solve this problem is multi-band sensing, which divides the wide bandwidth into multiple sub-bands and jointly make decisions for efficient resource utilisations [11].

However, this method requires a high sampling rate analogue-to-digital converter (ADC) as the signal needs to be sampled at or above the Nyquist rate. Alternatively, the parallel structure filter-bank algorithm may be used to avoid the high sampling rate [72], at the expense of increasing cost of RF component. To cope with the aforementioned drawbacks, sub-Nyquist sensing would be another solution. This method argues that the existing of primary user is sparse in some domain, and therefore the signal can be acquired with a relatively few measurements, using a sampling rate that lower than the Nyquist rate [73]. Some relevant works are summarised in [74].

• **Cooperative spectrum sensing**

The basic idea of cooperative spectrum sensing is to exploit the spatial diversity by using multiple sensing devices, making a global decision based on the combined measurements. It can overcome some limitations of local spectrum sensing, i.e., poor detection probability caused by the multipath or shadowing fading, but has a high implementation complexity due to the use of multiple devices and the consequent communication overhead. In general, current works can be categorised into centralised and distributed sensing schemes, depending on different model used in the fusion centre. In centralised schemes, the fusion centre collects the observations from all the sensing devices directly [75]. Good detection performance can be obtained as the decision is based on the whole data, but a high communication overhead is required. An alternative way is distributed sensing, where the sensing devices only send their local informations, i.e., the test statistic or local decision, to the fusion centre, and a final decision is made by using counting rules [76, 77] or optimisation techniques [78, 79].

2.2.2 Spectrum Sensing for Non-Gaussian noise

As mentioned above, most of the conventional spectrum sensing techniques make assumption on Gaussian noise as it accords with the CLT and offers mathematical tractability. However, this model is not always valid as the noise found in practical wireless communications often shows a non-Gaussian heavy-tailed behaviour [80]. The reason is that in addition to the Gaussian distributed thermal noise, there exists artificial noise as well which is impulsive in nature [7, 81]. In the presence of non-Gaussian noise, the performance of standard detectors becomes unpredictable due to the uncertain null distribution of the test statistic. Hence, the robust spectrum sensing methods are required to address possible deviations of the noise distribution from a Gaussian model.

In the literature, several spectrum sensing methods have been proposed to deal with non-Gaussian noise. In general, the heavy-tailed noise is modelled to be a broad class of circularly symmetric distributions which include Gaussian distribution as a special case. Depending on the *prior* knowledge of noise, they fall into two categories: the detection with full or partial noise knowledge [29, 31, 82] and the detection with unknown noise knowledge [32–35]. In this section, they will be briefly reviewed and a simple summary of these detection algorithms is given in Table 2.2.

Detection with full or partial noise knowledge

If the knowledge of non-Gaussian noise is fully or partially known by the cognitive radio user, detectors can be designed according the specified noise models.

• The authors in [29] considered α-stable distributed noise. The α-stable distribution, where the characteristic α is used to control the level of heaviness, is circularly symmetric but only has finite moments of order less than α. By assuming an M antenna assisted sensing device, the detection is based on the *covariation*[1] coefficient absolute value (CCAV) and exploits the structure of covariation matrix that the off-diagonal elements are zero under $\mathcal{H}_0$ and have non-zero value under $\mathcal{H}_1$. More precisely, let $\hat{\rho}_{\alpha,p}(i,j)$, $i,j = 1,2,...,M$, $1 < p < \alpha$, be the estimate of the covariation coefficient. The test is given by:

$$T(p) = \frac{\sum_{i=1}^{M}\sum_{j=1}^{M}\left|\hat{\rho}_{\alpha,p}(i,j)\right|}{\sum_{i=1}^{M}\left|\hat{\rho}_{\alpha,p}(i,i)\right|} \underset{\mathcal{H}_0}{\overset{\mathcal{H}_1}{\gtrless}} \gamma(p). \tag{2.21}$$

Ideally, $T(p)$ is around 1 when $\mathcal{H}_0$ holds and larger than 1 if the primary signal exists. In addition, the value of $T(p)$ also depends on p, which is picked by Monte Carol trails so that the root mean error of $\hat{\rho}_{\alpha,p}(i,j)$ is minimised. Since the choice of p and the null distribution of $T(p)$ depends on many mathematically intractable terms, the test threshold $\gamma(p)$ cannot be analytically expressed.

• Moreover, the authors in [82] considered the case of partially known noise knowledge. That is, the exact noise distribution is unknown, but its statistical moments are available. Based on

[1]Covariation, which is analogous to covariance, desirables the statistical property of a process that does not exist finite second order statistics. For the definition and more details, see [29].

Detector	REF	Assumptions	Closed form solutions for test threshold
LO	[31]	Noise distribution is known	No
CCAV	[29]	α-stable distributed noise	No
L_p-norm	[82]	The channel and noise statistics are known	No
Robust LO	[31]	$\epsilon-$contaminated noise model	No
Cyclic correlation	[33]	Cyclic frequency is known	Asymptotic solutions
PCA	[34]	Real-valued data	Analytical solutions
KS	[32]	Training noise samples	Analytical solutions
t-sensing	[35]	Training noise samples and non-zero mean primary signal	Asymptotic solutions

Table 2.2: *Summary of sensing algorithms for Non-Gaussian noise*

this, a L_p-norm detector was proposed by invoking assumption on low SNR. This work is originated from the LR detection, and the result is simplified by using a tunable parameter p to adapt to the underlying noise distribution. The decision statistic is given by:

$$T = \frac{1}{L}\sigma_h^2 \sum_l |y(l)|^p , \tag{2.22}$$

where σ_h^2 denotes the power of channel coefficient h, i.e., h is assumed to a random variate in this work, and p is obtained by solving an optimisation problem. Note that the L_p-norm detector does not need *prior* knowledge about the primary signal, but the statistical moments of the fading channel and the additive noise are required to be known.

• In addition, a locally optimal (LO) detector in NP sense was proposed in [31] for wideband sensing. The detector assumes arbitrary noise types, but the noise distribution must be known. The test statistic of the LO detector, expressed in frequency domain, is fundamentally a spectral estimation function that correlates the periodogram of observations with the known or estimated primary signal spectrum. The test statistic is complicated so that there does not exist closed form solutions for the test threshold.

Detection with unknown noise knowledge

By contrast to the aforementioned parametric approaches that depend on the known noise knowledge, some works have considered the case where the noise type is unknown, and only minimal assumptions are made on the noise distribution.

• A feature based detector was proposed in [33]. This detector uses a cyclic correlation estimator as the test statistic, requiring at least one cyclic frequency of the primary signal to be known. To make the detector quantitatively robust, the cyclic correlation estimator is based on the spatial sign function, which is defined in sense of complex-valued data:

$$S\left(y\left(l\right)\right)=\begin{cases}\frac{y(l)}{|y(l)|} & y\left(l\right)\neq 0\\ 0 & y\left(l\right)=0\end{cases} \tag{2.23}$$

Then given a cyclic frequency ξ and a set of time delays, $\tau_1, \tau_2, ..., \tau_N$, the decision rule is given by:

$$T=\sum_{i=1}^{N}\left|\hat{R}_s\left(\xi,\tau_i\right)\right|^2 \underset{\mathcal{H}_0}{\overset{\mathcal{H}_1}{\gtrless}} \gamma, \tag{2.24}$$

where

$$\hat{R}_s\left(\xi,\tau_i\right)=L\sum_{l=0}^{L-1}S\left(y\left(l\right)\right)S\left(y\left(l+\tau_i\right)^*\right)\exp\left(-j\xi l\right) \tag{2.25}$$

is the estimate of the sign cyclic correlation. The advantages of (2.24) are that only circularly symmetric process is made on the noise PDF, and the asymptotic null distribution of the test statistic has been derived. However, this detector is not fully nonparametric as it exploits the cyclostationarity so that at least one cyclic frequency of the primary signal is required to be known.

• In [32], a Kolmogorov-Smirnov (KS) test was proposed for nonparametric signal detection, which requires a sequence of noise samples for reference purposes. This test is a goodness-of-fit test that quantifies the distance between the empirical cumulative distribution function (CDF) of the observations and the CDF of the reference samples. For example, let $\hat{W}_{|w|}$ be the empirical CDF of the noise magnitude, and $\hat{W}_{|y|}$ be the empirical CDF of the observation magnitude. The test uses the largest absolute distance between the two CDFs as the goodness-of-fit statistic:

$$T=\max_{z}\left|\hat{W}_{|y|}\left(z\right)-\hat{W}_{|w|}\left(z\right)\right| \underset{\mathcal{H}_0}{\overset{\mathcal{H}_1}{\gtrless}} \gamma. \tag{2.26}$$

Equation (2.26) has an explanation that we will reject $\mathcal{H}_0$ when the deviation between the underlying distribution of the observations and the reference is larger than a given threshold. This test is easy to implement as no knowledge of the primary signal and the noise characteristic is required, and there exists numerical tables for computing the test threshold. In addition, the reference noise only samples are also achievable, i.e., they can be collected when the primary user is known for sure to be absent.

• Again, by assuming a sequence of noise samples is available, a asymptotically robust t-sensing was proposed in [35] to detect the non-zero mean primary signal. Initially derived in Gaussian, this detector is fundamentally a test of whether the mean of collected samples is equal to the mean of reference noise samples. Since the test statistic is asymptotically Gaussian, the t-sensing is asymptotically nonparametric and can be applied to non-Gaussian noise when the sample size is sufficiently large.

• A different path was considered in [34]. By considering a multiple antenna equipped receiver, a nonparametric polarity-coincidence-array (PCA) based detector was proposed, requiring no knowledge on the primary signal and noise characteristics. However, the detector is derived and discussed for real-valued measurements.

• In addition, a robust LO detector was also proposed in [31] by assuming the noise consists of $100\,(1-\epsilon)\%$ Gaussian and $100\epsilon\%$ unknown non-Gaussian parts. In this case, the initial spectral estimator is invalid and the authors propose a robust method by formulating a non-linear cost function that minimises the impact brought by the unknown non-Gaussian distributions. Results in [31] show that the robust approach performs slightly worse than the LO NP detector, but is nonparametric at the cost of increasing computational complexity.

As summarised in Table 2.2, most of the aforementioned detection methods are parametric or make assumptions on a specific signal type. Another concern is the selection of a test threshold is generally difficult as the test statistic's null distribution may be complicated and unknown in non-Gaussian noise.

2.3 Conclusion

In this section, we presented a literature review of the state-of-the-art spectrum sensing techniques, providing a background knowledge for the rest of the thesis. In particular, related

works for noise robust sensing algorithms have been highlighted and summarised in Table 2.1 and Table 2.2. In Chapter 3, we shall propose a novel F-test based detector to cope with the sensing problem in noise variance uncertainty. Under a Gaussian noise assumption, this detector is equivalent to the maximal likelihood ratio test. Then in Chapter 4 and Chapter 5, several robust sensing methods for non-Gaussian noise will be developed and the nonparametric bootstrap technique will be applied to avoid making assumptions on large samples or reproducible experiment conditions.

Chapter 3
F-test Based Spectrum Sensing

3.1 Introduction

The energy detector [8] is the most widely used sensing scheme due to its good detection performance and low implementation complexity. However, it requires accurate knowledge of noise power and even a mild noise variance uncertainty will lead to fundamental limit on its detection performance [12, 59]. As illustrated in Figure 3.6, in the presence of noise variance mismatch, the high false alarm probability and significant performance loss in detection probability will make the energy detector invalid.

To cope with this problem, most current research focuses on *blind* sensing schemes, which refer to the detection without knowing any knowledge of the transmitted primary signal, the channel coefficient and the power of the additive noise. They commonly assume a receiver antenna array so that the eigenstructure of the sample covariance matrix behaves differently under the null hypothesis and the alternative hypothesis. For example, a MME detection was proposed in [13], which assumes that when primary signal exists, the ratio of maximum eigenvalue to minimum eigenvalue will be relatively larger than for the noise only case. Another method is to construct the test statistic using likelihood ratio principle [56]. Given a specified data model, one uses the maximal likelihood to estimate all the unknowns which yields the well-known GLRT based detector [15–17]. As discussed in Chapter 2, the test statistics for those detectors are all functions of eigenvalues and the corresponding test thresholds may have to be evaluated empirically, as the closed form analytical solutions are generally difficult to obtain and the asymptotic results invoke assumptions on large data records and large array size. In addition, they are subject to limited test performance.

On the other hand, signal features can be considered in the design of detection criterion if the primary signal has some known statistical properties. For example, the detectors derived in [18, 19] exploit the non-stationary property of CP-OFDM signal without knowing the knowledge of noise power. In addition, many man-made signal give rise to a cyclostationarity property that can be utilised, requiring *prior* knowledge or accurate estimate of cyclic frequencies. The

examples of noise robust detectors using this property can be found in [20] and [21], where the eigenstructure of the cyclic covariance matrix and large sample statistics of the CAC functions are exploited, respectively. Compared with the *blind* detectors, the feature based detection methods offer a better detection performance by exploiting the inherent structure of primary signal. The cost is that they can only be applied to a specified signal type and generally high computational complexity is required for implementation.

In summary, most current detectors are sensitive to noise variance uncertainty or subject to limited test performance and high computational complexity. In this chapter, a novel multiple antenna assisted F-test based sensing technique is developed, which offers absolute robustness against noise variance uncertainty and is relatively easy to implement. It requires the CSI as *prior* knowledge, which may be imperfect due to the lack of reciprocal communication standard between the primary and secondary systems. Hence, the impact of channel uncertainty also needs to be addressed. The main contributions of this chapter are summarised as follows:

• An F-test based detection scheme is proposed. By taking the CSI as *prior* knowledge, the F-statistic is derived using likelihood ratio principle with all the unknowns estimated via ML method. It is insensitive to the noise variance uncertainty as no information of noise power is required.

• The test statistic follows an F-distribution under the null hypothesis and a noncentral F-distribution under the alternative hypothesis. Given a target false alarm probability, the exact value of test threshold and probability of detection are derived based on the statistical properties of F-distribution.

• The impact of channel uncertainty is investigated. Results show that the F-test based detector has constant false alarm probability, independent of the accuracy of channel estimation. The detection probability under imperfect CSI can be calculated using the doubly noncentral F-distribution. To avoid computational complexity, a simple approximated value for the detection probability is also presented.

• Simulation results show that the proposed F-test based detector achieves a significant performance improvement compared with the energy detector. In addition, it offers robustness against noise uncertainty and suffers a mild performance loss under imperfect CSI.

The remainder of this chapter is structured as follows. The signal model for multiple antenna

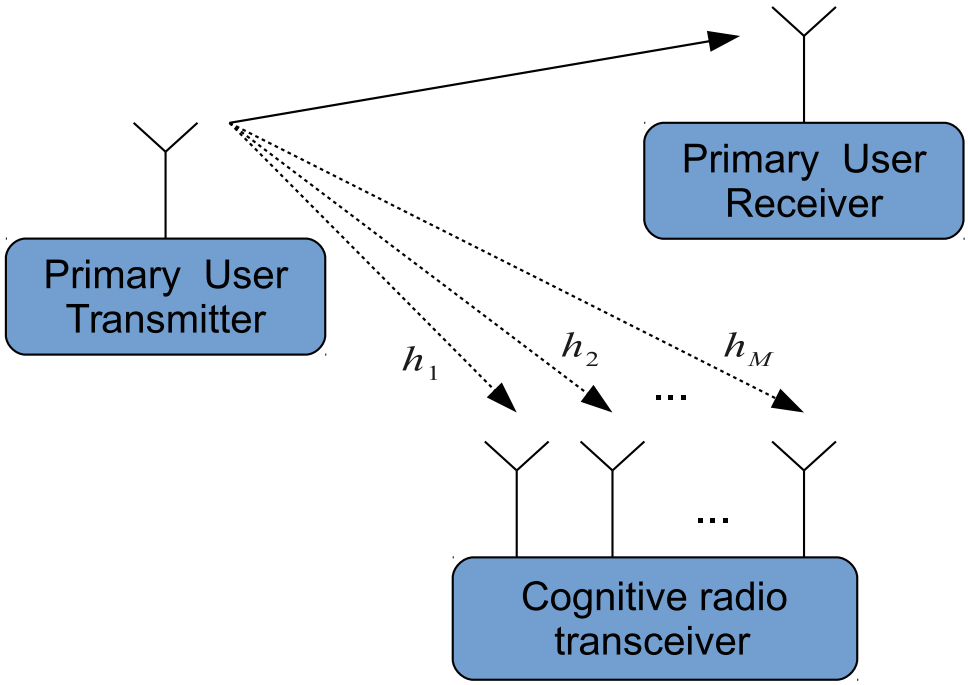

Figure 3.1: *SIMO network used for spectrum sensing.*

assisted spectrum sensing is described in Section 3.2. Section 3.3 introduces and derives the F-test. In Section 3.4, the F-test based detector is proposed, and its test threshold and detection probability are derived, respectively. Then the impact of CSI estimation error is discussed in Section 3.5. Simulation results are presented in Section 3.6. Finally, Section 3.7 concludes this chapter.

3.2 System Model

Consider a single-input multiple-output (SIMO) network as shown in Figure 3.1, where there is only one primary user and the cognitive radio transceiver is equipped with M antennas to sense the surrounding radio environment [1]. Note that the multiple receiver system is applied as it is less sensitive to multipath fading effects on the primary-secondary user channel and the F-test based detector can be applied to such system.

In spectrum sensing, we aim at finding the idle spectrum band unoccupied by the primary user within the range of secondary users. As discussed in Section 2.2, Chapter 2, the detection of

[1]The F-test can be easily extended to the case of multiple signal sources. In this work, SIMO network is applied for simplicity. In addition, spectrum sensing schemes are generally considered and designed for one primary signal.

primary user can be formulated as a hypothesis testing problem: the null hypothesis $\mathcal{H}_0$ implies that the primary user is not active; and the alternative $\mathcal{H}_1$ implies that the primary user is active. Let $\mathbf{y}(l) = [y_1(l), y_2(l), \ldots, y_M(l)]^T$, $(l = 0, 1, \ldots, L-1)$, denote the size M baseband signal vectors at the receiver antenna array with L denoting the sample size. Then the spectrum sensing problem can be expressed as the following hypothesis test:

$$\begin{aligned} \mathcal{H}_0 &: \mathbf{y}(l) = \mathbf{w}(l), \\ \mathcal{H}_1 &: \mathbf{y}(l) = \mathbf{h}s(l) + \mathbf{w}(l),\ l = 0, 1, ..., L-1, \end{aligned} \tag{3.1}$$

where $s(l)$ denotes the transmitted primary signal symbol at time instant l, which is assumed to be unknown and deterministic. The fading channel between the primary user to cognitive radio transceiver is represented by the known CSI vector $\mathbf{h} = [h_1, h_2, \ldots, h_M]^T$. We assume that $\mathbf{h}$ stays constant during the sensing period. The noise vector $\mathbf{w}(l) = [w_1(l), w_2(l), \ldots, w_M(l)]^T$ is characterised by an i.i.d complex Gaussian variate with zero-mean and covariance matrix $\sigma_w^2\mathbf{I}$, i.e., $\mathbf{w}(l) \sim \mathcal{CN}(\mathbf{0}, \sigma_w^2\mathbf{I})$, where σ_w^2 is unknown.

Since there is no existing reciprocal communication standard between primary and secondary systems, the problem of estimating the CSI $\mathbf{h}$ is still an open question. One solution to this problem was suggested in [10, 11, 83, 84]: the knowledge of CSI is acquired from the periodically transmitted pilot when the primary transmitter is active. Moreover, the authors in [84–86] developed joint estimation based sensing schemes in which the fading channel can be recursively estimated for improved sensing performance. The impact of CSI estimation mismatch will be discussed later in Section 3.5.

3.3 Preliminaries of F-test

The F-distribution is formed by the ratio of two independent chi-square variates [87], with each one divided by its degrees of freedom. Since it arises from chi-square, the F-distribution is characterised by positive values and non-symmetric distribution. The F-test is a statistical test in which the test statistic follows an F-distribution under the null hypothesis [88]. It is designed to find out whether the two population variances are equal using the ratio of two sample variances as the test statistic. So, if the null hypothesis is true, the test statistic should be near 1. We shall reject the null hypothesis when the ratio of variances is large enough to exceed a given threshold.

The F-test acts as an efficient tool for the hypothesis testing problems in regression analysis. Under a Gaussian error/noise assumption, it is equivalent to the maximal likelihood ratio test [88] and is thus optimal in the Neyman-Pearson sense [56]. In the following, we shall develop the F-test using the likelihood ratio principle.

Based on the signal model (3.1), the distribution of received data $\mathbf{y}(l)$ can be written in case by:

$$\begin{aligned} \mathcal{H}_0 &: \mathbf{y}(l) \sim \mathcal{CN}\left(0, \sigma_w^2 \mathbf{I}\right), \\ \mathcal{H}_1 &: \mathbf{y}(l) \sim \mathcal{CN}\left(\mathbf{h}s(l), \sigma_w^2 \mathbf{I}\right). \end{aligned} \tag{3.2}$$

Define $\mathbf{Y} \triangleq [\mathbf{y}(0), \mathbf{y}(1), \ldots, \mathbf{y}(L-1)]$ be the sample set. We apply the likelihood ratio principle to construct the test statistic:

$$T_{LR} = \max_{s(l), \sigma_w^2} \mathscr{L}\left(\mathbf{Y} \left| \mathcal{H}_1, s(l), \sigma_w^2 \right.\right) - \max_{\sigma_w^2} \mathscr{L}\left(\mathbf{Y} \left| \mathcal{H}_0, \sigma_w^2 \right.\right), \tag{3.3}$$

where

$$\mathscr{L}\left(\mathbf{Y} \left| \mathcal{H}_0, \sigma_w^2 \right.\right) = -ML \ln\left(\pi \sigma_w^2\right) - \frac{1}{\sigma_w^2} \sum_{l=0}^{L-1} \|\mathbf{y}(l)\|^2, \tag{3.4}$$

$$\mathscr{L}\left(\mathbf{Y} \left| \mathcal{H}_1, s(l), \sigma_w^2 \right.\right) = -ML \ln\left(\pi \sigma_w^2\right) - \frac{1}{\sigma_w^2} \sum_{l=0}^{L-1} \|\mathbf{y}(l) - \mathbf{h}s(l)\|^2, \tag{3.5}$$

are the concentrated log-likelihood functions under $\mathcal{H}_1$ and $\mathcal{H}_0$, respectively. $\|\cdot\|$ denotes the Euclidean norm of a vector.

By taking derivative of $\mathscr{L}\left(\mathbf{Y} \left| \mathcal{H}_0, \sigma_w^2 \right.\right)$ with respect to σ_w^2, we obtain the maximal likelihood estimate (MLE) of σ_w^2 under the null hypothesis $\mathcal{H}_0$:

$$\hat{\sigma}_{w,\mathcal{H}_0}^2 = \frac{1}{ML} \sum_{l=0}^{L-1} \|\mathbf{y}(l)\|^2. \tag{3.6}$$

Similarly, we obtain the MLE of $s(l)$ and σ_w^2 under $\mathcal{H}_1$:

$$\hat{s}(l) = \mathbf{h}^\dagger \mathbf{y}(l), \tag{3.7}$$

$$\hat{\sigma}_{w,\mathcal{H}_1}^2 = \frac{1}{ML} \sum_{l=0}^{L-1} \mathbf{y}(l)^H (\mathbf{I} - \mathbf{P}) \mathbf{y}(l), \tag{3.8}$$

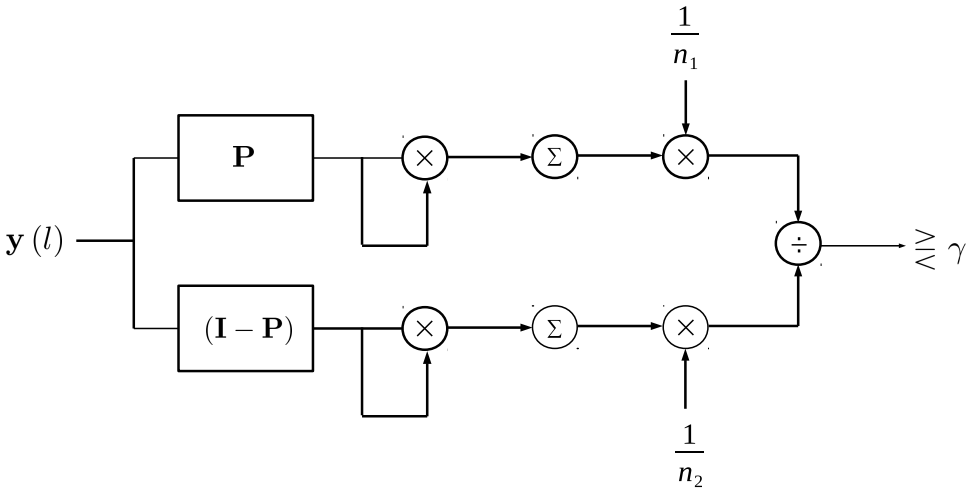

Figure 3.2: *Block diagram of the F-test with degrees of freedom n_1 and n_2 [56].*

where $\mathbf{h}^{\dagger} \triangleq \left(\mathbf{h}^H\mathbf{h}\right)^{-1}\mathbf{h}^H$ denotes the pseudo-inverse of $\mathbf{h}$ and $\mathbf{P} = \mathbf{h}(\mathbf{h}^H\mathbf{h})^{-1}\mathbf{h}^H$ represents the projection onto the subspace spanned by $\mathbf{h}$. Note that the solution to (3.5) is evaluated separately, where we maximise over $s(l)$ to obtain a function of σ_w^2 first and then maximise over σ_w^2 to get the whole solution.

Substituting the ML estimates, eqs. (3.6-3.8), in (3.4) and (3.5) leads to the following closed form optimisations:

$$\mathscr{L}\left(\mathbf{Y}\,|\mathcal{H}_0, \hat{\sigma}_w^2\right) = -\ln\left(\text{tr}\left[\hat{\mathbf{R}}_y\right]\right), \tag{3.9}$$

$$\mathscr{L}\left(\mathbf{Y}\,|\mathcal{H}_1, \hat{s}(l), \hat{\sigma}_w^2\right) = -\ln\left(\text{tr}\left[\left(\mathbf{I}-\mathbf{P}\right)\hat{\mathbf{R}}_y\right]\right). \tag{3.10}$$

Here $\hat{\mathbf{R}}_y = \frac{1}{L}\sum_{l=0}^{L-1}\mathbf{y}(l)\mathbf{y}(l)^H$ denotes the sample covariance matrix and tr $[\cdot]$ represents the trace operator which is defined to be the sum of the diagonal elements of a matrix. Subtracting (3.9) from (3.10) leads to the following maximal likelihood ratio test statistic:

$$\begin{aligned} T_{LR} &= \ln\left(1 + \frac{\text{tr}\left[\mathbf{P}\hat{\mathbf{R}}_y\right]}{\text{tr}\left[\left(\mathbf{I}-\mathbf{P}\right)\hat{\mathbf{R}}_y\right]}\right) \\ &= \ln(1 + \frac{n_1}{n_2}T_F), \end{aligned} \tag{3.11}$$

where T_F is the statistic given by:

$$\begin{aligned} T_F &= \frac{n_2}{n_1}\left(\frac{\hat{\sigma}^2_{w,\mathcal{H}_0}}{\hat{\sigma}^2_{w,\mathcal{H}_1}} - 1\right) \\ &= \frac{n_2}{n_1}\frac{\text{tr}\left[\mathbf{P}\hat{\mathbf{R}}_y\right]}{\text{tr}\left[(\mathbf{I}-\mathbf{P})\,\hat{\mathbf{R}}_y\right]} \end{aligned} \tag{3.12}$$

with degrees of freedom:

$$n_1 = 2L, \tag{3.13}$$

$$n_2 = 2L(M-1). \tag{3.14}$$

As shown in the block diagram of F-test in Figure 3.2, the statistic T_F, also known as the F-statistic, measures the ratio of the energy of $\mathbf{Y}$ that projects onto the subspace relates to the primary signal, $\mathbf{P}$, to the energy of $\mathbf{Y}$ that projects onto the orthogonal subspace, $(\mathbf{I}-\mathbf{P})$. When the null hypothesis holds, tr $\left[\mathbf{P}\hat{\mathbf{R}}_y\right]$ and tr $\left[(\mathbf{I}-\mathbf{P})\,\hat{\mathbf{R}}_y\right]$ are two independent chi-square distributed variates, and the statistic T_F follows an F_{n_1,n_2}-distribution with degrees of freedom n_1 and n_2 given in eqs. (3.13) and (3.14) [87].

Given a target significance value, known as the false alarm probability in spectrum sensing, the F-test then reject $\mathcal{H}_0$ when T_F exceeds a pre-determined threshold γ. Finally note that the monotonicity of the logarithm function in (3.11) ensures the equivalence between the maximal likelihood ratio test and the F-test.

3.4 F-test Based Detector

Recall the regression data model (3.1). Given the observation $\mathbf{Y}$ and CSI vector **h**, we apply the F-test to detect the existence of primary signal. As discussed above, the decision rule is given by:

$$T_F = \frac{n_2}{n_1}\frac{\text{tr}\left[\mathbf{P}\hat{\mathbf{R}}_y\right]}{\text{tr}\left[(\mathbf{I}-\mathbf{P})\,\hat{\mathbf{R}}_y\right]} \underset{\mathcal{H}_0}{\overset{\mathcal{H}_1}{\gtrless}} \gamma, \tag{3.15}$$

where the test threshold γ is selected to ensure a target probability of false alarm. Note that T_F can be seen as an estimate of the increased SNR induced by the primary signal [89]. Therefore, the decision rule (3.15) has an interpretation that we will accept the alternative hypothesis $\mathcal{H}_1$,

or declare the existence of primary signal, when the SNR estimate is large enough to exceed a given threshold γ.

When the null hypothesis $\mathcal{H}_0$ holds, the test statistic T_F is F_{n_1,n_2}-distributed, i.e., $T_F \sim F_{n_1,n_2}$. Let $W_{c,n1,n2}(x)$ be the CDF of the F-distribution with degrees of freedom n_1 and n_2, which is given by [87]:

$$W_{c,n1,n2}(x) = I_k\left(\frac{1}{2}n_1, \frac{1}{2}n_2\right), \tag{3.16}$$

where $k = n_1 x / (n_2 + n_1 x)$ and

$$I_k(\frac{1}{2}n_1, \frac{1}{2}n_2) = \frac{\int_0^k t^{\frac{1}{2}n_1-1}(1-t)^{\frac{1}{2}n_2-1}dt}{\int_0^1 t^{\frac{1}{2}n_1-1}(1-t)^{\frac{1}{2}n_2-1}dt} \tag{3.17}$$

is the regularised beta function.

Then given a target false alarm probability α, we can obtain the test threshold through the following relation:

$$\begin{aligned} \alpha &= \Pr\left(T_F \geq \gamma \,|\mathcal{H}_0\right) \\ &= 1 - W_{c,n1,n2}(\gamma). \end{aligned} \tag{3.18}$$

There are several tables of $W_{c,n1,n2}(x)$ and each one corresponds to a different significance value α. Hence, the test threshold γ can be easily obtained.

When the primary user is active, or $\mathcal{H}_1$ holds, the test statistic T_F is noncentral F-distributed [87], i.e., $T_F\left(\mathcal{H}_1\right) \sim F'_{n_1,n_2}(\delta^2)$. The noncentrality parameter δ^2 is given by:

$$\delta^2 = \frac{2\sum_{l=0}^{L-1} \|\mathbf{h}s(l)\|^2}{\sigma_w^2}. \tag{3.19}$$

The probability of detection is:

$$\begin{aligned} P_d &= \Pr(T_F > \gamma|\mathcal{H}_1) \\ &= 1 - W_{nc,n1,n2}. \end{aligned} \tag{3.20}$$

where $W_{nc,n1,n2}\left(x \mid \delta^2\right)$ denotes the CDF of the noncentral F-distribution. It is given by [87]:

$$W_{nc,n1,n2}\left(x \mid \delta^2\right) = \sum_{i=0}^{\infty} \varpi_{i,\delta^2} I_k\left(\frac{1}{2}n_1 + i, \frac{1}{2}n_2\right), \tag{3.21}$$

where

$$\varpi_{i,\delta^2} = \exp\left(-\delta^2/2\right) \frac{\left(\delta^2/2\right)^i}{i!}. \tag{3.22}$$

It is shown that P_d is an increasing function of the noncentrality parameter δ^2 [87]. From (3.19), we can conclude that a higher probability of detection can be obtained by increasing the sample size L.

It is worth mentioning that an harmonic-F test based method for spectrum sensing was discussed in [22], which is based on multitaper method to estimate the spectrum and the linear model for setting F-test is in the frequency domain. In order to reduce the variance of spectrum estimate, the data is firstly windowed by a set of orthogonal eigentapers. Then given the eigenspectra estimations and eigencoefficients (the discrete fourier transform of eigentapers), an F test is set up to test whether a colored component (primary signal) exists or not over a bandwidth [90]. It can be seen as a nonparametric wideband sensing and large sample size is required to achieve reasonable performance, i.e., 2200 samples is used in [22]. The proposed F-test based detector in this chapter, however, is based on a totally different signal model. It assumes a multiple antenna scenario and CSI is needed to construct the F-test. Moreover, to achieve reasonable performance, the required sample size is much smaller.

3.5 Impact of Imperfect CSI

Channel information $\mathbf{h}$ is needed for constructing the F-test based method in (3.15). As mentioned above, it could be acquired from the periodically transmitted pilot or be jointly estimated and updated during the sensing period. However, as shown in the data model (3.1), the fading channel $\mathbf{h}$ is not be always embedded in the observations. Particularly, the received data is noise only when $\mathcal{H}_0$ holds. Hence, due to the delayed update coupled with the estimation or quantisation errors, one only has access to the imperfect CSI, $\hat{\mathbf{h}} \in \mathbb{C}^{M\times 1}$, which can be modelled as follows:

$$\hat{\mathbf{h}} = \mathbf{h} + \triangle\mathbf{h}, \tag{3.23}$$

where $\triangle\mathbf{h} = [\triangle h_1, \triangle h_2, \ldots, \triangle h_M]^T$ denotes the uncertain term. Such uncertainty may degrade the performance of the proposed detector. In this section, the impact of channel uncertainty will be discussed.

Test threshold and false alarm probability

The selection of test threshold depends on the target false alarm probability, which is related to the null hypothesis $\mathcal{H}_0$. In this case, the received data only consists of noise so that the channel estimate may have a significant deviation from its true value.

Note that $\hat{\mathbf{h}}$ is a fixed parameter during a sensing period. Combining (3.15) and (3.12), the test statistic under channel uncertainty can be expressed as:

$$\begin{aligned} T_F\left(\hat{\mathbf{h}}|\mathcal{H}_0\right) &= \frac{n_2}{n_1}\frac{\mathrm{tr}\left[\hat{\mathbf{P}}\hat{\mathbf{R}}_y\right]}{\mathrm{tr}\left[\left(\mathbf{I}-\hat{\mathbf{P}}\right)\hat{\mathbf{R}}_y\right]} \\ &= \frac{n_2}{n_1}\frac{\sum_{l=0}^{L-1}\mathbf{w}\left(l\right)^H\hat{\mathbf{P}}\mathbf{w}\left(l\right)}{\sum_{l=0}^{L-1}\mathbf{w}\left(l\right)^H\left(\mathbf{I}-\hat{\mathbf{P}}\right)\mathbf{w}\left(l\right)}, \end{aligned} \tag{3.24}$$

where $\hat{\mathbf{P}} = \hat{\mathbf{h}}\left(\hat{\mathbf{h}}^H\hat{\mathbf{h}}\right)^{-1}\hat{\mathbf{h}}^H$ denotes the projection matrix onto the space spanned by the channel estimate $\hat{\mathbf{h}}$.

Since the noise $\{\mathbf{w}(l); l = 0, 1, \ldots, L-1\}$ is complex Gaussian distributed, the test statistic $T_F\left(\hat{\mathbf{h}}|\mathcal{H}_0\right)$ is F_{n_1,n_2}-distributed under the null hypothesis, with degrees of freedom n_1 and n_2 given by eqs. (3.13) and (3.14). Note that the characteristics of the F-distribution only relate to the degrees of freedom [87]. As there is no change in the null distribution of T_F as well as its corresponding degrees of freedom, the pre-computed threshold γ will still be effective to ensure the target false alarm probability as:

$$\begin{aligned} P_f &= \Pr\left(T_F\left(\hat{\mathbf{h}}\right) > \gamma|\mathcal{H}_0\right) \\ &= 1 - W_{c,n1,n2}\left(\gamma\right) \\ &= \alpha. \end{aligned} \tag{3.25}$$

In other words, the F-test based detector has constant false alarm probability, independent of the accuracy of channel estimation.

Detection probability

When the alternative hypothesis $\mathcal{H}_1$ holds, the received data consists of both signal and noise, implying that the observations will depend on the channel $\mathbf{h}$ and so does the detection probability. Based on eqs. (3.15) and (3.12), when the primary signal exists, the test statistic can be written as:

$$T_F\left(\hat{\mathbf{h}}|\mathcal{H}_1\right) = \frac{n_2}{n_1}\frac{\sum\limits_{l=0}^{L-1}\left(\mathbf{h}s\left(l\right)+\mathbf{w}\left(l\right)\right)^H\hat{\mathbf{P}}\left(\mathbf{h}s\left(l\right)+\mathbf{w}\left(l\right)\right)}{\sum\limits_{l=0}^{L-1}\left(\mathbf{h}s\left(l\right)+\mathbf{w}\left(l\right)\right)^H\left(\mathbf{I}-\hat{\mathbf{P}}\right)\left(\mathbf{h}s\left(l\right)+\mathbf{w}\left(l\right)\right)}, \tag{3.26}$$

which is doubly noncentral F-distribution (DNF) distributed, i.e., $T_F\left(\hat{\mathbf{h}}|\mathcal{H}_1\right) \sim F''_{n_1,n_2}\left(\delta_1^2,\delta_2^2\right)$ [87], with the noncentrality parameters:

$$\delta_1^2 = \frac{2}{\sigma_w^2}\sum_{l=0}^{L-1}\left\|\hat{\mathbf{P}}\mathbf{h}s(l)\right\|^2, \tag{3.27}$$

$$\delta_2^2 = \frac{2}{\sigma_w^2}\sum_{l=0}^{L-1}\left\|\left(\mathbf{I}-\hat{\mathbf{P}}\right)\mathbf{h}s\left(l\right)\right\|^2. \tag{3.28}$$

The corresponding detection probability can be obtained as:

$$\begin{aligned} P_d &= \Pr\left(T_F\left(\hat{\mathbf{h}}\right) > \gamma|\mathcal{H}_1\right) \\ &= 1 - W_{dnc,n_1,n_2}\left(\gamma|\delta_1^2,\delta_2^2\right), \end{aligned} \tag{3.29}$$

where $W_{dnc,n_1,n_2}\left(x \mid \delta_1^2,\delta_2^2\right)$ denotes the CDF of DNF distribution, which is given by:

$$W_{dnc,n1,n2}\left(x \mid \delta_1^2,\delta_2^2\right) = \sum_{i_2=0}^{\infty}\varpi_{i_2,\delta_2^2}\sum_{i_1=0}^{\infty}\varpi_{i_1,\delta_1^2}I_k\left(\frac{1}{2}n_1+i_1,\frac{1}{2}n_2+i_2\right). \tag{3.30}$$

For the definitions of ϖ_{i,δ^2} (ϖ_{i_1,δ^2} and ϖ_{i_2,δ^2}) and $I_k\left(\cdot\right)$, see in eqs. (3.22) and (3.17), respectively. It can be expected that the detection probability will be maximised when the perfect channel information is available, as shown in the following result.

Lemma 3.1. Given a test threshold γ, the detection probability of F-test based detector is maximised when $\hat{\mathbf{h}} = \mathbf{h}$.

Proof. Combining (3.27) and (3.28), and applying the property of the projection matrix $\hat{\mathbf{P}}$, we

have:

$$\begin{aligned}\delta_1^2+\delta_2^2 &= \frac{2}{\sigma_w^2}\left\{\sum_{l=0}^{L-1}\left\|\hat{\mathbf{P}}\mathbf{h}s(l)\right\|^2+\sum_{l=0}^{L-1}\left\|(\mathbf{I}-\hat{\mathbf{P}})\mathbf{h}s(l)\right\|^2\right\}\\ &= \frac{2}{\sigma_w^2}\sum_{l=0}^{L-1}\left\|\mathbf{h}s(l)\right\|^2. \end{aligned} \tag{3.31}$$

It has been shown that the probability of detection P_d given in (3.29) will rise when δ_1^2 increases or δ_2^2 decreases [91]. Since $\delta_1^2+\delta_2^2$ is constant and $\delta_2^2 \geqslant 0$, P_d will be maximised when

$$\delta_1^2 = \frac{2}{\sigma_w^2}\sum_{l=0}^{L-1}\left\|\mathbf{h}s(l)\right\|^2, \tag{3.32}$$

$$\delta_2^2 = 0. \tag{3.33}$$

Both the equalities hold when and only when $\hat{\mathbf{P}}$ is the projection onto the space spanned by $\mathbf{h}$, which implies that given γ, the detection probability of the F-test based detector, eq. (3.29), will reach its maximal at $\hat{\mathbf{h}}=\mathbf{h}$. □

From *lemma* 1, we conclude that the detection performance of the F-test based approach under perfect CSI offers a benchmark for comparison.

As shown in 3.30, the CDF of DNF distribution consists of doubly infinite sum of incomplete beta functions and thus is difficult to evaluate. Here, in order to simplify the computation, we apply a simple approach derived from the approximations to noncentral chi-squared distributions [87]. The approximation of the DNF distribution is given by:

$$\frac{1+\delta_1^2 n_1^{-1}}{1+\delta_2^2 n_2^{-1}}F_{v_1,v_2}, \tag{3.34}$$

with degrees of freedom:

$$v_1 = \left(n_1+\delta_1^2\right)^2\left(n_1+2\delta_1^2\right)^{-1}, \tag{3.35}$$

$$v_2 = \left(n_2+\delta_2^2\right)^2\left(n_2+2\delta_2^2\right)^{-1}. \tag{3.36}$$

Therefore, we can utilise the table of central F-distribution to calculate the approximated de-

Detector	Legend	Assumptions	Sensing Complexity
F-test based detector eq. (3.15)	F-test	Multiple receiving antennas CSI is known	$O\left(M^2L\right)$
Energy detector [8]	EG	Noise power σ_w^2 is known	$O\left(ML\right)$
GLRT based detector [15]	GLRT	Multiple receiving antennas	$O\left(M^3LN\right)$

Table 3.1: *Summary of the simulated detection algorithms. M: number of receiving antennas. L: sample size. N: Number of Monte carol trails.*

tection probability under channel uncertainty, that is:

$$P_d \approx 1 - W_{c,v_1,v_2}\left(\frac{1+\delta_2^2 n_2^{-1}}{1+\delta_1^2 n_1^{-1}}\gamma\right). \tag{3.37}$$

In addition, it is worth mentioning that the detection probability of F-test based detector is invariant to the gain and rotation transformation of channel, i.e., $\hat{\mathbf{h}} = G\mathbf{h}\exp\left(j\theta\right)$. The reason is that for this special case, $\hat{\mathbf{P}}$ is still the projection onto $\mathbf{h}$ as:

$$\begin{aligned}\hat{\mathbf{P}} &= \hat{\mathbf{h}}\left(\hat{\mathbf{h}}^H\hat{\mathbf{h}}\right)^{-1}\hat{\mathbf{h}}^H \\ &= \frac{G^2}{G^2}\exp\left(j0\right)\mathbf{h}(\mathbf{h}^H\mathbf{h})^{-1}\mathbf{h}^H \\ &= \mathbf{P}.\end{aligned} \tag{3.38}$$

3.6 Simulation Results

In this section, the proposed F-test based sensing technique will be evaluated numerically and compared with the other two widely used detectors, namely the energy detector [8] and the GLRT based detector [15] (given in eqs. (2.8) and (2.16), Chapter 2). A simple summary of the three detectors to be simulated is outlined in Table 3.1. Given a target false alarm probability, which is generally set as 0.1 due to the current requirements on spectrum sensing [92], the test thresholds of the F-test based detector and the energy detector are evaluated using tables of F-distribution and chi-squared distribution [8], respectively; while the threshold for the GLRT based detector is obtained using $N = 5000$ Monte Carlo trails.

All results are obtained by averaging over 5000 independent Monte Carlo trials. In each trial,

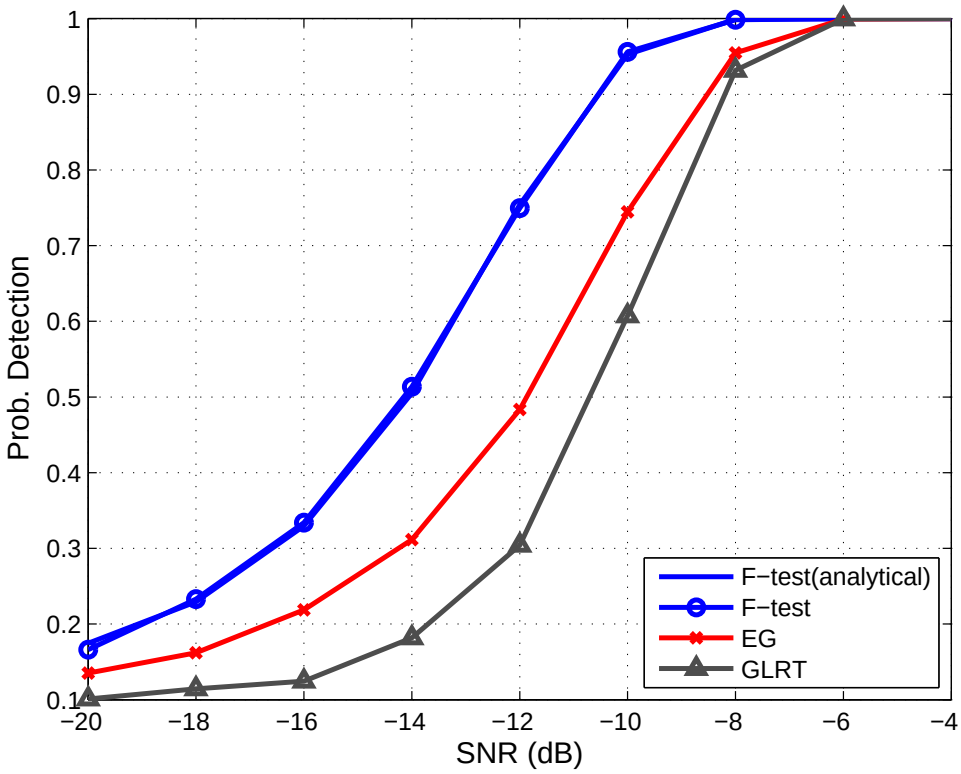

Figure 3.3: *Probability of detection versus SNR. Target false alarm probability* $P_f = 0.1$ *,* $M = 4$ *receiving antennas and* $L = 100$ *samples.*

the channel coefficient $\mathbf{h}$, the primary signal $s(l)$ and the additive white noise $\mathbf{w}(l)$ are generated by the zero-mean complex Gaussian distributed variates. Both the channel $\mathbf{h}$ and $s(l)$ are normalised so that $\|\mathbf{h}\|^2 = \|s(l)\|^2 = \|\mathbf{h}s(l)\|^2 = 1$. The noise power σ_w^2 are selected according to the SNR level defined as:

$$\text{SNR} \triangleq \frac{\|\mathbf{h}s(l)\|^2}{M\sigma_w^2}. \tag{3.39}$$

Performance under perfect CSI

In the first experiment, we assume the perfect channel knowledge $\mathbf{h}$ is available to the F-test based method and the accurate noise power σ_w^2 is known to the energy detector.

The detection probability P_d against SNR is plotted in Figure 3.3 with $M = 4$ receiving an-

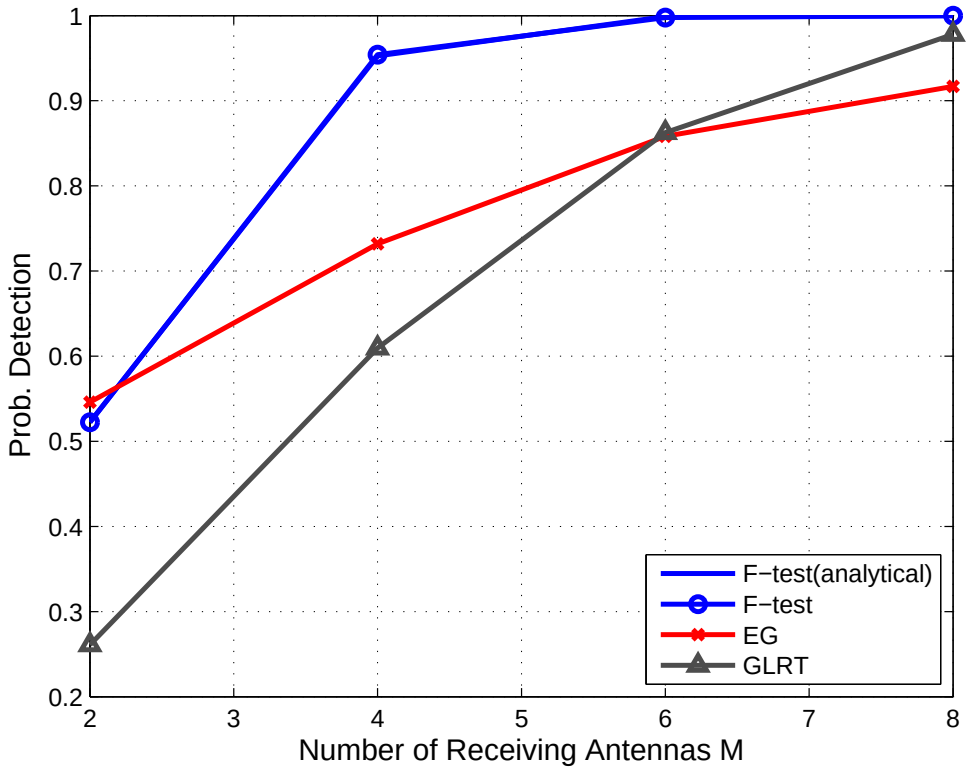

Figure 3.4: *Probability of detection versus number of receiving antennas M. Target false alarm probability $P_f = 0.1$, $L = 100$ samples and SNR $= -10$ dB.*

tennas, $L = 100$ samples and $P_f = 0.1$. We can find that the proposed F-test based method achieves the best detection probability. For example, to achieve a 90% detection probability, the proposed sensing method offers a 2 dB and 2.2 dB SNR gain compared with the energy detector (EG) and the GLRT based detector, respectively. In addition, as shown in the figure, the analytical formula for detection probability P_d, eq. (3.20) and marked as F-test (analytical), gives an accurate description. Since the GLRT based detection method is *blind*, which does not require any *prior* knowledge, it performs worse than the energy detector when the noise power is exactly known.

In Figure 3.4, the impact of the receiver array size M is presented, where we fix the SNR $= -10$ dB and vary the number of receiving antennas from 2 to 8. It shows that when M is small, i.e., $M = 2$, the proposed F-test has nearly the same detection probability as the energy detector. However, when M increases, the F-test based sensing technique has a significant performance improvement. This is due to the linear regression involved in the proposed approach,

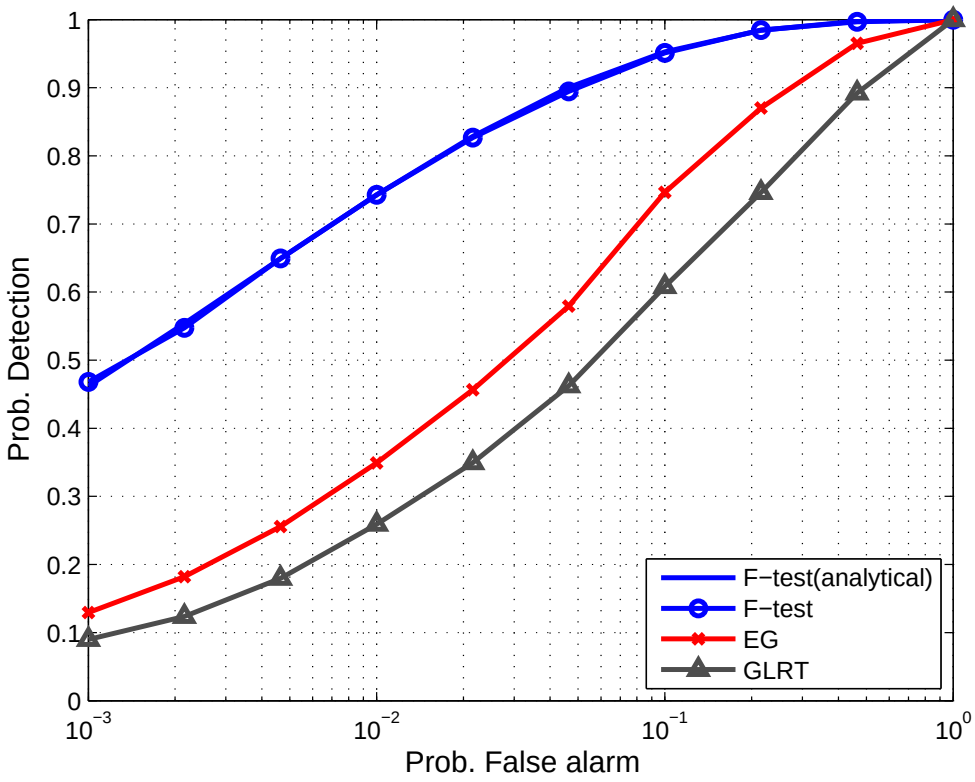

Figure 3.5: *ROC curve, for $M = 4$ receiving antennas, $L = 100$ samples and SNR $= -10$ dB.*

e.g., it takes the channel $\mathbf{h}$ as the regressor and the received signal $\mathbf{y}(l)$ as the response variable. In other words, the F-test based detection method compares the linear similarity between the received signal and CSI. Therefore, a higher detection probability can be expected when more antennas i.e., larger size of the regressor $\mathbf{h}$, are available, further justifying the selection of $M = 4$ in other simulations.

In addition, to quantify the trade-off between the false alarm probability and detection probability, we draw the Receiver Operating Characteristics (ROC) curve in Figure 3.5 with the SNR fixed at -10 dB. Note that the test thresholds of all detectors change according to the different levels of target false alarm probability. It shows that given a certain false alarm rate, the proposed F-test based method provides a much higher probability of detection than other detectors. For example, when P_f is fixed at 5×10^{-2}, the detection probability gain of the F-test based method is about 40% for the energy detector and approximately 50% for the GLRT based detector. This means that to achieve the same spectrum efficiency, the proposed F-test based detector causes less interference to the primary user.

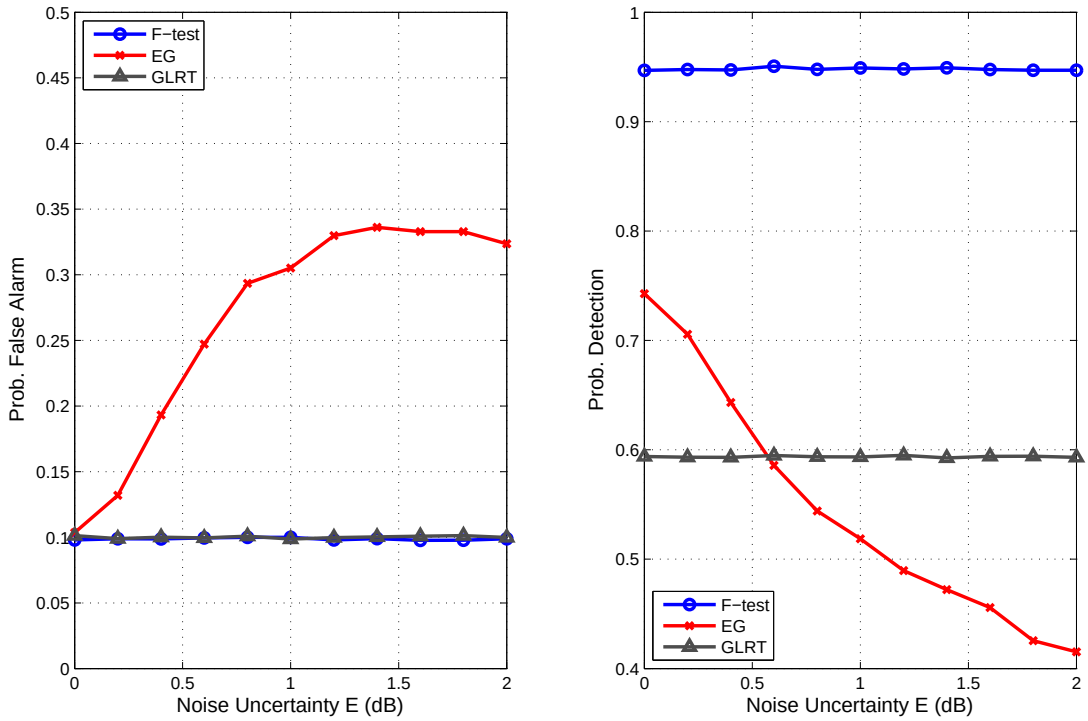

(a) **(b)**

Figure 3.6: *Performance v.s. noise uncertainty E. The performance for: (a) False Alarm Probability; and (b) Detection probability is plotted. Target false alarm probability $P_f = 0.1$, $M = 4$ receiving antennas, $L = 100$ samples and SNR $= -10$ dB.*

Performance under noise variance uncertainty

As mentioned above, the energy detector has a significant performance loss under noise variance uncertainty and the proposed F-test based sensing method enjoys the robustness. To validate this property numerically, we assume that only the estimated noise power $\hat{\sigma}_w^2 = \eta\sigma_w^2$ is available. The uncertainty factor $10\log_{10}\eta$ (in dB scale) is considered as a uniformly distributed random variable in the interval $[-E, E]$ [13]. Note that the estimated noise power is varied in each realisation to a certain degree as mentioned above and is used to decide the test threshold of the energy detector.

Figure 3.6 shows the detection performance against noise mismatch E (in dB) for $M = 4$ receiving antennas, $L = 100$ samples and SNR $= -10$ dB. It can be observed that the performance of the energy detector degrades severely under mismatched noise variance. For example, in the typical uncertainty range $E \in [1, 2]$ [13], Figure 3.6(a) indicates that the false alarm rate

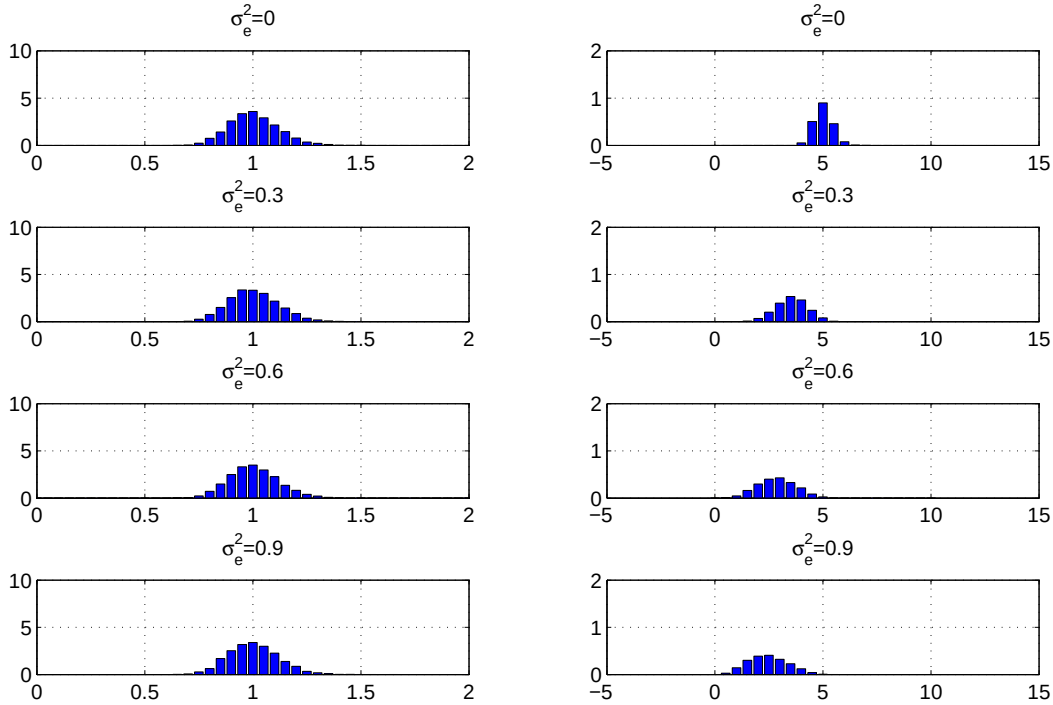

Figure 3.7: *Normalised histogram of the test statistic for F-test based method under channel uncertainty: (a) $T_F\left(\hat{\mathbf{h}}|\mathcal{H}_0\right)$; and (b) $T_F\left(\hat{\mathbf{h}}|\mathcal{H}_1\right)$. The uncertainty level is selected as σ_e^2 =0, 0.3, 0.6 and 0.9, respectively, for $M = 4$ receiving antennas, SNR $=$ 0 dB and $L = 100$ samples.*

of the energy detector far exceeds the target limit 0.1. In addition, Figure 3.6(b) shows that the corresponding detection probability degrades severely and becomes substantially worse than the GLRT based method. On the other hand, the F-test based detector and the GLRT based detector are robust against the uncertain noise level as expected, while the F-test exhibits superior detection probability.

Performance under imperfect CSI

In the following experiments, we consider the case of CSI uncertainty, i.e., only the imperfect channel estimate $\hat{\mathbf{h}}$ is available to the F-test based detector. In simulation, the error term $\triangle\mathbf{h}$ in (3.23) varies in each trial, which is generated by an i.i.d. complex Gaussian distributed variate with zero-mean and variance $\sigma_e^2\mathbf{I}$. The variance of each entry is assumed to be from zero to

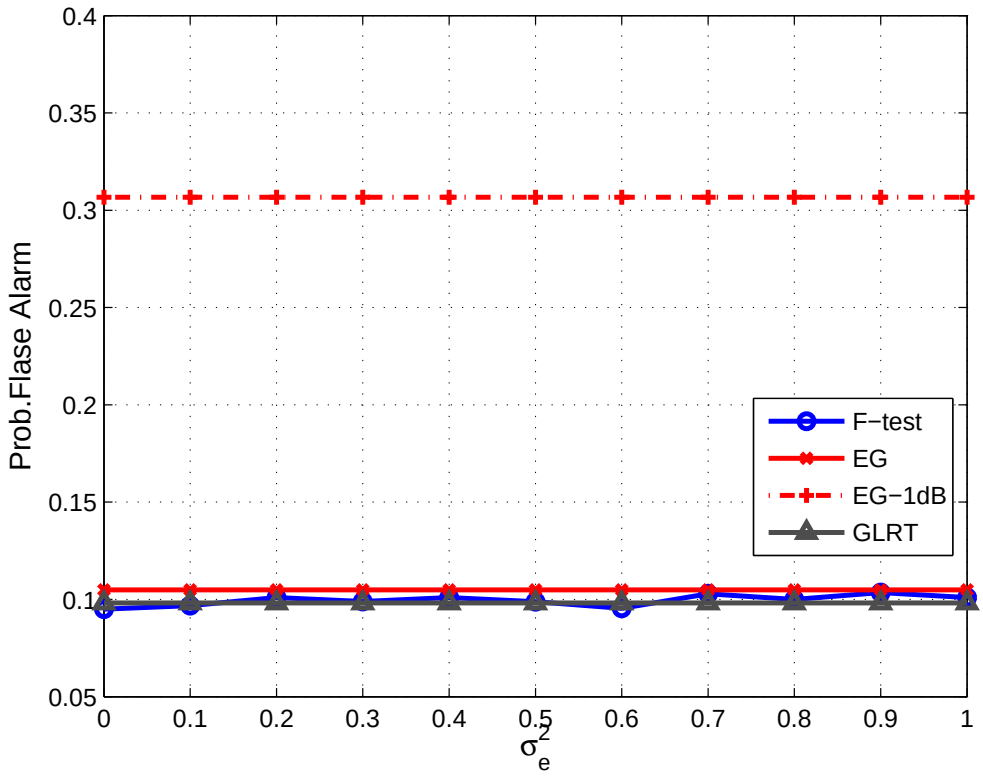

Figure 3.8: *False alarm probability v.s. channel uncertainty σ_e^2. Target false alarm probability $P_f = 0.1$, $M = 4$ receiving antennas, $L = 100$ samples and SNR $= -10$ dB.*

one, i.e., $0 \leq \sigma_e^2 \leq 1$. Since we have normalised the CSI, $\mathbf{h}$, the level of channel uncertainty can be viewed as from 0% to 100%.

Firstly, to get an insight into the impact of channel uncertainty into the F-test based method, we plot the normalised histogram of the test statistic under $\mathcal{H}_0$ and $\mathcal{H}_1$ in Figure 3.7. The error variance σ_e^2 is set as 0, 0.3, 0.6 and 0.9 with the corresponding uncertainty level as 0%, 30%, 60% and 90%, respectively. Figure 3.7(a) shows that the null distribution of test statistic, $T_F\left(\hat{\mathbf{h}}|\mathcal{H}_0\right)$, does not vary with channel uncertainty, verifying our analysis that the F-test based method has constant false alarm rate. While in Figure 3.7(b), we can find that when the alternative hypothesis $\mathcal{H}_1$ holds, the histogram of test statistic $T_F\left(\hat{\mathbf{h}}|\mathcal{H}_1\right)$ shrinks to a smaller value when σ_e^2 rises, which implies that the probability of detection will decrease with growing channel uncertainty.

Then in Figure 3.8 and Figure 3.9, the false alarm probability and the detection probability

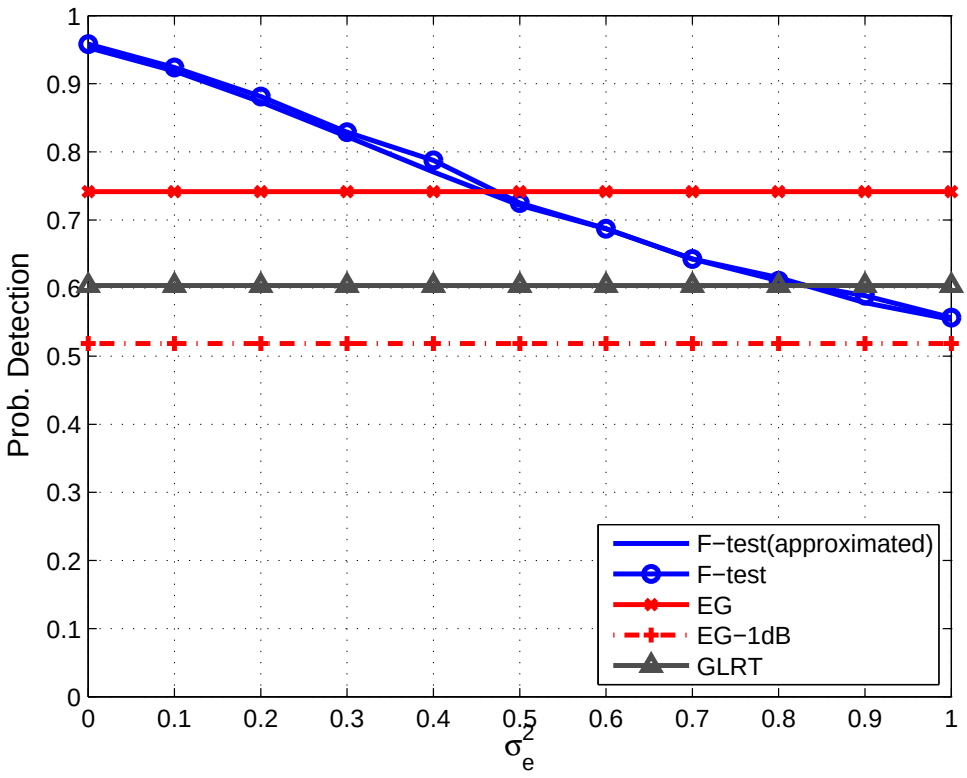

Figure 3.9: *Detection probability v.s. channel uncertainty* σ_e^2*. Target false alarm probability* $P_f = 0.1$ *,* $M = 4$ *receiving antennas,* $L = 100$ *samples and SNR* $= -10$ *dB.*

against the channel uncertainty are presented, with $M = 4$ receiving antennas $L = 100$ samples and SNR $= -10$ dB. Note that the plot for the energy detector with 1 dB noise mismatch (EG $-$ 1 dB) acts as a basis of comparison. Figure 3.8 shows that unlike the energy detector, the false alarm probability of the F-test based method is still around the pre-defined level, 0.1, in the situation with parameter uncertainty. The detection probability of the proposed detector, as shown in Figure 3.9, has a degradation under CSI error. However, with channel uncertainty up to 47%, the F-test based detector still outperforms the ideal energy detector. Besides, it performs better than the GLRT based detector with channel uncertainty up to 83%. Moreover, compared with the energy detector with 1 dB noise mismatch, the F-test has a better detection performance over the entire range of CSI error. In addition, the approximated value for detection probability, given in eq. (3.37), marked here as F-test(approximated), is quite accurate.

In Figure 3.10, we increase the number of receiving antennas to 8. It can be observed that the

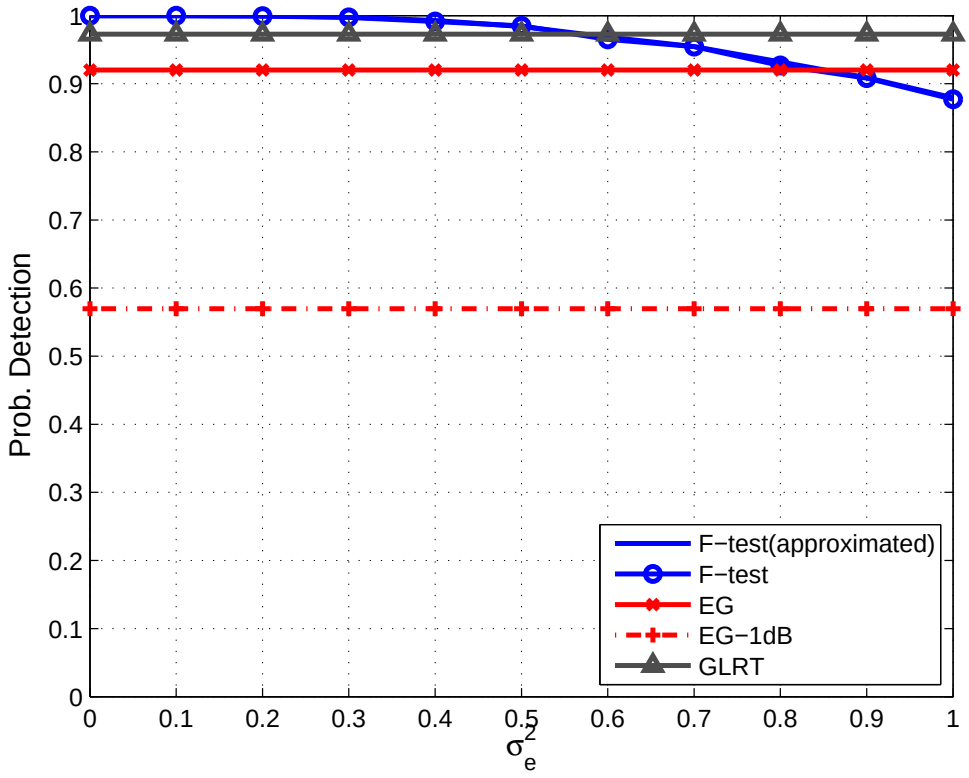

Figure 3.10: *Detection probability v.s. channel uncertainty σ_e^2. Target false alarm probability $P_f = 0.1$, $M = 8$ receiving antennas, $L = 100$ samples and SNR $= -10$ dB.*

performance loss of F-test based approach caused by channel uncertainty becomes insignificant. For instance, Figure 3.10 shows that the detection probability only has an up to 12% degradation over the whole uncertainty interval. This is also due to the fact that the F-test based sensing method uses linear regression models, as discussed in Figure 3.4.

Discussion

In summary, in addition to enhanced robustness against noise variance uncertainty, the F-test based detector is more powerful than several popular spectrum sensing techniques. Compared with the traditional robust or blind detectors [13, 15], the proposed detector can be easily constructed and the computational complexity is moderate. The only *prior* information needed is CSI, which can be seen as the price for improved robustness against uncertain noise level and performance gain. Moreover, the F-test performs reasonably well for moderate CSI uncertainty

and its false alarm probability is unchanged.

3.7 Conclusion

An F-test based approach for spectrum sensing is proposed in this chapter. This method can be applied for multiple antenna cognitive radio systems without the knowledge of noise statistic. It offers absolute robustness against noise variance mismatch as the test statistic is independent from noise power. Statistical properties of F-distribution are applied to derive the test threshold and evaluate the detection probability. The only *prior* information needed is CSI, which can be seen as the price for improved robustness against noise variance uncertainty and performance gain. The detection performance under CSI error has been discussed and results show that the proposed F-test based approach has constant false alarm probability and the detection probability can be evaluated.

Simulations have been carried out to verify the proposed method. The detection performance of the F-test based sensing schemes is superior to the widely used energy detector as a 2.2 dB SNR gain can be achieved to obtain a 90% detection probability. When perfect channel information is not available, the F-test based detector suffers a mild performance loss in probability of detection and its false alarm probability remains unchanged. In addition, the analytical results are verified to be sufficiently accurate. Given its superior performance, the F-test based detector is an attractive approach for spectrum sensing.

Note that in this chapter, the F-test based detection method is developed and studied based on a Gaussian noise assumption. In the following Chapter 4 and Chapter 5, the sensing problem in non-Gaussian noise will be considered.

Chapter 4
Spectrum Sensing for Non-Gaussian Noise Using Bootstrap Techniques

4.1 Introduction

The majority of current spectrum sensing methods consider Gaussian noise. Following the CLT, the Gaussian distribution provides a good model for noise caused by natural sources, such as thermal noise. In addition, it generally offers mathematically tractable results as the Gaussian distribution can be fully characterised by the mean and the variance. However, the Gaussian noise model cannot perfectly model reality as another important noise source in practical wireless communications is man-made, which is impulsive by nature and makes the whole noise distribution heavy-tailed [7, 80, 81]. In the case of non-Gaussian noise, the performance of standard detectors becomes unpredictable due to the uncertain distribution of the test statistic.

In the literature, several sensing methods have been proposed to deal with detection in non-Gaussian noise [29, 31–35, 82]. As summarised in Table 2.2, Chapter 2, many of them require *prior* knowledge of the noise distribution. For example, a LO detector for wideband sensing assumes a perfectly known noise distribution [31]. It uses a spectral estimator as the test statistic, which correlates the periodogram of transformed observations with the primary signal spectrum. In addition, α-stable distributed noise is assumed in [29] and the detector exploits the particular *covariation* properties of the α-stable distribution. Moreover, the authors in [82] considered the situation in which the exact noise distribution is unknown but its statistical moments are available. By invoking a low SNR assumption, a L_p-norm detector was proposed where p is the tunable parameter used to adapt to the underlying non-Gaussian noise.

Other existing approaches consider the case of unknown noise type and only minimal assumptions are made on the noise model. For instance, a nonparametric KS based detector was proposed in [32], which uses a sequence of noise samples for a goodness-of-fit comparison. In addition, some robust detectors are derived without knowing the statistics of the noise, but particular assumptions are made on the primary signal. For example, a cyclic correlation based

detector was studied in [33] which requires knowledge of at least one of the cyclic frequencies of the primary signal. In [34], a PCA detector was proposed for real-valued observations and in [35], a asymptotically robust t-sensing was proposed for non-zero mean primary signal.

As discussed in the background chapter, most of the aforementioned detection methods are parametric, i.e., requiring *prior* knowledge of the signal and noise characteristics, or making particular assumptions on the signal type. In addition, the selection of a test threshold is generally difficult, especially for parametric detectors as their test statistics are relatively complicated and may depend on several unknowns. In this chapter, we shall apply the powerful bootstrap technique to overcome those challenges. By using the bootstrap procedure, two detection methods are proposed which can be applied to arbitrary noise types with finite power. Firstly, by using multiple antennas at the sensing device, a *blind* eigenvalue based detector is developed by exploiting the eigenstructure of the sample covariance matrix. Next, the noise power is assumed to be known and we generalise the conventional energy detector to non-Gaussian noise by studentizing its test statistic. For both detectors, there are no closed form expressions for the test statistic's null distribution due to the unknown noise distribution. We shall apply the bootstrap resampling to overcome this difficulty.

The main contributions of this chapter are summarised as follows:

• An eigenvalue based detector is proposed for unknown noise power and noise types. By using multiple receiving antennas, this method is fundamentally a binary hypothesis test for the difference between sample eigenvalues. In addition, in order to reduce the bias of sample eigenvalues, a nonparametric bootstrap bias correction step is also proposed.

• Assuming that the noise power is known, an energy based detector is developed with the test statistic being studentized, i.e., the statistic is divided by the estimate of its standard deviation. By doing this, the conventional energy detector is generalised to non-Gaussian noise.

• For both detectors, the nonparametric bootstrap procedure is applied to estimate the test statistic's null distribution. It works without requirements on reproducible experimental conditions and large samples. The advantage of bootstrap is highlighted and its accuracy is described.

• Simulation results show that the bootstrap method gives a sufficiently accurate result for short data records. In non-Gaussian noise, the eigenvalue based detector offers an overall better detection probability while the energy based detector illustrates its superiority in the low SNR

regime.

The remainder of this chapter is organised as follows. The signal model is described in Section 4.2. Section 4.3 introduces the bootstrap techniques. The non-parametric eigenvalue based detector is proposed in Section 4.4 and the energy based detector is proposed in Section 4.5, respectively. The accuracy of bootstrap method is highlighted in Section 4.6. Simulation results are shown in Section 4.7. Finally, Section 4.8 concludes the chapter.

4.2 System Model

Recall the SIMO system model defined in Chapter 3, Section 3.2. The baseband received signal vector $\mathbf{y}\,(l)$ can be expressed as:

$$\begin{aligned} \mathcal{H}_0 \quad &: \quad \mathbf{y}\,(l) = \mathbf{w}\,(l)\,, \\ \mathcal{H}_1 \quad &: \quad \mathbf{y}\,(l) = \mathbf{h}s\,(l) + \mathbf{w}\,(l)\,,\ l = 0, 1, ..., L-1. \end{aligned} \tag{4.1}$$

Here we assume $s(l)$ is the zero-mean complex primary signal with unknown power σ_s^2. The vector $\mathbf{h} = [h_1, h_2, \ldots, h_M]^T$ denotes the unknown fading channel, which remains unchanged during the sensing period. The noise $\mathbf{w}(l) = [w_1(l), w_2(l), \ldots, w_M(l)]^T$ consists of i.i.d complex-valued elements, $w_i(l), i = 1, 2, ..., M$, with zero-mean and finite variance σ_w^2. Note that no assumption is made on the distribution of noise or signal. In addition, the primary signal, channel and noise are assumed to be mutually independent.

4.3 Preliminaries of Bootstrap Techniques

The bootstrap is a data-based simulation method, which is an attractive tool for estimating parameters or finding confidence intervals [93]. Unlike conventional asymptotic/analytical methods, which may assume Gaussian noise or invoke large sample sizes, the bootstrap method is non-parametric and works for moderate sample sizes. In the following, we shall give an introduction to the bootstrap principle and then describe its application to the hypothesis testing problem.

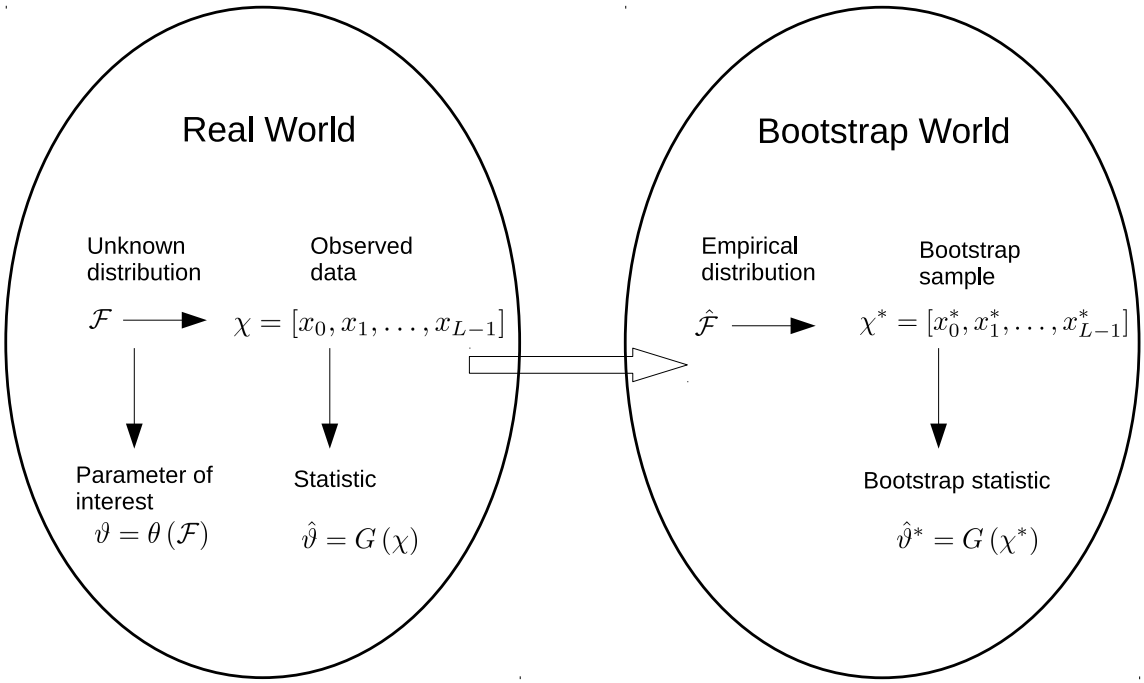

Figure 4.1: *A schematic diagram of the bootstrap principle [94].*

General Concept

A schematic diagram of the bootstrap principle is shown in Figure 4.1 [94]. In the "real world" an unknown distribution $\mathcal{F}$ provides a set of random observed data $\chi = [x_0, x_1, \ldots, x_{L-1}]$. Here, "random" means that the samples x_l, $l = 0, 1, \ldots, L-1$, is i.i.d, following the same distribution $\mathcal{F}$. Let $\vartheta = \theta(\mathcal{F})$ denote the parameter of interest, such as the mean or variance, which is estimated by the statistic $\hat{\vartheta} = G(\chi)$. Note that the "parameter" is a function of the distribution $\mathcal{F}$ and the "statistic" is a function of the data χ.

The problem of interest is to find the statistical behaviour, i.e, bias and variance, or the distribution of $\hat{\vartheta}$ on the basis of observed data χ. By contrast to the conventional Monte Carlo method which repeats the experiment for a sufficient number of times [36], the bootstrap method, enables us to resample from a distribution in a way that approaches $\mathcal{F}$ in some sense. For example, the observed data set χ, which can be seen as an empirical distribution $\hat{\mathcal{F}}$, approaches the true distribution $\mathcal{F}$ as the sample size L grows large [95].

The Bootstrap Principle

1) Given an i.i.d data set $\chi = [x_0, x_1, \ldots, x_{L-1}]$.
2) Draw a bootstrap sample set $\chi^* = [x_0^*, x_1^*, \ldots, x_{L-1}^*]$ via resampling χ with replacement. An example can be : $\chi^* = [x_1, x_1, \ldots, x_8]$.
3) Compute the bootstrap statistic $\hat{\vartheta}^*$ from χ^*.
4) Repeat 2) and 3) B times to obtain a set of bootstrap statistics $\{\hat{\vartheta}^*(b), b = 1, 2, \ldots, B\}$.
5) Using the empirical distribution of $\hat{\vartheta}^*$ to approximate the statistical behaviour or the distribution of $\hat{\vartheta}$.

The "bootstrap world" can be explained in an analogous manner to the "real world". As shown in the bootstrap side of Figure 4.1, the empirical distribution $\hat{\mathcal{F}}$, i.e., the original data χ, gives the bootstrap sample $\chi^* = [x_0^*, x_1^*, \ldots, x_{L-1}^*]$ from resampling with replacement. By "resampling with replacement " it is meant that χ^* may contain repeated data as it is drawn randomly from χ, with each x_i has an equal probability to be selected. Using χ^*, the bootstrap statistic $\hat{\vartheta}^*$ can be evaluated. A major advantage of bootstrap is that we can obtain as many replications of $\hat{\vartheta}^*$ as we need. This yields a set of bootstrap statistics, $\left\{\hat{\vartheta}^*(b), b = 1, 2, \ldots B\right\}$, from which we approximate the behaviour or distribution of $\hat{\vartheta}$ by that of $\hat{\vartheta}^*$.

Bootstrap for Hypothesis Testing

As an extension of distribution estimate, the bootstrap procedure can be easily adapted to find a confidence interval of $\hat{\vartheta}$ or construct a hypothesis test. Consider a problem for testing the null hypothesis $\mathcal{H}_0 : \vartheta \leq \vartheta_0$ against the alternative $\mathcal{H}_1 : \vartheta > \vartheta_0$, where ϑ_0 is a given bound. The test statistic is defined as:

$$\hat{\mathcal{T}} = \frac{\hat{\vartheta} - \vartheta_0}{\hat{\sigma}}, \tag{4.2}$$

where $\hat{\sigma} = \sqrt{\hat{\sigma}^2}$ and $\hat{\sigma}^2$ is an estimate of the variance of $\hat{\vartheta}$. Given a significant value α, one can compute the test threshold γ based on the bootstrap approximation, $\left\{\hat{\mathcal{T}}^* = \frac{\hat{\vartheta}^* - \hat{\vartheta}}{\hat{\sigma}^*}\right\}$, through the following relation:

$$\alpha = \frac{1}{B}\sum_{b=1}^{B} I\left[(\hat{\mathcal{T}}^*(b) > \gamma\right], \tag{4.3}$$

where $I[x] = \begin{cases} 1 & x > 0 \\ 0 & x \leqslant 0 \end{cases}$ denotes the indicator function.

Note that we resample $\hat{\vartheta}^* - \hat{\vartheta}$ instead of $\hat{\vartheta}^* - \vartheta_0$ for the purpose of increasing detection probability [96]. By using a set of bootstrap statistics as reference basis, the test will reject $\mathcal{H}_0$ when $\hat{\vartheta} - \vartheta_0 > 0$ is relatively large. If the alternative hypothesis $\mathcal{H}_1$ is true and the value of ϑ is ϑ_1, i.e., $\theta\left(\mathcal{F}\,|\mathcal{H}_1\right) = \vartheta_1$, then the detection probability is expected to increase to 1 as $\vartheta_1 - \vartheta_0$ grows. However, when $\mathcal{H}_1$ holds, the value of $\hat{\vartheta} - \vartheta_0$ will never be too large if we use the bootstrap distribution based on $\hat{\vartheta}^* - \vartheta_0$ for comparison. On the contrary, the detection probability may degrade to at most the false alarm probability. Hence, a more appropriate comparison is with the bootstrap distribution based on $\hat{\vartheta}^* - \hat{\vartheta}$. Moreover, resampling $\hat{\vartheta}^* - \hat{\vartheta}$ is important to ensure the level of accuracy, which will be discussed later in Section 4.6.

In addition, the inclusion of $\hat{\sigma}$ and $\hat{\sigma}^*$ is known as bootstrap pivoting [96]. Under the null hypothesis $\mathcal{H}_0$, the asymptotic distribution of $\hat{\vartheta} - \vartheta_0$ and $\hat{\vartheta}^* - \hat{\vartheta}$ may depend on an unknown scale. To increase the accuracy of bootstrap approximation, the method of dividing by $\hat{\sigma}^*$ and $\hat{\sigma}$ are necessitated to ensure that the asymptotic distributions of $\hat{\mathcal{T}}^*$ and $\hat{\mathcal{T}}$ do not depend on any unknowns as $L \to \infty$. However, this technique may only be used when the square root of variance estimate, $\hat{\sigma}$, is perfectly known or can be effectively evaluated. There do exist cases where $\hat{\sigma}$ is difficult to evaluate, i.e., when the statistic $\hat{\vartheta}$ is a complex function of several unknowns. Although the bootstrap can also be applied blindly to estimate $\hat{\sigma}$, it may be computationally expensive as it invokes nested bootstrap resampling, especially when the function $G\left(\chi\right)$ is nonlinear. In such cases, the bootstrap pivoting might be disregarded, or we can apply other techniques such as bias reduction to improve the accuracy of bootstrap estimate [97].

4.4 Nonparametric Eigenvalue Based Detector

In this section, the noise power σ_w^2 is assumed to be unknown. By using multiple receiving antennas, we propose an eigenvalue based detector which exploits the eigenvalue property of sample covariance matrix. Inspired by [98], the bootstrap resampling is applied to estimate the null distribution of the test statistic. Note that the bootstrap technique works in arbitrary noise and does not require a large sample size. However, when no assumption is made on large samples, as it is in this chapter, the bias in sample eigenvalues may be significant and

degrade the test performance. Therefore, a nonparametric bootstrap bias correction step is also proposed.

Based on the signal model defined in (4.1), the received data $\mathbf{y}(l)$ can be seen as an i.i.d. random variate with zero-mean and covariance matrix:

$$\begin{aligned} \mathcal{H}_0 &: \quad \mathbf{R}_y = \sigma_w^2 \mathbf{I}, \\ \mathcal{H}_1 &: \quad \mathbf{R}_y = \sigma_s^2 \mathbf{h}\mathbf{h}^H + \sigma_w^2 \mathbf{I}. \end{aligned} \tag{4.4}$$

The corresponding eigenvalues [99] λ_i, $i = 1, 2, ..., M$ are:

$$\begin{aligned} \mathcal{H}_0 &: \quad \lambda_1 = \lambda_2 = \ldots = \lambda_M = \sigma_w^2, \\ \mathcal{H}_1 &: \quad \lambda_1 > \lambda_2 = \ldots = \lambda_M = \sigma_w^2. \end{aligned} \tag{4.5}$$

Equation (4.5) has an interpretation that, when $\mathcal{H}_0$ holds, all the eigenvalues represent noise only. However, when $\mathcal{H}_1$ is true, the largest eigenvalue $\lambda_1 = \mathbf{h}^H \mathbf{h} \sigma_s^2 + \sigma_w^2$ is contributed by both the primary signal and noise.

Based on our assumption, the covariance matrix $\mathbf{R}_y$ is unknown. The one we can obtain is the sample covariance matrix:

$$\hat{\mathbf{R}}_y = \frac{1}{L-1} \sum_{l=0}^{L-1} \mathbf{y}(l) \mathbf{y}(l)^H. \tag{4.6}$$

When the sample size L is finite, the sample eigenvalue β_i, $i = 1, 2, ..., M$ obtained from $\hat{\mathbf{R}}_y$ are definitely distinct [99] under both $\mathcal{H}_0$ and $\mathcal{H}_1$:

$$\beta_1 > \beta_2 > \ldots > \beta_M. \tag{4.7}$$

By employing the difference of eigenvalues, the hypothesis test in (4.5) can be rewritten as:

$$\begin{aligned} \mathcal{H}_0 &: \quad \lambda_1 - \frac{1}{M-1} \sum_{i=2}^{M} \lambda_i = 0, \\ \mathcal{H}_1 &: \quad \lambda_1 - \frac{1}{M-1} \sum_{i=2}^{M} \lambda_i > 0. \end{aligned} \tag{4.8}$$

Considering that we can only obtain the sample eigenvalues, the test statistic for the above

hypothesis testing problem (4.8) is given as follows:

$$\hat{T}_{EV} = \beta_1 - \frac{1}{M-1}\sum_{i=2}^{M}\beta_i. \tag{4.9}$$

Since the sample eigenvalues β_i, $i = 1, 2, ..., M$, are distinct from each other with probability one, the test statistic $\hat{T}_{EV}$ will be non-zero under both $\mathcal{H}_0$ and $\mathcal{H}_1$. However, a reasonable assumption can be made that $\hat{T}_{EV}$ will be large when primary signal exists but relatively small in the noise only case. Therefore, the hypothesis testing problem (4.8) can be converted to the following decision rule:

$$\hat{T}_{EV} \underset{\mathcal{H}_0}{\overset{\mathcal{H}_1}{\gtrless}} \gamma, \tag{4.10}$$

where γ is the test threshold to ensure a target false alarm probability.

Note that the evaluation of γ needs the null distribution of the test statistic $\hat{T}_{EV}$. To the best of our knowledge, there are no existing results on the joint distribution of eigenvalues without additional assumptions on the Gaussian distributed entries. We shall apply the bootstrap procedure [94] to overcome this difficulty.

The hypothesis testing problem (4.8) can be reformulated as:

$$\begin{aligned} \mathcal{H}_0 &: \quad T_{EV} = 0, \\ \mathcal{H}_1 &: \quad T_{EV} > 0, \end{aligned} \tag{4.11}$$

where

$$T_{EV} = \lambda_1 - \frac{1}{M-1}\sum_{i=2}^{M}\lambda_i \tag{4.12}$$

with $\hat{T}_{EV}$ in (4.9) as the estimator. By definition, T_{EV} and $\hat{T}_{EV}$ are non-negative. As discussed in Section 4.3, the test threshold γ can be evaluated based on the bootstrap approximation for the null distribution of $\hat{T}_{EV}$. The detection procedure is outlined in Table 4.1 where the included eigenvalue bias reduction step will be discussed later.

Note that the test statistic $\hat{T}_{EV}$ is unpivoted due to the difficulty of computing the variance, and some investigations have shown that the extra computational cost for evaluating the standard deviation of sample eigenvalues is unnecessary [100].

Input: $\mathbf{Y} = [\mathbf{y}(0), \mathbf{y}(1), \ldots, \mathbf{y}(L-1)]$ and target false alarm probability α.

1) Compute the bias corrected sample eigenvalues using eq. (4.15)
and obtain the test statistic:
$\hat{T}_{EV} = \hat{\beta}_1 - \frac{1}{M-1}\sum_{i=2}^{M}\hat{\beta}_i$.

2) Draw a bootstrap sample set $\mathbf{Y}^*$ from $\mathbf{Y}$.

3) Compute the bias corrected bootstrap test statistic:
$\hat{T}^*_{EV} = \hat{\beta}^*_1 - \frac{1}{M-1}\sum_{i=2}^{M}\hat{\beta}^*_i$.

4) Repeat 2) and 3) B times. Ranking the bootstrap statistics as:
$(\hat{T}^*_{EV}(1) - \hat{T}_{EV}) \leq \ldots \leq (\hat{T}^*_{EV}(k) - \hat{T}_{EV}) \leq \ldots \leq (\hat{T}^*_{EV}(B) - \hat{T}_{EV})$

5) From the ordered statistics, choose the index k by:
$1 - \frac{k+1}{B} \leq \alpha \leq 1 - \frac{k}{B}$.
The test threshold is then obtained as:
$\gamma = \hat{T}^*_{EV}(k) - \hat{T}_{EV}$.

Output: Hypothesis testing $\hat{T}_{EV} \underset{\mathcal{H}_0}{\overset{\mathcal{H}_1}{\gtrless}} \gamma$.

Table 4.1: *The bootstrap procedure for the eigenvalue based detection problem*

Bootstrap Bias Reduction

As mentioned above, the test statistic $\hat{T}_{EV}$ is constructed by the sample eigenvalues. However, as discussed in [98, 99], the sample eigenvalue contributed by the primary signal is asymptotically unbiased, whereas the one contributed by the noise only is asymptotically biased. When the sample size is small, the bias becomes quite significant, i.e., $\hat{T}_{EV}$ may be large even if no primary signal exists. Note that in this chapter, we do not make assumption of large data sizes. Therefore, a bias reduction is necessary to ensure the accuracy of the sample eigenvalues.

Define the bias of sample eigenvalue β_i as the difference between the expectation of β_i and the exact eigenvalue λ_i, that is:

$$\text{Bias}(\beta_i) = \text{E}\left[\beta_i\right] - \lambda_i,\ i = 1, 2, \ldots, M. \tag{4.13}$$

Since no assumption is made on the distribution of signal and noise, we apply the distribution-

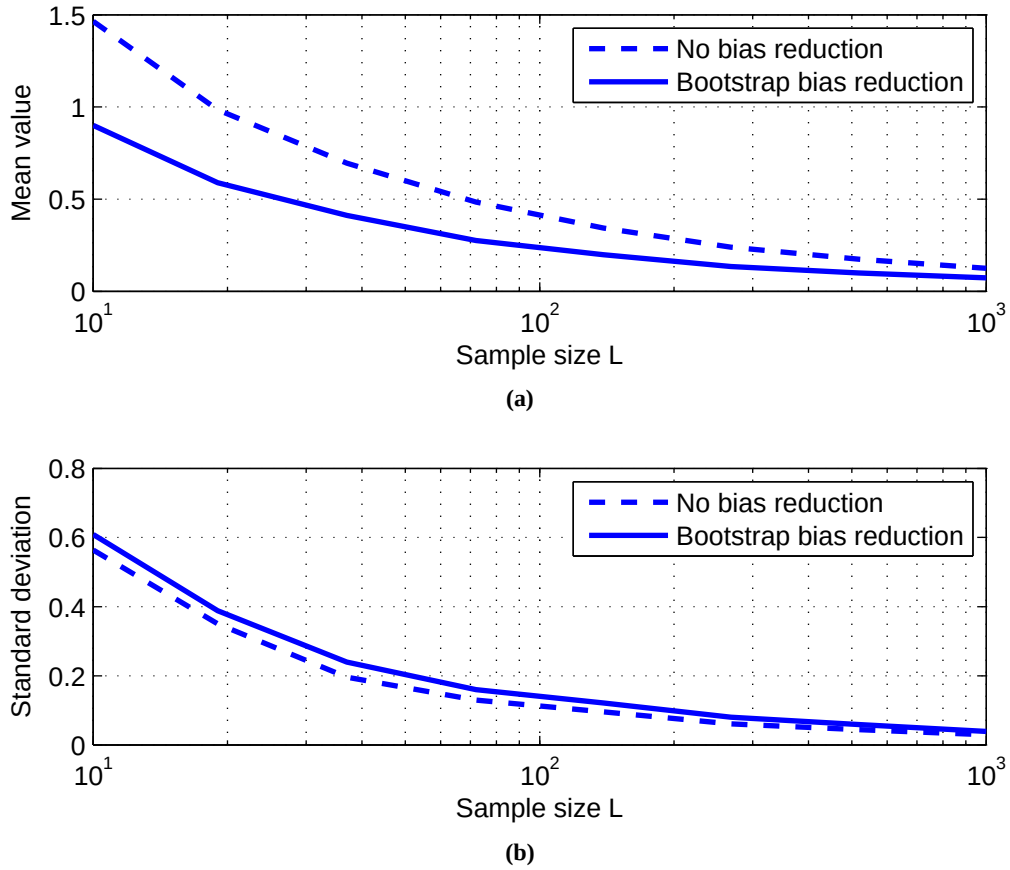

Figure 4.2: *The: (a) mean; and (b) standard deviation of the test statistic* $\hat{T}_{EV}$ *versus the sample size* L*, for Laplacian distributed data with Identity covariance matrix and corresponding eigenvalues* $[1,\ 1,\ 1,\ 1]^T$*. Number of bootstrap replications* $B_1 = 30$*,* $M = 4$ *receiving antennas and* $L = 100$ *samples.*

free bootstrap method [94] to estimate the bias of sample eigenvalue β_i. That is:

$$\hat{\text{Bias}}(\beta_i) = \frac{1}{B_1}\sum_{b=1}^{B_1}\beta_i^*(b) - \beta_i,\ i = 1, 2, \ldots, M, \tag{4.14}$$

where B_1 is the number of bootstrap replications and empirically, $B_1 = 30$ gives quite satisfactory results for the bias estimate [94]. The corrected sample eigenvalue is given by:

$$\begin{aligned}\hat{\beta}_i &= \beta_i - \hat{\text{Bias}}(\beta_i) \\ &= 2\beta_i - \frac{1}{B_1}\sum_{b=1}^{B_1}\beta_i^*(b),\ i = 1, 2, \ldots, M.\end{aligned} \tag{4.15}$$

In Figure 4.2 and Figure 4.3, we plot the mean value and standard deviation of the test statistic

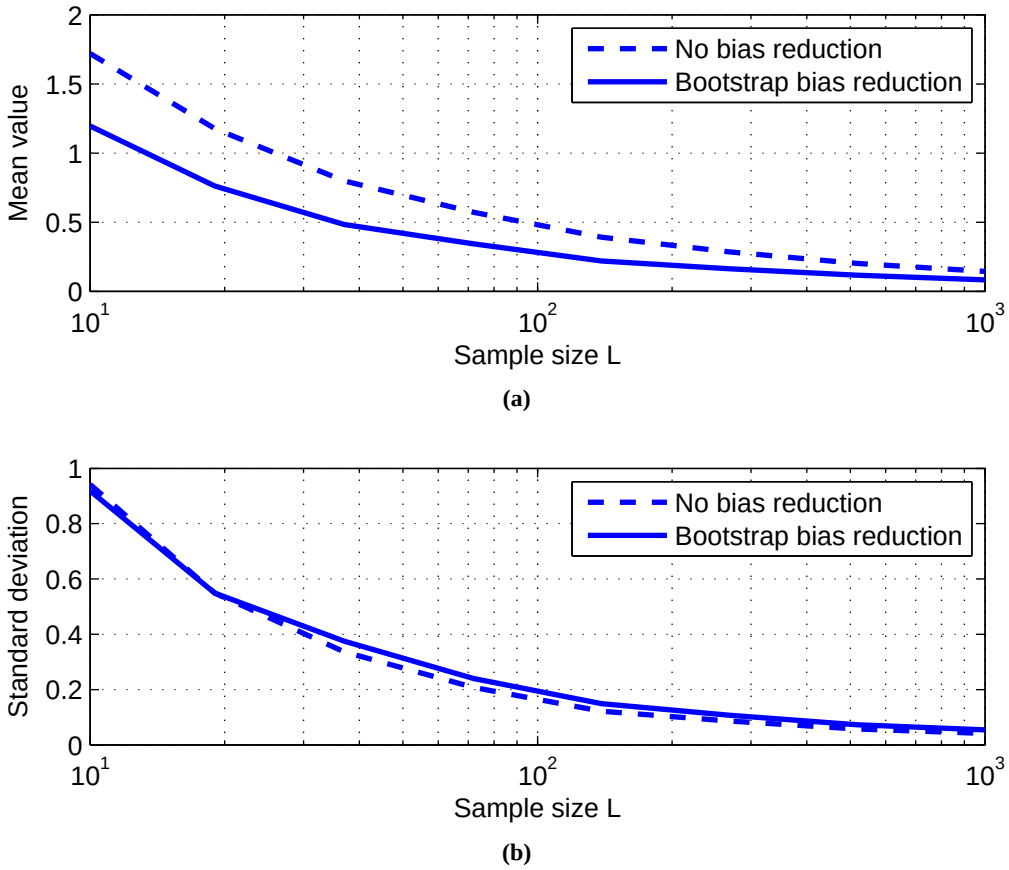

Figure 4.3: *The: (a) mean; and (b) standard deviation of the test statistic $\hat{T}_{EV}$ versus the sample size L, for Gaussian Mixture distributed data with Identity covariance matrix and corresponding eigenvalues $[1,\ 1,\ 1,\ 1]^T$. Number of bootstrap replications $B_1 = 30$, $M = 4$ receiving antennas and $L = 100$ samples.*

$\hat{T}_{EV}$ with and without bootstrap bias reduction. To test the distribution-free property of the bias reduction procedure, the data is generated by the zero-mean Laplacian and Gaussian Mixture (defined later in eq. (4.25)) distributed variates, with identity covariance matrix and eigenvalues $[1,\ 1,\ 1,\ 1]^T$. Theoretically, $\hat{T}_{EV}$ should be near zero in this case. However, due to the bias of sample eigenvalues, both Figure 4.2(a) and Figure 4.3(a) show that the mean value of $\hat{T}_{EV}$ exceeds the zero line over the full range of sample size L, especially when L is small. Such bias can be efficiently decreased by applying the bias reduction procedure. For example, there is a notable 40% decrease in the mean value of $\hat{T}_{EV}$ at $L = 100$ samples by using the bias-corrected sample eigenvalues, while the increase in the standard deviation, shown in Figure 4.2(b) and Figure 4.3(b), is not significant.

4.5 Energy Based Detector

Among current spectrum sensing techniques, the energy detector [8] is the most widely used method due to its simplicity and good detection performance. It takes the energy of received signal as the test statistic, which follows a chi-squared distribution under null hypothesis $\mathcal{H}_0$ for Gaussian noise. However, when the Gaussian noise assumption no longer holds, the null distribution of the test statistic becomes uncertain and may make the detection result become invalid. For example, as shown in Section 4.6, the false alarm probability of the energy detector far exceeds the target level under heavy-tailed noise, which leads to unexpected harmful interference to the primary user. In this section, we generalize the conventional energy detector to the case of non-Gaussian noise by applying the bootstrap procedure. Note that the noise power σ_w^2 is required as *prior* knowledge.

Recall the signal model (4.1). Define

$$Y(l) \triangleq \|\mathbf{y}(l)\|^2,\ l = 0, 1, \ldots, L-1, \tag{4.16}$$

be the received signal energy, which can be seen as an i.i.d. variate since the sample $\mathbf{y}(l)$ is assumed to be i.i.d. The statistical expectation of $Y(l)$ can be written as:

$$\begin{aligned} \mathcal{H}_0 &: \quad \mathrm{E}[Y(l)] = M\sigma_w^2, \\ \mathcal{H}_1 &: \quad \mathrm{E}[Y(l)] > M\sigma_w^2. \end{aligned} \tag{4.17}$$

The expectation $\mathrm{E}[Y(l)]$ can be estimated by the sample mean of $Y(l)$, i.e., $\frac{1}{L}\sum_{l=0}^{L-1} Y(l)$, which is the test statistic of the conventional energy detector [8]. In this work, we take $\mathrm{E}[Y(l)]$ as the parameter of interest and $\frac{1}{L}\sum_{l=0}^{L-1} Y(l)$ as its estimator. As discussed in Section 4.3, the statistic for hypotheses testing problem (4.17) can be written as:

$$\hat{T}_{EG} = \frac{\frac{1}{L}\sum_{l=0}^{L-1}\left(Y(l) - M\sigma_w^2\right)}{\sqrt{\frac{1}{L(L-1)}\sum_{l=0}^{L-1}\left(Y(l) - \frac{1}{L}\sum_{l=0}^{L-1} Y(l)\right)^2}}. \tag{4.18}$$

Here $\hat{T}_{EG}$ is studentized, where the pivotal

$$\hat{\sigma}_Y = \sqrt{\frac{1}{L(L-1)}\sum_{l=0}^{L-1}\left(Y(l) - \frac{1}{L}\sum_{l=0}^{L-1}Y(l)\right)^2} \tag{4.19}$$

is as an estimate of the standard deviation of $\frac{1}{L}\sum_{l=0}^{L-1}Y(l)$.

The bootstrap resampling procedure for hypothesis testing problem (4.17) is summarised in Table 4.2. Note that the bootstrap version of the test statistic $\hat{T}^*_{EG}$ should also be asymptotically pivotal, where we use

$$\hat{\sigma}^*_Y = \sqrt{\frac{1}{L(L-1)}\sum_{l=0}^{L-1}\left(Y^*(l) - \frac{1}{L}\sum_{l=0}^{L-1}Y^*(l)\right)^2} \tag{4.20}$$

to estimate the standard deviation $\frac{1}{L}\sum_{l=0}^{L-1}Y^*(l)$.

4.6 The Accuracy of Bootstrap

In previous sections, the bootstrap procedure is applied to solve the spectrum sensing problem for non-Gaussian noise. One issue we may raise is how much the information from the original data can be kept via the bootstrap resampling. In this section, several theoretical results are given to answer this question and we shall emphasize the important role played by the bootstrap pivoting.

Given an i.i.d. sample set $\chi = [x_0, x_1, \ldots, x_{L-1}]$, let ϑ be the parameter of interest with $\hat{\vartheta}$ as its estimator. Hall [95] gives the following results by using Edgeworth expansion:

Result 1. Consider the pivotal statistic $\mathcal{T}_p = \sqrt{L}\left(\hat{\vartheta} - \vartheta\right)/\hat{\sigma}$, where $\hat{\sigma}$ is an estimate of the standard deviation of $\sqrt{L}\hat{\vartheta}$. Let $\mathcal{T}^*_p = \sqrt{L}\left(\hat{\vartheta}^* - \hat{\vartheta}\right)/\hat{\sigma}^*$ be the bootstrap version of $\mathcal{T}_p$, derived from resampling χ. We have:

$$\Pr\left(\mathcal{T}^*_p \le x \,|\chi\right) - \Pr\left(\mathcal{T}_p \le x\right) = O\left(L^{-1}\right), \tag{4.21}$$

where $O\left(L^{-1}\right)$ represents the error term which is of order L^{-1}, i.e., $\frac{\Pr\left(\mathcal{T}^*_p \le x|\chi\right) - \Pr(\mathcal{T}_p \le x)}{L^{-1}}$ is bounded with probability one.

Input: I.i.d energy samples $\mathcal{Y} = [Y(0), Y(1), \ldots, Y(L-1)]$, noise power σ_w^2 and target false alarm probability α .

1) Compute the test statistic:
$$\hat{T}_{EG} = \frac{\frac{1}{L}\sum_{l=0}^{L-1} Y(l) - M\sigma_w^2}{\sqrt{\frac{1}{L(L-1)}\sum_{l=0}^{L-1}\left(Y(l) - \frac{1}{L}\sum_{l=0}^{L-1} Y(l)\right)^2}}.$$

2) Draw a bootstrap sample set $\mathcal{Y}^*$ from $\mathcal{Y}$.

3) Compute the bootstrap test statistic:
$$\hat{T}^*_{EG} = \frac{\frac{1}{L}\sum_{l=0}^{L-1} Y^*(l) - \frac{1}{L}\sum_{l=0}^{L-1} Y(l)}{\sqrt{\frac{1}{L(L-1)}\sum_{l=0}^{L-1}\left(Y^*(l) - \frac{1}{L}\sum_{l=0}^{L-1} Y^*(l)\right)^2}}.$$

4) Repeat 2) and 3) B times. One obtains a set of bootstrap statistics: $[T^*(1), T^*(2), \ldots, T^*(B)]$.

5) Ranking the bootstrap statistics as: $\hat{T}^*_{EG}(1) \leq \ldots \leq \hat{T}^*_{EG}(k) \leq \ldots \leq \hat{T}^*_{EG}(B)$

5) Choose the index k by: $1 - \frac{k+1}{B} \leq \alpha \leq 1 - \frac{k}{B}$.
The test threshold is then obtained as: $\gamma = \hat{T}^*_{EG}(k)$.

Output: Hypothesis testing $\hat{T}_{EG} \underset{\mathcal{H}_0}{\overset{\mathcal{H}_1}{\gtrless}} \gamma$,

Table 4.2: *The bootstrap procedure for the energy based detection problem*

The result shown above means that the bootstrap approximation to the distribution of $\mathcal{T}_p$ is in error by L^{-1}. This is a significant improvement compared with the standard Gaussian approximation, i.e., $\Pr(\mathcal{T}_p \leq x) \sim \Phi(x)$ where $\Phi(x) \triangleq \exp\left(-\frac{1}{2}x^2\right)/\sqrt{2\pi}$, which is in error by $L^{-1/2}$ [95].

Result 2. Consider the non-pivotal statistic $\mathcal{T}_{np} = \sqrt{L}\left(\hat{\vartheta} - \vartheta\right)$ and its bootstrap version $\mathcal{T}^*_{np} = \sqrt{L}\left(\hat{\vartheta}^* - \hat{\vartheta}\right)$. We have:

$$\Pr\left(\mathcal{T}^*_{np} \leq x \,|\chi\right) - \Pr\left(\mathcal{T}_{np} \leq x\right) = O\left(L^{-1/2}\right). \tag{4.22}$$

Now the error term between the distribution of non-pivotal statistic $\mathcal{T}_{np}$ and its bootstrap approximation is in a order of $L^{-1/2}$ rather than L^{-1}. The performance loss is due to the absence of the scale factor $\hat{\sigma}$, justifying the necessity of pivoting. From Result 1 and 2, we can conclude that the bootstrap resamples contain the statistical information embedded in the original

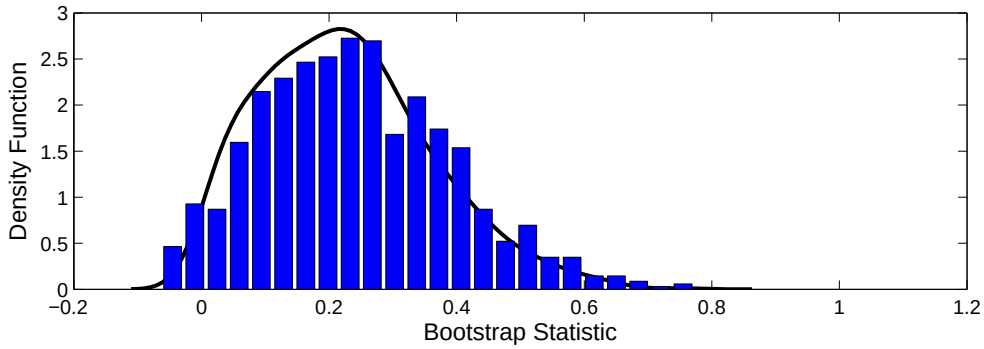

(a)

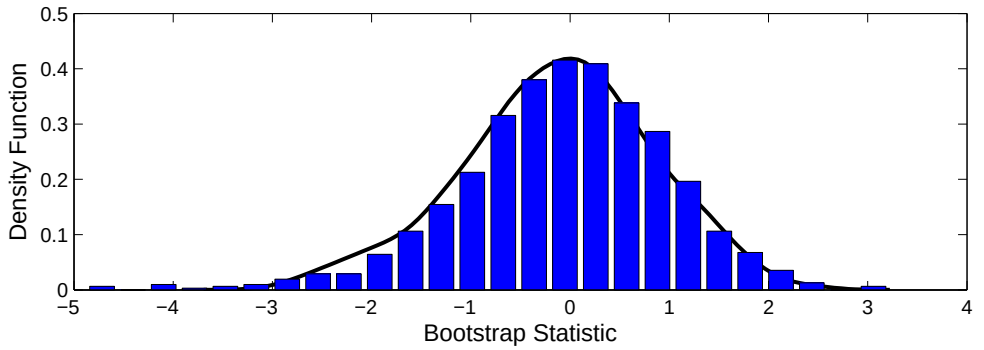

(b)

Figure 4.4: *Normalised histogram of* 500 *bootstrap statistic for: (a) eigenvalue based approach; and (b) energy based approach. Laplacian data is applied. The solid line is the probability density function of their test statistic under null hypothesis, obtained from* 1000 *Monte Carlo simulations.* $M = 4$ *receiving antennas and* $L = 100$ *samples.*

sample, which is of importance to the bootstrap hypothesis testing that we have discussed.

Recall the proposed eigenvalue based and energy based detectors. When the null hypothesis $\mathcal{H}_0$ holds, the bootstrap approximation for the null distribution of the test statistic, eqs. (4.9) and (4.18), are approximately in error by $L^{-1/2}$ and L^{-1}, respectively. Since the test threshold aims at maintaining a target false alarm probability, i.e., declaring $\mathcal{H}_1$ when $\mathcal{H}_0$ holds, its accuracy only relates to the null distribution of the test statistic. As shown in the results, when L is large, the accuracy of the test thresholds derived from bootstrap statistics can be guaranteed. In addition, the accuracy for the eigenvalue based detectors can be further improved by the bias reduction procedure. As shown in the simulations, empirically $L \sim 10^1$ leads to sufficiently accurate results.

To have an insight into the bootstrap approximation, we plot the density function of the test

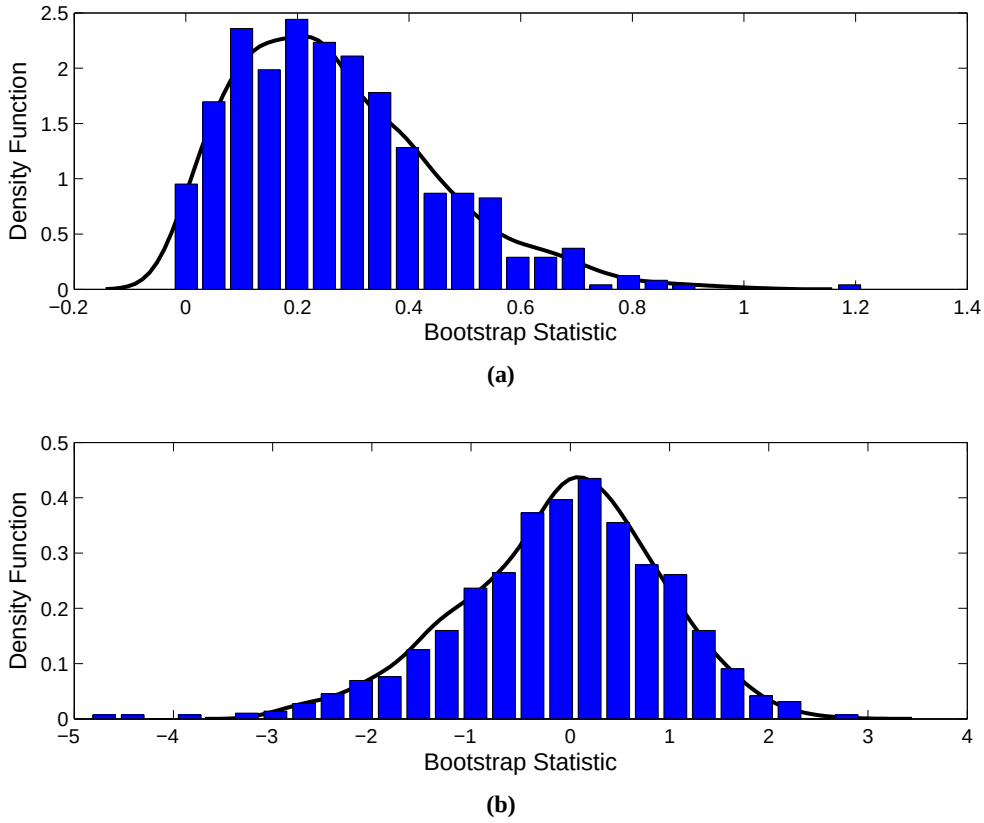

Figure 4.5: *Normalised histogram of* 500 *bootstrap statistic for: (a) eigenvalue based approach; and (b) energy based approach. Gaussian Mixture data is applied.* $M = 4$ *receiving antennas and* $L = 100$ *samples.*

statistics $\hat{T}_{EV}$ and $\hat{T}_{EG}$ under the null hypothesis, and the histogram of their bootstrap estimates in Figure 4.4 and Figure 4.5. Laplacian and Gaussian Mixture noise (defined later in eq. (4.25)) are applied, for $M = 4$ receiving antennas and sample size $L = 100$. It can be observed that for both the eigenvalue based and energy based detectors the bootstrap gives a sufficiently accurate approximation for the null distribution of the test statistic. In addition, Figure 4.4(b) and Figure 4.5(b) show that the pivotal statistic $\hat{T}_{EG}$ and its bootstrap version are approximately Gaussian distributed, regardless of noise types. This is a great advantage as with the help of pivoting, we only need to deal with a standard distribution instead of a broad class of distributions.

4.7 Simulation Results

In this section, the test performance of the proposed methods will be demonstrated by numerical experiments and we shall compare them with the conventional energy detector [8] and the KS

Detector	Legend	Assumptions	Sensing Complexity
Eigenvalue based detector, Table 4.1	Bootstrap-EV	Multiple receiving antennas	$O\left(BB_1M^3L\right)$
Energy based detector, Table 4.2	Bootstrap-EG	Noise power σ_w^2 is known	$O\left(BML\right)$
Conventional energy detector [8]	EG(Original)	Gaussian noise with known noise power σ_w^2	$O\left(ML\right)$
Kolmogorov-Smirnov based detector [32]	KS	Training noise samples with size L	$O\left(ML\right)$

Table 4.3: *Summary of the simulated detection algorithms. M: number of receiving antennas. L: sample size. B and B_1 denote the number of bootstrap replications for distribution approximation and sample eigenvalue bias correction, respectively.*

based detector [32] (given in eqs. (2.8) and (2.26), Chapter 2). As discussed in Chapter 2, the KS based detector, which requires a sequence of noise samples for training purpose, is another robust approach that can be applied to arbitrary noise types. A simple summary of the detectors to be simulated is outlined in Table 4.3.

For simplicity, both the primary signal and the fading channel $\mathbf{h}$ are generated by the zero-mean complex Gaussian distributed variates. According to the current requirements [92], the target false alarm is set as $P_f = 0.1$. The number of bootstrap replications for the null distribution approximation, i.e., B, and the sample eigenvalue bias reduction, i.e., $B1$, are set to be 500 and 30, respectively. All results are obtained by averaging over 5000 independent Monte Carlo trials. In addition, the SNR is defined as:

$$\text{SNR} \triangleq \frac{\sigma_s^2 \left\|\mathbf{h}\right\|^2}{M\sigma_w^2}. \tag{4.23}$$

To test the distribution-free property of the proposed detectors, we consider the following non-Gaussian noise types that are relevant in the context of cognitive radio:

1. Generalised Gaussian Model (GGM): The GGM is a broad family which adds a shaping parameter to the Gaussian distribution [101]. It is widely used to model the non-Gaussian noise such as heavy-tailed and impulsive noise [102]. The probability density function

(PDF) of GGM with a variance σ^2 and shape parameter ρ is given by:

$$f_w(w) = \frac{\rho\Gamma\left(4/\rho\right)}{2\pi\sigma^2\left(\Gamma\left(2/\rho\right)\right)^2}\exp\left(-\frac{1}{c}\left(\frac{|w|}{\sigma}\right)^{\rho}\right), \tag{4.24}$$

where $c \triangleq (\Gamma(2/\rho)\Gamma(4/\rho))^{\rho/2}$ and $\Gamma(\rho) = \int_0^\infty x^{\rho-1}e^{-x}dx$.

The GGM is short-tailed when $\rho > 2$ and heavy-tailed when $0 < \rho < 2$. The Gaussian ($\rho = 2$) and Laplacian ($\rho = 1$) distribution are special cases of GGM. In simulations, heavy-tailed Laplacian noise is applied.

2. Gaussian Mixture Model (GMM): The GMM is another popular model to describe the heavy-tailed non-Gaussian noise [81]. The corresponding PDF is:

$$f_w(w) = \sum_{i=1}^{I}\frac{c_i}{\pi\sigma_i^2}\exp\left(-\frac{|w|^2}{\sigma_i^2}\right), \tag{4.25}$$

where $c_i, \sigma_i^2 > 0$, $\sum_{i=1}^{I} c_i = 1$ and $\sum_{i=1}^{I} c_i\sigma_i^2 = \sigma^2$. A special case is ε-mixture model, where $I = 2$, $c_1 = 1-\epsilon$, $c_2 = \epsilon$, $\sigma_1^2 = \sigma^2/(1-\epsilon+\eta\epsilon)$ and $\sigma_2^2 = \eta\sigma_1^2$. Here, we choose $\epsilon = 0.06$ and $\eta = 10$ to model the man-made noise.

Accuracy of bootstrap

In this chapter, the nonparametric eigenvalue based detector, summarised in Table 4.1, and the energy based detector, summarised in Table 4.2, are proposed for spectrum sensing in arbitrary noise types with finite power. For both detectors, bootstrap procedures are applied to evaluate the test thresholds. In the first experiment, we test their accuracy under the GGM (Laplacian noise is applied as special case of GGM) and GMM distributed noise by evaluating their false alarm probability P_f against the sample size L in Figure 4.6 with $M = 4$ receiving antennas.

On one hand, it can be observed that both the two proposed bootstrap based detectors meet the target 10% false alarm probability for short data records, i.e., with $L = 100$ or less. Especially for the non-pivotal eigenvalue based method, with the help of bias reduction procedure, its accuracy is guaranteed in small samples. On the other hand, as shown in the figure, the conventional energy detector (marked as EG(Original)) fails in non-Gaussian noise as its false alarm probability far exceeds the target limit. For instance, given 0.1 as the target value, the false alarm probability of EG(Original) is approximately 0.2 and 0.27 under Laplacian and Gaussian Mixture noise, respectively. The reason is that its test threshold is evaluated based on

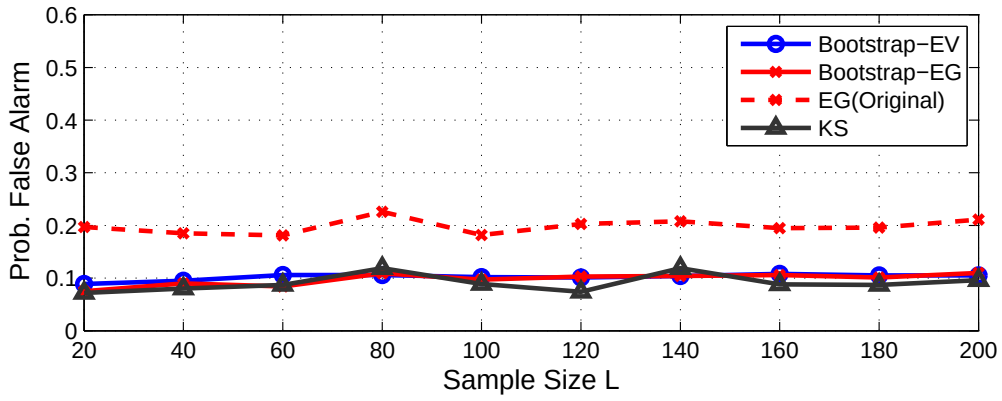

(a)

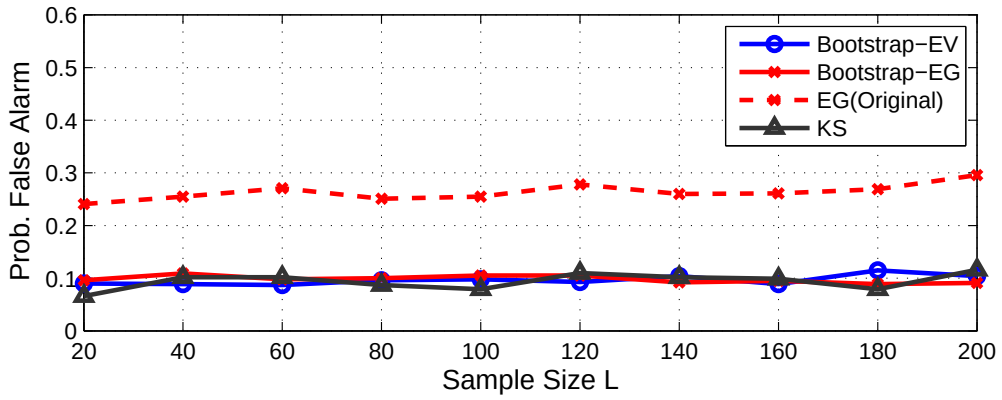

(b)

Figure 4.6: *Probability of false alarm versus sample size L, for: (a) Laplacian noise; (b) Gaussian Mixture noise. Target false alarm probability $P_f = 0.1$ and $M = 4$ receiving antennas are applied.*

the Gaussian noise assumption.

Detection performance

In the following experiments, the detection probability of the eigenvalue based detector and the energy based detector will be evaluated and compared with the KS based detector and the conventional energy detector. Note that the two proposed detectors and the KS based detector are distribution-free so they can be applied to both Gaussian and non-Gaussian noise.

In Figure 4.7, the detection probability P_d against SNR in Gaussian noise is presented, with $M = 4$ receiving antennas, sample size $L = 100$ and target false alarm probability $P_f = 0.1$. It can be observed that in Gaussian noise, the energy based detector performs the best and

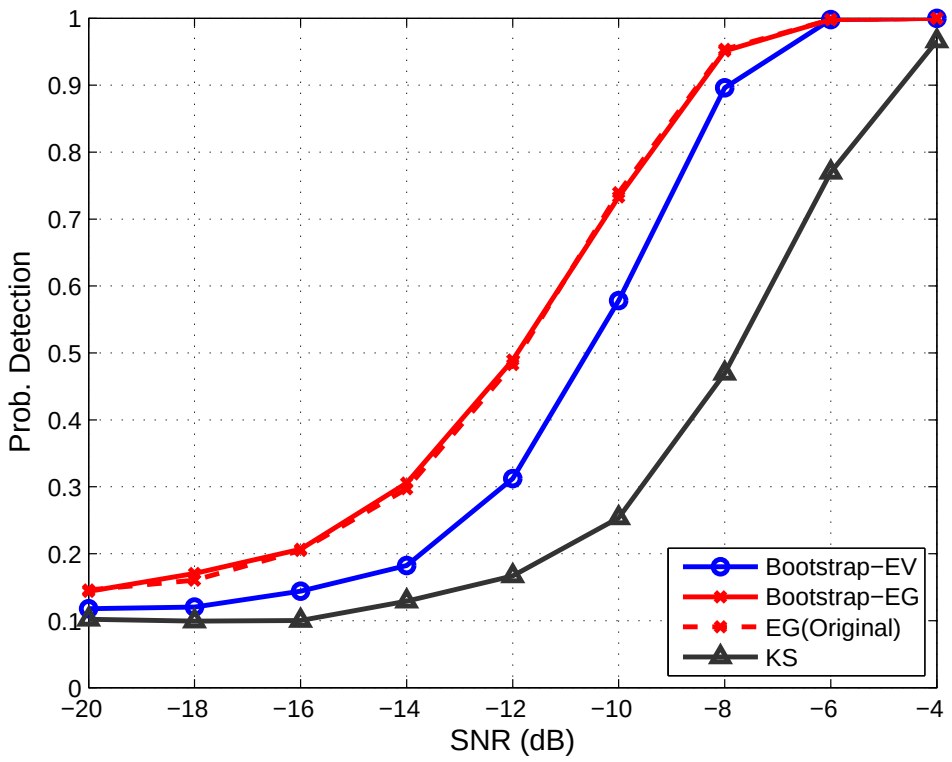

Figure 4.7: *Probability of detection versus SNR under Gaussian noise. Target false alarm probability* $P_f = 0.1$*,* $M = 4$ *receiving antennas and* $L = 100$ *samples.*

the nonparametric eigenvalue based detector has a better detection probability compared with the KS based detector. In addition, it is shown that the proposed energy based detector and the conventional energy detector have nearly the same detection probability in Gaussian noise. The reason is that the test statistic $\hat{T}_{EG}$ in (4.18) can be seen as a scaled test statistic of the conventional energy detector, i.e., eq. (2.8) in Chapter 2.

Then in Figure 4.8 and Figure 4.9, their detection performance in non-Gaussian noise, i.e., Laplacian noise and GMM noise, is investigated. Note that the performance gain achieved by the conventional energy detector, EG(original), should be ignored since it is impaired by the high false alarm probability in such cases, i.e., see in Figure 4.6(a) and Figure 4.6(b). Among the other three distribution-free detectors, the nonparametric eigenvalue based detector offers an overall superior detection performance in both Laplacian and GMM noise. For example, for GMM noise in Figure 4.8(b), to obtain a 90% detection probability, the eigenvalue based detector provides a 1 dB SNR gain compared with the energy based detector and KS detector.

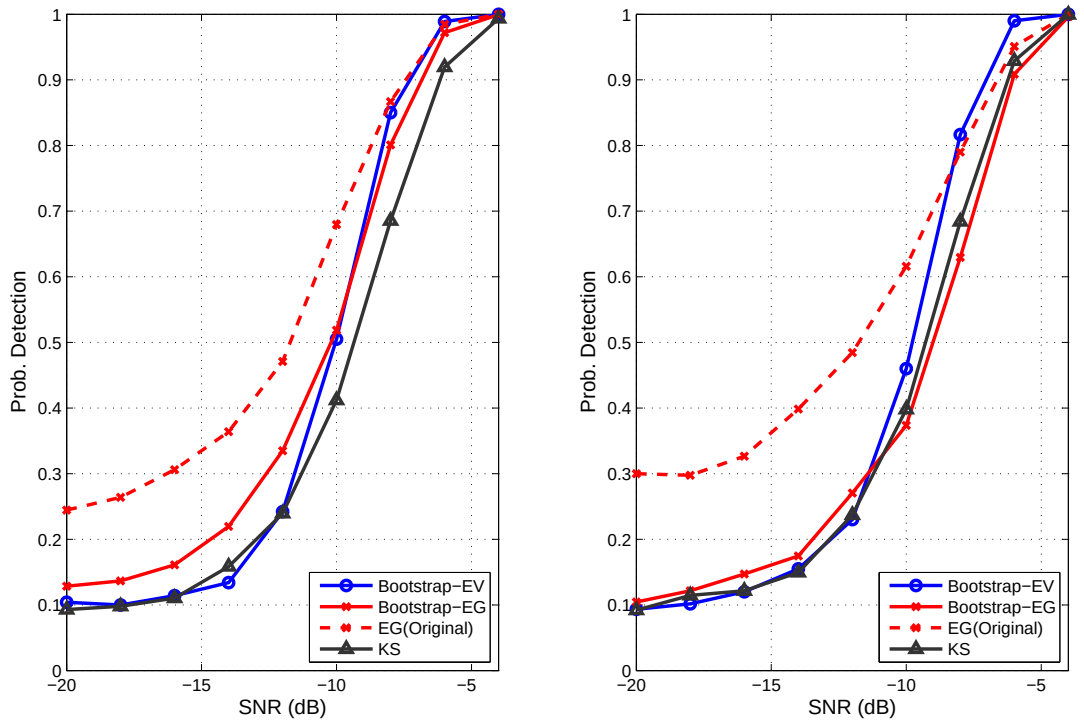

Figure 4.8: *Probability of detection versus SNR under: (a) Laplacian noise; and (b) Gaussian Mixture noise. Target false alarm probability* $P_f = 0.1$, $M = 4$ *receiving antennas and* $L = 100$ *samples.*

In addition, the proposed energy based detector holds its superiority in low SNR regime, i.e., an up to 2 dB SNR gain is achieved by Bootstrap-EG, as shown in Figure 4.8(a) for Laplacian noise.

In Figure 4.9, the impact of the receiver array size M is presented, where we fix the SNR $= -8$ dB and vary the number of antennas from 2 to 8. Note that the eigenvalue based method requires at least two antennas to exploit the eigenstructure of sample covariance matrix while others do not make this assumption. It can be observed that when $M = 2$, the eigenvalue based detector is inferior to the energy based detector and KS based detector. However, when M increases, a significant performance improvement can be achieved by the eigenvalue based approach, i.e., it performs the best when $M \geq 4$ in both Laplacian and Gaussian mixture noise. The reason is that the eigenvalue based approach measures the difference between sample eigenvalues. When SNR in (4.23) is fixed, larger M indicates a relatively bigger response

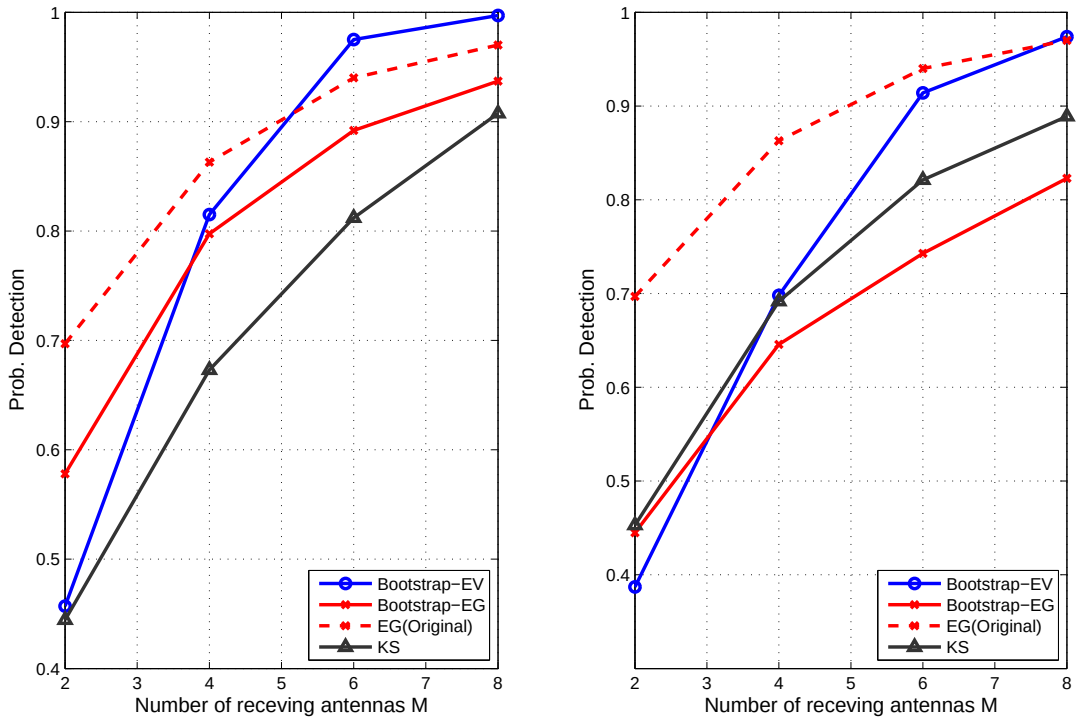

Figure 4.9: *Probability of detection versus number of receiving antennas,* M*, under: (a) Laplacian noise; and (b) Gaussian Mixture noise. Target false alarm probability* $P_f = 0.1$*, SNR* $= -8$ *dB and* $L = 100$ *samples.*

in the signal dimension and a more significant difference between sample eigenvalues. Hence, a performance gain can be expected for the eigenvalue based detector when multiple antennas are available.

Discussion

In summary, by applying the bootstrap resampling procedure, both the eigenvalue based and energy based detectors maintain the predetermined false alarm probability in a variety of noise types. By contrast, most of state-of-art methods tend to yield unacceptably high false alarm probabilities in non-Gaussian noise.

When the noise is non-Gaussian, the eigenvalue based detector has an overall better detection probability. The energy based detector is simple to implement and has a good performance in

the low SNR regime. The main issue for these two detectors is the computational complexity. As they rely on random resampling with replacement, the complexity will grow linearly with the number of bootstrap replications, i.e., see in Table 4.3. However, when the sample size is moderate, such complexity is compatible with the computer power today.

4.8 Conclusion

In this chapter, we studied the spectrum sensing problem in the situation of unknown noise type, introduced and highlighted the powerful bootstrap technique.

Two detection methods are proposed by using the bootstrap procedure. The first eigenvalue based detector is *blind*, which is fundamentally a binary hypothesis test for the difference between sample eigenvalues. We assume that when primary signal exists, the difference between eigenvalues will be relatively larger than the noise only case. When the sample size is small, the bias in sample eigenvalue may make the test statistic under null and alternative hypothesis not be well separated. To improve the accuracy of the test statistic, we also propose a bootstrap bias reduction procedure. The second energy based detector, similar to the conventional energy detector, assumes the value of noise power is known and compares it with the received sample energy. The difference is that we studentize the test statistic and generalize its application to arbitrary noise types by using bootstrap.

For both detectors, the bootstrap resampling is applied to non-parametrically estimate the test statistic's null distribution. It is shown that for a moderate sample size, such as 100 samples, the bootstrap gives a sufficiently accurate approximation, leading to a test threshold that maintaining a target false alarm probability. In addition, the important role of pivot is discussed. We showed that the bootstrap test with pivoting, such as the energy based detection, has a standardizing null distribution that does not depend on the unknown noise types.

The detection performance of proposed detectors is evaluated numerically and compared with the nonparametric KS detector and the conventional energy detector. Simulation results have shown that both the proposed detectors are valid in a variety of noise types. In non-Gaussian noise, the eigenvalue based method offers an overall better detection probability and a performance gain can be expected when the more receiving antennas are available. The energy based detector has relatively low computational complexity and outperforms other simulated detection methods in the low SNR regime.

In Chapter 5, another sensing technique for non-Gaussian noise, i.e., the F-statistic based sensing, will be proposed. This detector is based on the F-test discussed in Chapter 3 and we shall generalise its application to non-Gaussian noise. The bootstrap technique will be applied to estimate the null distribution of the F-statistic when the *prior* knowledge on the noise is limited.

Chapter 5
F-statistic Based Spectrum Sensing for Non-Gaussian Noise

5.1 Introduction

This chapter develops a robust F-statistic based detection method for spectrum sensing in non-Gaussian noise. It is well known that in linear regression with Gaussian errors, the F-statistic follows an F-distribution under the null hypothesis. Motivated by the invariance property under different noise levels, an F-test based spectrum sensing scheme was presented in Chapter 3. Simulation results therein showed that in addition to enhanced robustness against noise level uncertainty, the F-test based detector is more powerful than several standard spectrum sensing techniques. In this chapter, we shall generalise its application to non-Gaussian noise.

When the noise distribution is not Gaussian, a major concern is to control the false alarm probability as the null distribution of the F-statistic becomes unpredictable. For example, as shown in Section 5.6, the false alarm probability of the conventional F-statistic based detector far exceeds the target value under heavy-tailed noise, leading to unexpected interference to the primary user. To tackle this problem, the null distribution of the F-statistic for general noise distributions needs to be addressed.

Several papers in the statistical literature have considered this issue. In [103, 104], a general investigation was carried out by evaluating the cumulants of a linear function used in the F-test. The authors in [105] considered the case of global null, i.e., assuming the data is noise only under the null hypothesis, and they approximated the mean and the variance of $\log F$ statistic by its permutation moments. It is shown that the sensitivity to non-Gaussian distribution depends highly on the numerical values of regression variables. In [106], a more general null hypothesis was considered and a simple degrees-of-freedom modification method was proposed to approximate the null distribution of the F-statistic. Note that all the previous studies focus on real-valued data, which needs to be extended to complex-valued data for I/Q-demodulation that is used in practical communication systems.

In this chapter, we consider a robust F-statistic based detector for non-Gaussian noise with complex-valued measurements. By exploiting different *prior* knowledge of the noise, two novel methods are developed to estimate the null distribution of the F-statistic. The main contributions are summarised as follows:

• Firstly, we assume that the normalised kurtosis of the noise is finite and known. The null distribution of the F-statistic is approximated by an F-distribution with modified degrees of freedom (MDOF), where a simple closed form result is obtained by matching the first two moments of the log test statistic with those of a log$F$ distribution.

• Secondly, we relax the assumption on the noise kurtosis and propose a nonparametric approach which is based on the numerical bootstrap procedure. Given a moderate size of training noise samples, the bootstrap approach approximates the null distribution of the test statistic by resampling the training data and no knowledge of the underlying noise statistics is required.

• Simulation results show that by applying either of the two proposed methods with samples $L > 500$, good detection probability is achieved by the F-statistic based detector under non-Gaussian noise while maintaining the predetermined false alarm probability.

• The robust F-statistic based detector has general validity which could be generalised to other linear regression problems with complex number measurements.

The rest of this chapter is structured as follows. The data model and problem statement are demonstrated in Section 5.2. Then the degrees-of-freedom modification approach for the null distribution approximation is developed in Section 5.3. The bootstrap based method is discussed in Section 5.4. In Section 5.5, we extends our results to a more general linear regression hypothesis testing problem. Simulation results are presented in Section 5.6 and Section 5.7 concludes the chapter.

5.2 System Model and Problem Statement

Recall the SIMO system model defined in Chapter 3, Section 3.2. As shown in Figure 3.1, we consider a cognitive radio network where one primary signal source may exist within the range of the secondary user and the sensing device comprises M antennas.

Let $\mathbf{y}(l) = [y_1(l), y_2(l), \ldots, y_M(l)]^T$, $(l = 0, 1, \ldots, L-1)$, be the size M baseband signal

vectors at the receiver antenna array with L denoting the sample size. Then the spectrum sensing problem can be formulated as the following hypothesis test:

$$\begin{aligned} \mathcal{H}_0 &: \mathbf{y}(l) = \mathbf{w}(l), \\ \mathcal{H}_1 &: \mathbf{y}(l) = \mathbf{h}s(l) + \mathbf{w}(l),\ l = 0, 1, ..., L-1. \end{aligned} \tag{5.1}$$

where $s(l)$ represents the primary signal, which is assumed to be unknown and deterministic. The vector $\mathbf{h} = [h_1, h_2, \ldots, h_M]^T$ denotes the known time-invariant propagation channel. The noise $\mathbf{w}(l) = [w_1(l), w_2(l), \ldots, w_M(l)]^T$ is characterised by a circular, symmetric distribution with zero mean and covariance $\sigma_w^2\mathbf{I}$. Note that the noise variance σ_w^2 is assumed to be finite.

As mentioned in Chapter 3, Section 3.2, the acquisition of CSI $\mathbf{h}$ is still an open question in spectrum sensing due to lack of reciprocal communication standards between primary and secondary users. Possible solutions are acquiring $\mathbf{h}$ via the periodically transmitted pilot primary signal [11, 83, 84] or recursively estimating it during the sensing period [84–86].

Given the signal model (5.1) and a Gaussian noise assumption, an F-test can be applied to decide whether primary signals exist or not. As discussed in Chapter 3, the decision rule is given by:

$$T_F \underset{\mathcal{H}_0}{\overset{\mathcal{H}_1}{\gtrless}} \gamma, \tag{5.2}$$

where γ denotes the test threshold and the test statistic T_F, also known as the F-statistic, is given by:

$$T_F = \frac{n_2}{n_1} \frac{\sum_{l=0}^{L-1} \mathbf{y}(l)^H \mathbf{P} \mathbf{y}(l)}{\sum_{l=0}^{L-1} \mathbf{y}(l)^H (\mathbf{I} - \mathbf{P}) \mathbf{y}(l)}, \tag{5.3}$$

where $\mathbf{P} = \mathbf{h}(\mathbf{h}^H\mathbf{h})^{-1}\mathbf{h}^H$ represents the projection onto the subspace spanned by $\mathbf{h}$. When the noise is complex Gaussian distributed, i.e., $\mathbf{w}(l) \sim \mathcal{CN}\left(0, \sigma_w^2\mathbf{I}\right)$, the test statistic T_F under the null hypothesis $\mathcal{H}_0$ is F_{n_1,n_2}-distributed with degrees of freedom [87]:

$$n_1 = 2L, \tag{5.4}$$

$$n_2 = 2L(M-1). \tag{5.5}$$

Given a target false alarm rate α, the test threshold γ can be easily obtained using numerical tables of the F-distribution. In this chapter, the null distribution of the F-statistic in (5.3) may

no longer be F-distributed as the noise is not necessarily Gaussian distributed. In the following sections, two approaches will be proposed to tackle this problem by exploiting different *prior* knowledge of the noise.

It is worth mentioning that the impact of CSI uncertainty in estimates of $\mathbf{h}$ is studied in Chapter 3. Results show that under a Gaussian noise assumption, the F-test based detector has a fixed false alarm rate, independent of the accuracy of channel estimation. The reason is that the null distribution of the F-statistic remains unchanged in this case. When the noise is not Gaussian distributed, as it is in this chapter, a constant false alarm rate can also be obtained as the test statistic (5.3) and the following approaches for the null distribution approximation are all based on the CSI estimates.

5.3 Degrees-of-Freedom Modification

In this section, we assume the normalised kurtosis of the noise is finite and known. We shall use it to approximate the test statistic's null distribution by an F-distribution with modified degrees of freedom (MDOF). This approach is inspired by the robust F-tests suggested in [88, 106] for real number problems. For wireless communication systems, the results therein need to be generalised to complex-valued samples.

Preliminaries

To begin with, we define the normalised kurtosis [107] of a complex random variable $\mathcal{Z}$ as:

$$K_c\left[\mathcal{Z}\right] \triangleq \frac{\mathrm{E}\left[\left|\mathcal{Z}\right|^4\right] - \left|\mathrm{E}[\mathcal{Z}^2]\right|^2}{\left[\mathrm{E}\left[\left|\mathcal{Z}\right|^2\right]\right]^2} - 2. \tag{5.6}$$

The kurtosis $K_c\left[\mathcal{Z}\right]$ is a measure of whether the probability distribution of $\mathcal{Z}$ is peaked or flat compared with a Gaussian distribution. The "minus 2" in this formula acts as a correction factor so that the kurtosis of Gaussian distribution becomes zero. The variate with positive kurtosis tends to have a peak probability density near the mean value so that it becomes heavy-tailed. On the contrary, the one with negative kurtosis tends to have a flat top near the mean and thus has short tail.

Since the noise elements $w_i(l), i = 1, 2, ..., M$, are circularly symmetric and i.i.d, the corre-

sponding normalised kurtosis κ can be expressed as:

$$\kappa \triangleq K_c\left[w_i(l)\right] = \frac{\mu_4}{\sigma_w^4} - 2, \tag{5.7}$$

where $\mu_4 \triangleq \mathrm{E}\left[|w_i(l)|^4\right]$ and $\sigma_w^4 \triangleq \mathrm{E}\left[|w_i(l)|^2\right]^2$.

Define $\mathbf{P}_1 \triangleq \mathbf{P}$, with rank $r_1 = 1$, and $\mathbf{P}_2 \triangleq \mathbf{I}_M - \mathbf{P}$, with rank $r_2 = M - 1$. The quadratic form of the data vector $\mathbf{y}(l)$ has the following properties.

Property 5.1. $\mathbf{P}_k$ $(k = 1, 2)$ is the projection matrix with rank r_k. Define $\mathbf{p}_k$ be the column vector consisting of diagonal elements of $\mathbf{P}_k$. When the null hypothesis $\mathcal{H}_0$ holds, the expectation, variance and covariance of the quadratic form $\sum_{l=0}^{L-1}\mathbf{y}(l)^H\mathbf{P}_k\mathbf{y}(l)$ are given as follows:

$$\mathrm{E}\left[\sum_{l=0}^{L-1}\mathbf{y}(l)^H\mathbf{P}_k\mathbf{y}(l)|\mathcal{H}_0\right] = L\sigma_w^2 r_k. \tag{5.8}$$

$$\mathrm{Var}\left[\sum_{l=0}^{L-1}\mathbf{y}(l)^H\mathbf{P}_k\mathbf{y}(l)|\mathcal{H}_0\right] = L\sigma_w^4\left(r_k + \kappa\left\|\mathbf{p}_k\right\|^2\right). \tag{5.9}$$

$$\mathrm{Cov}\left[\sum_{l=0}^{L-1}\mathbf{y}(l)^H\mathbf{P}_1\mathbf{y}(l),\ \sum_{l=0}^{L-1}\mathbf{y}(l)^H\mathbf{P}_2\mathbf{y}(l)|\mathcal{H}_0\right] = L\sigma_w^4\kappa\mathbf{p}_1'\mathbf{p}_2. \tag{5.10}$$

Proof. See Appendix A. □

Note that the proof of Property 5.1 is similar to those based on real-valued data [88]. The main difference is that the analysis of eqs. (A.3) - (A.10) in Appendix A takes the properties of complex samples into account.

The properties of the F-statistic in (5.3) is difficult to evaluate numerically as it consists of a ratio of two variates. To simplify calculations, the logarithm of the F-statistic is considered instead, as shown in Property 5.2.

Property 5.2. Consider the logarithm of F-statistic:

$$Z = \frac{1}{2}\log T_F(n_1, n_2) = \frac{1}{2}(\log S_1^2 - \log S_2^2), \tag{5.11}$$

where

$$S_k^2 = \sum_{l=0}^{L-1}\mathbf{y}\left(l\right)^H\mathbf{P}_k\mathbf{y}\left(l\right)/2Lr_k,\ k = 1, 2. \tag{5.12}$$

Under the null hypothesis $\mathcal{H}_0$ and for large Lr_k, the expectation and variance of Z can be expressed approximately as:

$$\mathrm{E}[Z|\mathcal{H}_0] \sim \left(r_2^{-1} + r_2^{-2}\kappa \left\|\mathbf{p}_2\right\|^2 - r_1^{-1} - r_1^{-2}\kappa \left\|\mathbf{p}_1\right\|^2\right)/4L, \tag{5.13}$$

$$\mathrm{Var}[Z|\mathcal{H}_0] \sim \left(r_1^{-1} + r_1^{-2}\kappa \left\|\mathbf{p}_1\right\|^2 + r_2^{-1} + r_2^{-2}\kappa \left\|\mathbf{p}_2\right\|^2 - 2r_1^{-1}r_2^{-1}\kappa\right)/4L. \tag{5.14}$$

Proof. See Appendix B . □

The results described above are derived from the Taylor expansion of $\log S_k^2$ around $\log \sigma_w^2/2$ up to the third and second order term (see eqs. (B.1) and (B.5) in Appendix B), respectively. Since S_k^2 in (5.12) is an unbiased estimate of $\sigma_w^2/2$ under the null hypothesis $\mathcal{H}_0$, the higher order terms $O\left(\left(S_k^2 - \sigma_w^2/2\right)^3\right)$ for $\mathrm{E}[Z|\mathcal{H}_0]$ and $O\left(\left(S_k^2 - \sigma_w^2/2\right)^2\right)$ for $\mathrm{Var}[Z|\mathcal{H}_0]$ can be neglected for large value of Lr_k.

In practical communication systems, i.e., for a typical narrowband RF channel with 10kHz bandwidth, the power of thermal noise is generally around -134 dBm and man-made noise may be 20 dB stronger [108]. Hence, the noise power σ_w^2 is usually in the order of $10^{-15} \sim 10^{-17}$ and so is the variance estimate S_k^2. The approximation errors in (B.1) and (B.5) are in the order of $10^{-30} \sim 10^{-34}$ and $10^{-45} \sim 10^{-51}$, respectively. Therefore, the accuracy of eqs. (5.13) and (5.14) should hold in practical systems.

Modified Degrees of Freedom (MDOF) Approach

In Property 5.2, we derived the approximate mean and variance of the logarithm of F-statistic for arbitrary noise types in terms of the noise kurtosis κ. For Gaussian noise, $\kappa = 0$, leading to the following expressions:

$$\mathrm{E}[Z_F|\mathcal{H}_0] \sim \frac{(\frac{m_2}{2L})^{-1} - (\frac{m_1}{2L})^{-1}}{4L}, \tag{5.15}$$

$$\mathrm{Var}[Z_F|\mathcal{H}_0] \sim \frac{(\frac{m_2}{2L})^{-1} + (\frac{m_1}{2L})^{-1}}{4L}. \tag{5.16}$$

Where $Z_F = \frac{1}{2}\log F(m_1, m_2)$ denotes a special case of $Z = \frac{1}{2}\log T_F(n_1, n_2)$ with $T_F(n_1, n_2)$ replaced by an F_{m_1,m_2}-distributed random variable.

To approximate the null distribution of $T_F(n_1, n_2)$ in (5.3) with an F-distribution, we compare the mean and variance in the Gaussian case, i.e., eqs (5.15) and (5.16), with that for the

non-Gaussian case, i.e., eqs (5.13) and (5.14), respectively and obtain the modified degrees of freedom as follows:

$$m_1 = n_1 \left(1 + 2L\kappa \left(\frac{\|\mathbf{p}_1\|^2}{n_1} - \frac{\mathbf{p}_1'\mathbf{p}_2}{n_2}\right)\right)^{-1}, \tag{5.17}$$

$$m_2 = n_2 \left(1 + 2L\kappa \left(\frac{\|\mathbf{p}_2\|^2}{n_2} - \frac{\mathbf{p}_1'\mathbf{p}_2}{n_1}\right)\right)^{-1}, \tag{5.18}$$

where the degrees of freedom $n_1 = 2Lr_1$ and $n_2 = 2Lr_2$. In other words, when the noise kurtosis κ is known, the null distribution of the test statistic T_F and test threshold γ can be approximated by the F-distribution with the help of eqs. (5.17) and (5.18).

Since the MDOF approach is based on the first two moments, its accuracy will depend on the similarity between the F-distribution and the underlying distribution of T_F. The F-statistic originally arises as the ratio of two chi-squared variates [87] and the test statistic T_F can be written as $T_F = S_1^2/S_2^2$ where $S_k^2(k = 1, 2)$ is given in (5.12). According to the CLT, for large L, both the chi-squared variate and S_k^2 are approximately Gaussian distributed [109]. Therefore, the proposed MDOF method will approach the null distribution of T_F when L is large and empirically it has been found that $L \sim 10^1$ is sufficient, as shown in the simulation results.

5.4 The Bootstrap Approximation

As discussed in Chapter 4, the bootstrap is a data-based method that can estimate the empirical distribution of a statistic via resampling with replacement. In this section, we apply the bootstrap procedure to approximate the null distribution of the log F-statistic in non-Gaussian noise. Unlike the MDOF method which takes knowledge of noise kurtosis κ as a *prior*, the bootstrap approach is nonparametric and requires a set of noise samples with size L for training purposes, i.e., $\mathcal{W} = [\mathbf{w}(0), \mathbf{w}(1), \ldots, \mathbf{w}(L-1)]$, which can be collected when the primary user is known for sure to be absence. The null distribution of the test statistic is approximated by resampling the data set $\mathcal{W}$ repeatedly, leading to a test threshold that ensures a target false alarm probability. Note that the assumption on $\mathcal{W}$ is exactly the same as used in the conventional energy detector which estimates the noise power from training noise samples.

Recall the hypothesis testing problem in (5.2). When $Z = \frac{1}{2}\log T_F(n_1, n_2)$ is used as the test

Input:	Training noise samples $\mathcal{W} = [\mathbf{w}(0), \mathbf{w}(1), \ldots, \mathbf{w}(L-1)]$. Target false alarm probability α.
1)	Draw a bootstrap sample set $\mathcal{W}^*$ via resampling $\mathcal{W}$ with replacement. An example can be : $\mathcal{W}^* = [\mathbf{w}(1), \mathbf{w}(7), \mathbf{w}(7), \ldots, \mathbf{w}\,(2)]$.
2)	Compute the bootstrap test statistic Z^* using $\mathcal{W}^*$.
3)	Repeat 1) and 2) B times. One obtains the bootstrap test statistics : $[Z^*(1), Z^*(2), \ldots, Z^*(B)]$.
4)	Correct the mean of bootstrap test statistics: $\hat{Z}^*(b) = Z^*(b) - \frac{1}{B}\sum_{b=1}^{B} Z^*(b)$
5)	Ranking the bootstrap statistics as: $\hat{Z}^*(1) \leq \hat{Z}^*(2) \leq \ldots \leq \hat{Z}^*(B)$.
6)	From the ordered statistics, choose the index b_α by: $1 - \frac{b_\alpha+1}{B} \leq \alpha \leq 1 - \frac{b_\alpha}{B}$.
Output:	The test threshold $\gamma = \hat{Z}^*(b_\alpha)$.

Table 5.1: *The bootstrap procedure for approximating the null distribution of Z*

statistic, the decision rule becomes:

$$Z \underset{\mathcal{H}_0}{\overset{\mathcal{H}_1}{\gtrless}} \gamma, \tag{5.19}$$

where γ is the corresponding test threshold. The statistic Z is applied as a sample mean correction step will be involved later and the statistical exception of a log statistic is easier to obtain. In addition, using (5.19) is equivalent to (5.2) due to the monotonicity of the logarithm function.

When the null hypothesis $\mathcal{H}_0$ holds, the statistic $Z(\mathcal{H}_0)$ can be written as:

$$Z(\mathcal{H}_0) = \frac{1}{2}\log\frac{n_2}{n_1}\frac{\sum_{l=0}^{L-1}\mathbf{w}(l)^H\mathbf{P}\mathbf{w}(l)}{\sum_{l=0}^{L-1}\mathbf{w}(l)^H(\mathbf{I}_M - \mathbf{P})\mathbf{w}(l)}. \tag{5.20}$$

To obtain the test threshold γ, we run the algorithm of Table 5.1. By resampling $\mathcal{W}$ with replacement, the distribution of $Z(\mathcal{H}_0)$ is approximated by a set of bootstrap statistics, i.e., $\left\{\hat{Z}^*\,(b)\,,\, b = 1, 2, ..., B\right\}$. Then given a target false alarm probability, the test threshold γ can be derived from the bootstrap approximation of the null distribution.

It is worth mentioning that the bootstrap resampling for testing regression hypothesis should be based on the estimation of the i.i.d residuals [97], i.e., $\hat{\mathbf{w}}(l)$. The evaluation of $\hat{\mathbf{w}}(l)$ arises a

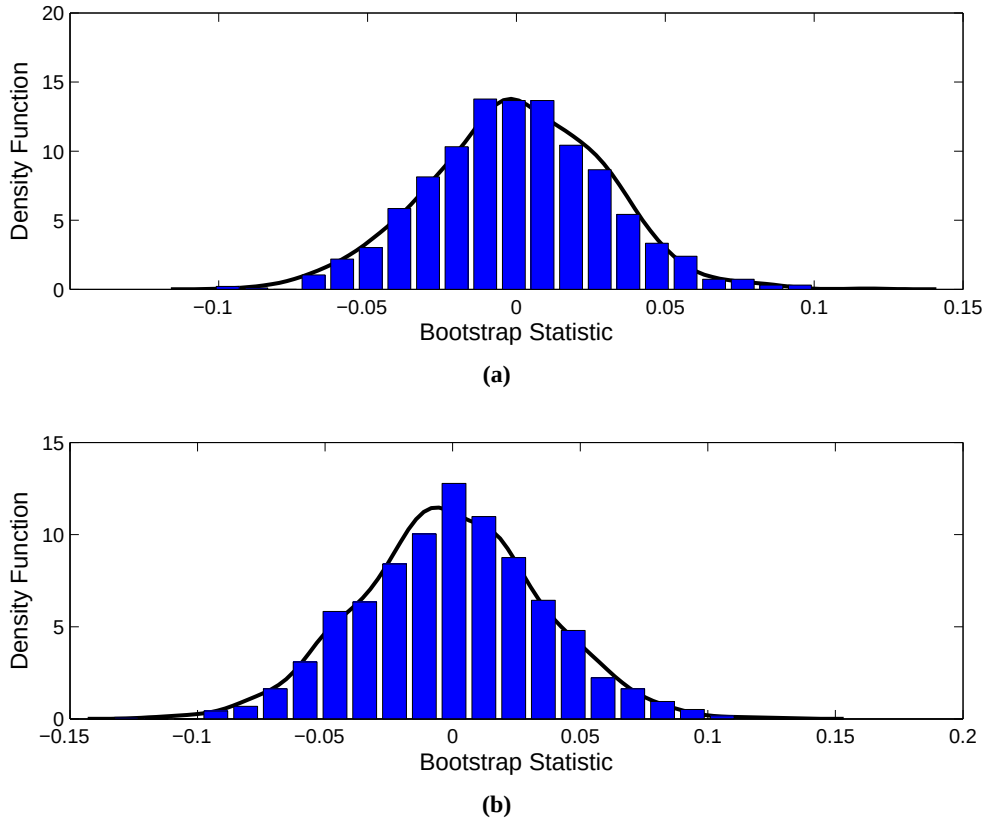

Figure 5.1: *Normalised histogram of* 500 *bootstrap statistics,* $\hat{Z}^*$*, under: (a) Laplacian noise; and (b) Gaussian Mixture noise. The solid line is the empirical probability density function of* $Z(\mathcal{H}_0)$*, obtained from* 1000 *Monte Carlo simulations.* $L = 500$ *samples and* $M = 4$ *receiving antennas.*

problem that whether we impose the null hypothesis or not, and the corresponding effects have been investigated in [110]. Here, this problem is simplified as we assume the noise only data $\mathcal{W}$ is available so that the bootstrap data in Table 5.1 is generated via resampling $\mathcal{W}$ directly.

To improve the accuracy of the bootstrap estimate, a sample mean correction step [97] is also included in Table 5.1, where the bootstrap statistic $Z^*(b)$ will be corrected by:

$$\hat{Z}^*(b) = Z^*(b) - \left(\frac{1}{B} \sum_{b=1}^{B} Z^*(b) - \mathrm{E}[Z|\mathcal{H}_0] \right). \tag{5.21}$$

As shown in the proof of Property 5.2, the first two terms of the approximation for $\mathrm{E}[Z|\mathcal{H}_0]$ are constant, independent of the higher order statistical moments of the noise. Replacing $\mathrm{E}[Z|\mathcal{H}_0]$ in (5.21) with the Taylor expansion up to second order terms in (B.5) and combining with (B.7)

lead to the following result:

$$\mathrm{E}[Z|\mathcal{H}_0] \sim 0. \tag{5.22}$$

Note that the higher order terms for $\mathrm{E}[Z|\mathcal{H}_0]$ in (5.22) becomes $O\left(\left(S_k^2 - \sigma_w^2/2\right)^2\right)$ rather than $O\left(\left(S_k^2 - \sigma_w^2/2\right)^3\right)$ for $\mathrm{E}[Z|\mathcal{H}_0]$ in (5.13). As discussed above, the two order approximation is still sufficiently accurate as the error is generally in a order of $10^{-30} \sim 10^{-34}$ in practical systems.

Consequently, the corrected bootstrap statistic becomes:

$$\hat{Z}^*(b) = Z^*(b) - \frac{1}{B}\sum_{b=1}^{B} Z^*(b). \tag{5.23}$$

The coverage error for this non-pivotal bootstrap regression approximation is generally $O(L^{-1/2})$ [95]. To guarantee a typical 10% false alarm probability [92], L should be larger than 10^3 samples. However, we find that empirically $L = 500$ gives satisfactory results for the simulated noise distributions. An example is presented in Figure 5.1. It can be observed that under Laplacian noise and Gaussian Mixture noise, the histogram of bootstrap statistic $\hat{Z}^*$ and the empirical distribution of $Z(\mathcal{H}_0)$ are well matched with $L = 500$ samples. Although the sample needed is larger than the MDOF approach, note that the bootstrap method is nonparametric and does not require knowledge of the noise kurtosis κ.

5.5 Extensions

In addition to the spectrum sensing problem, the robust F-statistic based methods can be applied to other linear regression problems with complex number measurements. Previous sections refer only to the case of single primary signal source and global null hypothesis, i.e., the data is assumed to be noise only under the null hypothesis. In this section, we shall extend the previous results by considering a more general linear regression problem.

Consider a linear data model :

$$\mathcal{H}_1 : \mathbf{y}(l) = \sum_{i=1}^{p} \mathbf{h}_i s_i(l) + \mathbf{w}(l),\ l = 0, 1, ..., L-1, \tag{5.24}$$

where $\mathbf{y}(l) = [y_1(l), y_2(l), \ldots, y_M(l)]^T$ is the size M observation vector. $s_i(l)$ is the ith regres-

sion coefficient and $\mathbf{h}_i = [h_{i,1}, h_{i,2}, \ldots, h_{i,M}]^T$ denotes the corresponding regressor vector, for $i = 1, 2, \ldots, p$ and $p < M$. $\mathbf{w}(l) = [w_1(l), w_2(l), \ldots, w_M(l)]^T$ denotes the i.i.d error/noise term.

The problem of interest is whether we can set some regression coefficients to be zero. Consider a null hypothesis with $s_{q+1}(l) = s_{q+2}(l) = \ldots = s_p(l) = 0$, then the corresponding data model becomes:

$$\mathcal{H}_0 : \mathbf{y}(l) = \sum_{i=1}^{q} \mathbf{h}_i s_i(l) + \mathbf{w}(l),\ l = 0, 1, ..., L-1. \tag{5.25}$$

To test $\mathcal{H}_0$ in (5.25) against the alternative $\mathcal{H}_1$ in (5.24), the F-statistic based detector can be applied, with the test statistic given by:

$$\Lambda_F = \frac{n_{\Lambda,2}}{n_{\Lambda,1}} \frac{\sum_{l=0}^{L-1} \mathbf{y}(l)^H \left(\mathbf{P}_A - \mathbf{P}_N\right) \mathbf{y}(l)}{\sum_{l=0}^{L-1} \mathbf{y}(l)^H \left(\mathbf{I} - \mathbf{P}_A\right) \mathbf{y}(l)}, \tag{5.26}$$

where $\mathbf{P}_A$ and $\mathbf{P}_N$ denote the projection onto the subspaces spanned by $[\mathbf{h}_1, \ldots, \mathbf{h}_p]$ and $[\mathbf{h}_1, \ldots, \mathbf{h}_q]$, respectively. When the error/noise term $\mathbf{w}(l)$ is complex Gaussian distributed, the test statistic Λ_F follows an $F_{n_{\Lambda,1}, n_{\Lambda,2}}$-distribution, with degrees of freedom:

$$n_{\Lambda,1} = 2L(p-q), \tag{5.27}$$

$$n_{\Lambda,2} = 2L(M-p). \tag{5.28}$$

Note that F-statistic in (5.3) used for spectrum sensing problem considers the special case with $p = 1$ and $q = 0$.

When $\mathbf{w}(l)$ is not Gaussian distributed, the results in Property 5.1 and Property 5.2 still hold since $(\mathbf{P}_A - \mathbf{P}_N)$, $(\mathbf{I} - \mathbf{P}_A)$ and $(\mathbf{P}_A - \mathbf{P}_N) + (\mathbf{I} - \mathbf{P}_A) = (\mathbf{I} - \mathbf{P}_N)$ are projection matrix. Hence, the proposed MDOF and bootstrap methods are also valid to estimate the null distribution of Λ_F.

On one hand, the MDOF method can be applied if the kurtosis of $w_i(l)$, κ, is known. That is, the null distribution of Λ_F can be approximated by an F-distribution with the modified degrees

of freedom:

$$m_{\Lambda,1} = n_{\Lambda,1}\left(1+2L\kappa\left(\frac{\|\mathbf{p}_1\|^2}{n_1}-\frac{\mathbf{p}_1'\mathbf{p}_2}{n_2}\right)\right)^{-1}, \tag{5.29}$$

$$m_{\Lambda,2} = n_{\Lambda,2}\left(1+2L\kappa\left(\frac{\|\mathbf{p}_2\|^2}{n_2}-\frac{\mathbf{p}_1'\mathbf{p}_2}{n_1}\right)\right)^{-1}. \tag{5.30}$$

Where $\mathbf{p}_1$ and $\mathbf{p}_2$ denote the column vector consisting of diagonal elements of $(\mathbf{P}_A - \mathbf{P}_N)$ and $(\mathbf{I} - \mathbf{P}_A)$, respectively.

On the other hand, when the noise kurtosis κ is unknown, we can apply the bootstrap method summarised in Table 5.1 to estimate the null distribution. Here, the training samples needed are the observations under the null hypothesis, i.e., the model given in eq. (5.25), instead of the noise only data $\mathcal{W}$. In addition, the log statistic $Z = \frac{1}{2}\log T_F(n_1, n_2)$ should be replaced by $\frac{1}{2}\log \Lambda_F(n_{\Lambda,1}, n_{\Lambda,2})$.

5.6 Simulation Results

In this section, we shall investigate the performance of the proposed methods by numerical experiments. Both the primary signal and CSI vector are generated by the normalised zero mean complex Gaussian distributed variates. We require the false alarm probability $P_f \leqslant 0.1$ and define SNR as $\text{SNR} \triangleq \|\mathbf{h}s(l)\|^2/M\sigma_w^2$. For the bootstrap approximation, the number of replications are set as $B = 500$. All results are obtained by averaging over $N = 5000$ independent Monte Carlo trials.

The Generalised Gaussian Model (GGM) and Gaussian Mixture Model (GMM), see eqs. (4.24) and (4.25) in Chapter 4, are used to generate non-Gaussian noise. As the parameters we previously used, the GGM is simulated by Laplacian noise with kurtosis $\kappa = 1.5$ in the complex-valued case. For GMM noise, we choose $\epsilon = 0.06$ and $\eta = 10$ to model the heavy-tailed noise with the kurtosis $\kappa = 2\left[\frac{1-\epsilon+\eta^2\epsilon}{(1-\epsilon+\eta\epsilon)^2}-1\right] = 3.85$.

Accuracy of the proposed methods

In this chapter, the MDOF method, discussed in Section 5.3, and the bootstrap method, summarised in Table 5.1, are proposed to estimate the null distribution of the F-statistic for non-

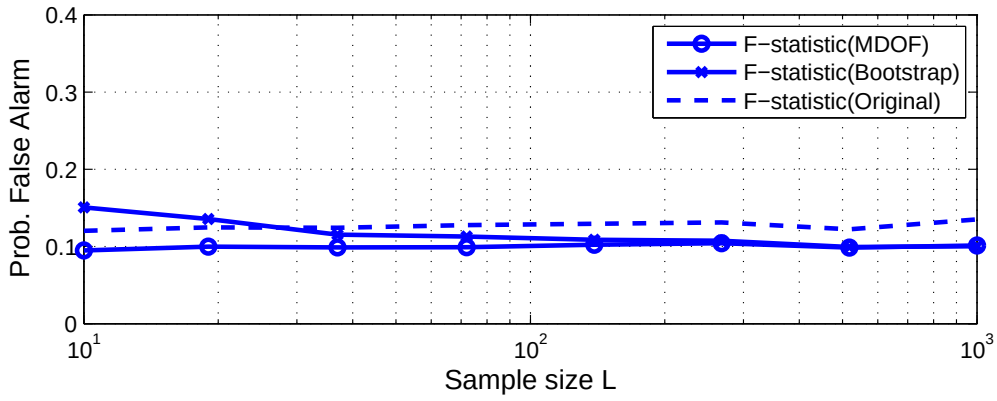

(a)

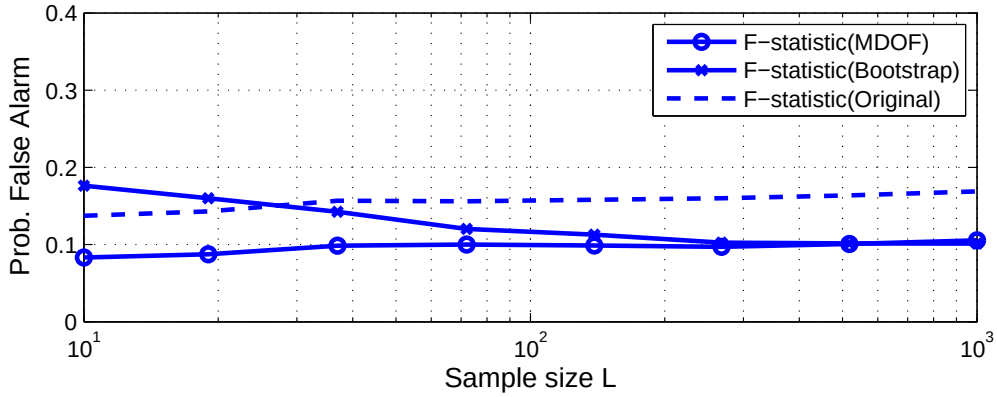

(b)

Figure 5.2: *Probability of false alarm versus sample size, L, for three methods calculating the test threshold, under: (a) Laplacian noise; and (b) Gaussian Mixture noise. Target false alarm probability $P_f = 0.1$ and $M = 4$ receiving antennas.*

Gaussian noise. In the first experiment, we test their accuracy under the Laplacian (special case of GGM) and GMM distributions above by evaluating their false alarm probability P_f against the sample size L with $M = 4$ receiving antennas. As shown in Figure 5.2, both methods can achieve the desired false alarm rate, 0.1, in the non-Gaussian noise scenario. The sample size L needed for the MDOF method to ensure the target false alarm is less than the bootstrap method. For example, $L \sim 10^1$ is sufficient for the MDOF method to obtain an accurate approximation of the null distribution, whereas the bootstrap approach needs $L \sim 10^2$. If we use the threshold derived using the Gaussian noise assumption, the P_f (marked as Original) is higher than the target value over the full range of L.

The probability of detection P_d versus the sample size L at SNR $= -14$ dB is plotted in

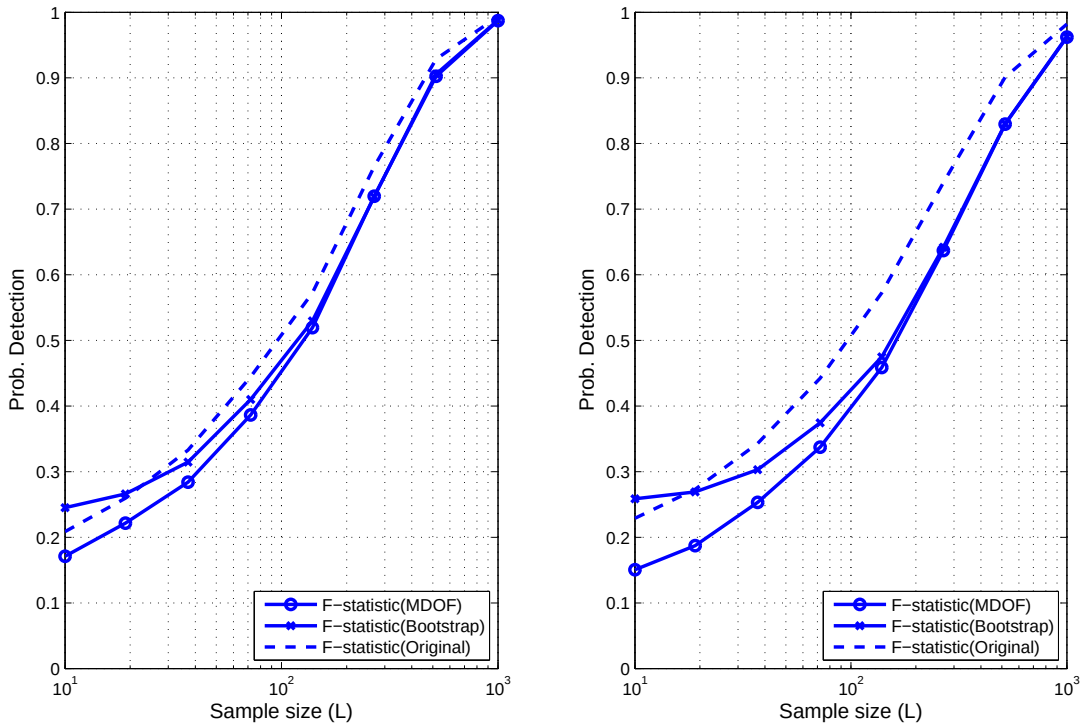

Figure 5.3: *Probability of detection versus sample size, L, for three methods calculating the test threshold,under: (a) Laplacian noise; and (b) Gaussian Mixture noise. Target false alarm probability $P_f = 0.1$, SNR $= -14$ dB and $M = 4$ receiving antennas.*

Figure 5.3 for Laplacian and GMM noise. Note that the performance gain achieved by the bootstrap and the original methods for small value of L can be ignored due to the high false alarm probability results in Fig.5.2. For $L \geqslant 500$, it can be observed that the proposed MDOF and bootstrap approaches have nearly the same probability of detection. Comparing the results with Figure 5.2, we conclude that the MDOF and bootstrap method have very similar test performance, when the sample size L is sufficiently large to ensure the pre-specified false alarm rate. For $L < 500$, the MDOF method can keep the P_f below the target level, but it requires additional information on the noise statistic, i.e., the kurtosis κ.

Comparison with other detectors

In the following experiments, we shall compare the detection probability of the F-statistic based method with other detection algorithms that are valid in non-Gaussian noise, i.e., the

Detector	Assumptions	Sensing Complexity
F-statistic:	Multiple receiving antennas known CSI	
MDOF, Section 5.3	Noise kurtosis κ is known	$O\left(M^2L\right)$
Bootstrap, Table 5.1	Training noise samples with size L	$O\left(BM^2L\right)$
Bootstrap-EV, Table 4.1	Multiple receiving antennas	$O\left(BB_1M^3L\right)$
Bootstrap-EG, Table 4.2	Noise power σ_w^2 is known	$O\left(BM^3L\right)$
L_p-norm [30]	The statistics of CSI and noise are known	$O\left(MLN\right)$

Table 5.2: *Summary of the simulated detection algorithms. M: number of receiving antennas. L: sample size. N: Number of Monte carol trails. B and B_1 denote the number of bootstrap replications for distribution approximation and sample eigenvalue bias correction, respectively.*

eigenvalue based detector, the energy based detector and the L_p-norm detector [30]. A simple summary of the four detectors to be simulated is outlined in Table 5.2. Note that the tunable parameter p for the L_p-norm detector, eq. (2.22) in chapter 2, is obtained by simulations . The sample size is chosen to be $L = 500$ so that both the MDOF and bootstrap methods have the same probability of detection. In Figure 5.4 and Figure 5.5, we elect to simulate the MDOF method for the F-statistic based detection.

Figure 5.4 presents the probability of detection versus SNR with $M = 4$ receiving antennas. Results show that the F-statistic based method has the best detection performance. For instance, as shown in Figure 5.4(a), to obtain a 90% detection probability in Laplacian noise, the F-statistic based method provides a 2.5 dB and 4 dB SNR gain compared with the eigenvalue based detector and the energy based detector, respectively. In addition, since the F-statistic is initially derived from Gaussian, a more significant performance gain can be expected when the noise distribution is near Gaussian, i.e., with a smaller noise kurtosis κ. For example, in Gaussian mixture noise with $\kappa = 3.85$, the SNR gap between the F-statistic based detector and L_p-norm based detector is 0.8 dB at 90% probability of detection. While if the noise is Laplacian distributed with $\kappa = 1.5$, the SNR gap between them will increase to 2 dB.

The impact of the number of receiving antennas M is shown in Figure 5.5, where we vary the number of antennas from 2 to 8 and fix the SNR at -14 dB. When $M = 2$, the F-statistic based detector still has a superior detection probability than the eigenvalue based and the energy based detector, whereas its performance is inferior to the L_p-norm based detector. However,

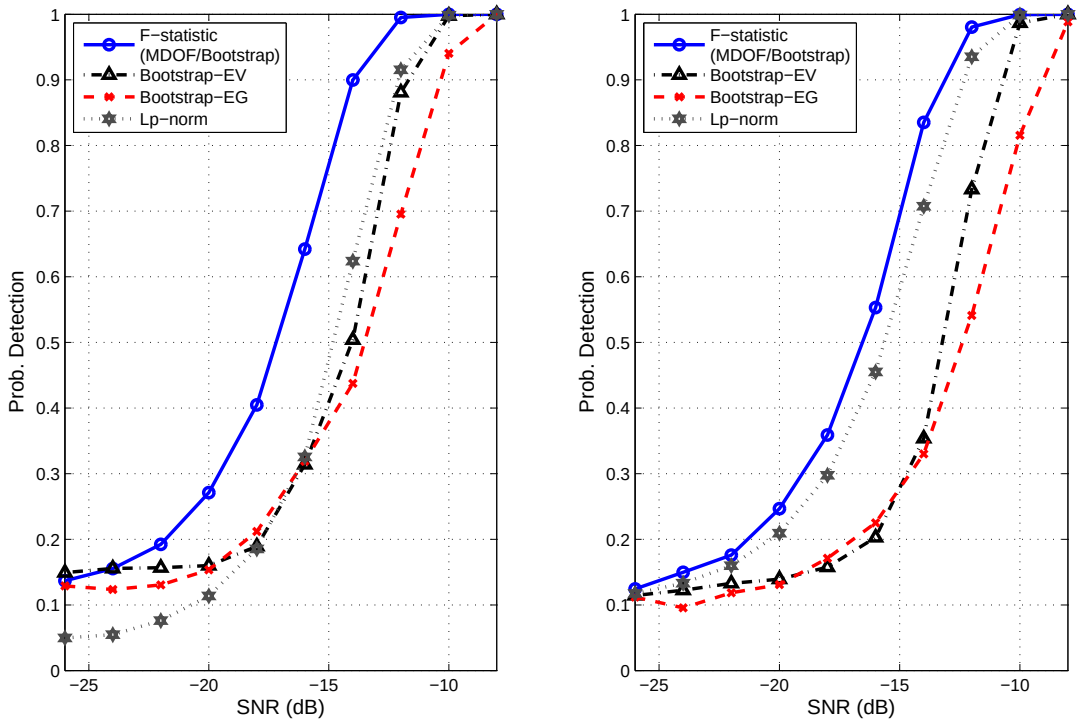

Figure 5.4: *Probability of detection versus SNR(dB) under: (a) Laplacian noise; and (b) Gaussian Mixture noise. Target false alarm probability* $P_f = 0.1$, $M = 4$ *receiving antennas and* $L = 500$ *samples.*

when M increases, a significant performance improvement can be achieved by the F-statistic based approach. As the F-statistic uses linear regression models, the detection probability increases rapidly with the regressor size M.

Discussion

In summary, the MDOF method requires less samples to meet a target false alarm probability and is relatively easy to implement. However, *prior* knowledge of the noise kurtosis κ is required. The bootstrap method is more computationally expensive (see in Table 5.2) but only requires a sequence of noise samples for training purpose. By applying either of the two proposed methods with $L > 500$, good detection probability is achieved by the F-statistic based detector under non-Gaussian noise while maintaining the predetermined false alarm probability.

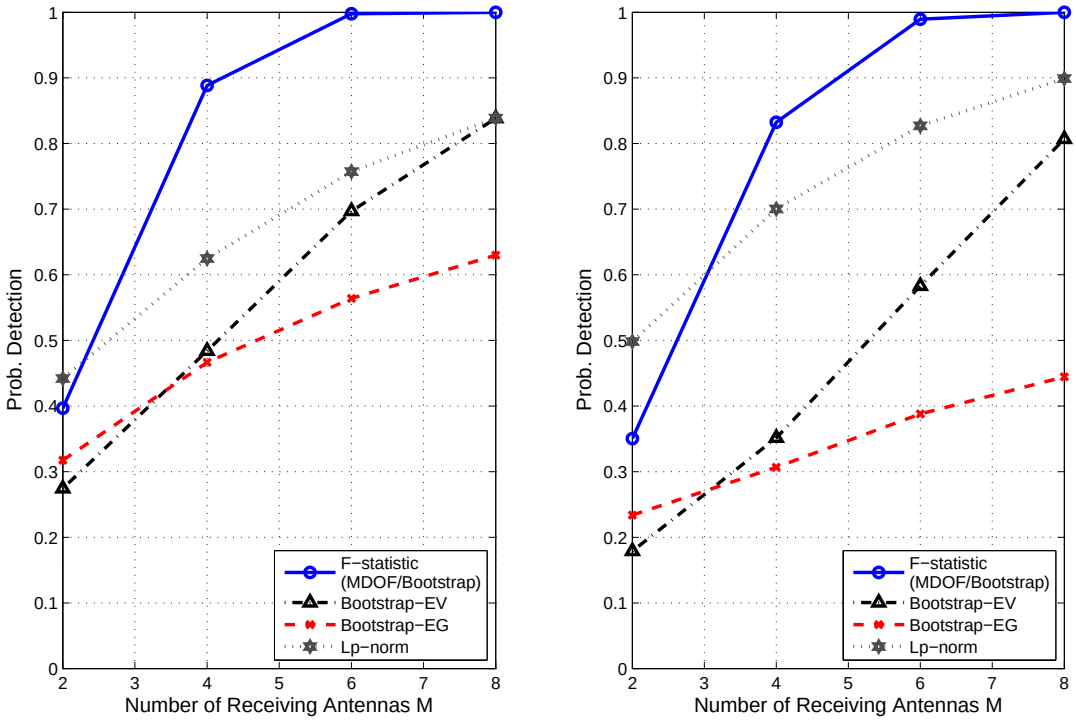

Figure 5.5: *Probability of detection versus number of receiving antennas, M, under: (a) Laplacian noise; and (b) Gaussian Mixture noise. Target false alarm probability $P_f = 0.1$, SNR $= -14$ dB and $L = 500$ samples.*

The main issue for the F-statistic based detector is the acquiring of CSI. As mentioned in Chapter 3, the CSI can be estimated using the primary pilot signal but may be imperfect due to the delay update and estimation error. In this chapter, the impact of CSI uncertainty does not be discussed in detail as it is another topic which needs to be further investigated. Actually, when the null hypothesis holds, the false alarm probability of the F-statistic based method remains unchanged, independent of the accuracy of CSI estimation. The reason is that the test statistic and the two proposed approaches for the null distribution approximation are all derived from the CSI estimation. However, when the alternative hypothesis holds, the imperfect CSI will lead to performance loss in detection probability.

5.7 Conclusion

In this chapter, we investigated the F-statistic based spectrum sensing schemes for cognitive radio, which are valid for any circularly symmetric distributed noise with finite power. To maintain the pre-determined false alarm probability in non-Gaussian noise, two methods are proposed to estimate the null distribution of test statistic. The first approach assumes a known noise kurtosis and matches the first two moments of the log test statistic with those of a log$F$ distribution. By doing this, the null distribution of the test statistic is approximated by the F-distribution with modified degrees of freedom and the results are obtained in closed form. The second approach, which relaxes the assumption on the noise kurtosis, applies the non-parametric bootstrap procedure to a set of noise only data and constructs the null distribution by resampling. Theoretical and simulation results show that both methods achieve accurate approximations with moderate samples, i.e., the sample size in a order of 10^1 and 10^2 are sufficient for the MDOF method and the bootstrap method, respectively.

The detection performance of proposed detectors in non-Gaussian noise is evaluated numerically and compared with other robust detection methods. Simulation results have shown that the F-statistic based sensing schemes achieved an overall superior detection probability for the GGM and GMM noise, i.e., compared with the energy based detector a 4 dB SNR gain can be achieved to obtain a 90% detection probability in Laplacian noise. In addition, since the F-statistic based detector uses linear regression models, a significant performance gain can be expected up to array size of $M = 4 - 8$.

These new detection techniques now offer the potential of improved performance for primary signal detection in non-Gaussian noise. Furthermore, the robust F-statistic based detector has general validity which can be extended to other linear regression problems with complex number measurements.

Chapter 6
Conclusions and Future Work

6.1 Conclusions

Today the rapid growth of wireless industry has contributed to huge demand for higher data rates wireless products and ever more bandwidth. Facing the future generation wireless services, the spectrum shared technology, cognitive radio, has received much research interest. This thesis has focused on the noise robust spectrum sensing designs in cognitive radio networks. Gaussian distributed noise with exactly known power is a common assumption made in current spectrum sensing schemes. However, such a assumption is not always valid in practical wireless communication systems. In order to achieve a more reliable detection, two challenging sensing conditions, e.g., the detection in unknown noise variance and the detection in non-Gaussian noise, have been considered in this thesis.

In Chapter 3, an F-test based sensing method has been proposed which overcomes the problem of noise variance uncertainty. It considers a multiple antenna cognitive radio system and assumes the CSI is known. Since the test statistic, F-statistic, is independent of the noise power, this approach offers absolute robustness against noise variance mismatch. By invoking a Gaussian noise assumption, easily evaluated expressions for the test threshold and the detection probability have been derived, respectively. Theoretical analysis indicates that when the *prior* knowledge of CSI is imperfect, the false alarm probability remains unchanged and the degraded detection probability can be evaluated. Simulation results have shown that the F-test based detector performs superior to the widely used energy detector as a 2.2 dB SNR gain can be achieved to obtain a 90% detection probability. When the CSI is imperfect, the proposed approach has constant false alarm probability and suffers from a mild performance loss in detection probability, but still has an overall better performance compared with the energy detector with 1 dB noise mismatch. In addition, since the F-test uses linear regression models, the detection probability will increase rapidly with the regressor size, i.e., number of receiving antennas M. When $M = 8$ antennas are applied, simulation results suggest that the performance loss caused by CSI uncertainty becomes insignificant.

While a Gaussian noise assumption was made in Chapter 3, Chapter 4 and Chapter 5 relaxed this requirement and considered the spectrum sensing problem for non-Gaussian noise. In Chapter 4, by using the bootstrap technique, two detection methods have been developed which can be applied to arbitrary noise types with finite power. Firstly, a nonparametric eigenvalue based detector was proposed which can be applied to multiple antenna assisted cognitive radio systems. It is fundamentally a binary hypothesis test for the difference between sample eigenvalues. Secondly, by assuming the noise power is known, the conventional energy detector was generalised to non-Gaussian noise. For both detectors, the nonparametric bootstrap technique has been applied to estimate the null distribution of the test statistic via resampling the collected data with replacement. A major advantage of the bootstrap is that it offers sufficiently accurate approximation in a variety of non-Gaussian noise types for short data records, leading to a test threshold that maintaining a target false alarm probability. In addition, the important role of bootstrap pivot has been described. The bootstrap test with a pivoting statistic, such as the energy based detection, has been shown to have a standardizing null distribution that independent of the unknown noise types. The detection performance of proposed detectors have been evaluated numerically. The results illustrated that in non-Gaussian noise, the energy based detector is a superior approach in low SNR regime and the eigenvalue based method offers an overall better detection performance, e.g., to obtain a 90% detection probability, the eigenvalue based detector provides an up to 1.5 dB SNR gain compared with the energy based detector.

Then in Chapter 5, the F-test based detector proposed in Chapter 3 was generalised to non-Gaussian noise. The noise distribution is characterised by circularly symmetric with finite kurtosis and is not necessary to be Gaussian. To maintain the pre-determined false alarm probability, two methods have been proposed to estimate the null distribution of the F-statistic. The first MDOF approach requires *prior* knowledge of the noise kurtosis. The null distribution is approximated by an F-distribution with modified degrees of freedom and the expressions are obtained in closed form. The second approach applies the nonparametric bootstrap procedure to a set of noise only data and constructs the null distribution by resampling. It incurs computational complexity but can work without the knowledge of noise kurtosis. Theoretical analysis shows that both methods can yield accurate statistical approximations in non-Gaussian noise, while the sample size required for the MDOF method is less than the bootstrap method. For example, given a target 10% false alarm probability, it has been verified that the sample size in a order of 10^1 is sufficient for the MDOF method, while the bootstrap method requires 10^2. When the sample size is sufficiently large to ensure the pre-specified false alarm rate, it can

be observed that the two proposed approaches have nearly the same probability of detection. Compared with other state-of-the-art robust detectors, the F-statistic based detector are shown to have a good detection probability under various types of non-Gaussian noise. For example, it is illustrated that in Laplacian noise, the SNR gap between the F-statistic based detector and the energy detector is 4 dB at 90% detection probability.

6.2 Limitations and Future Work

This thesis has developed robust sensing techniques that consider more reasonable noise models in cognitive radio networks. However, due to the initial assumptions made on the data model and applied techniques, there exists certain limitations and more efforts can be made to generalise the proposed approaches. In addition, based on this thesis, several interesting topics are worth further investigation.

6.2.1 Limitations

• *Chapter 3 and Chapter 5* : The F-statistic based approaches require *prior* knowledge of CSI. However, in the context of cognitive radio, the acquisition of CSI is an open issue due to the lack of reciprocal standard between primary and secondary systems. Suggested by the previous literature, possible solutions to this problem include acquiring CSI from the periodically transmitted pilot [11, 83, 84], or estimating the fading gains and the state of primary signal jointly [85, 86]. As discussed in this thesis, the imperfect CSI leads to performance loss in detection probability. Fortunately, when the primary user is absent, i.e., the null hypothesis $\mathcal{H}_0$ holds, the CSI uncertainty will not degrade the performance as the false alarm probability of the F-statistic based detector remains unchanged in this case.

• *Chapter 4 and Chapter 5*: Bootstrap resampling is applied to control the false alarm probability of sensing methods in non-Gaussian noise. This leads to increased computational cost as the complexity will grow linearly with the number of bootstrap replications. Such a problem is more significant in eigenvalue based method as it involves double bootstrap.

6.2.2 Future Work

• In addition to the detectors proposed in Chapter 4 and Chapter 5, the bootstrap technique can be further applied to other robust sensing designs by non-parametrically estimating their test statistics' null distributions. For example, the cyclostationarity based detection methods for non-Gaussian noise can be considered so that the signals from the primary user and interferences can be differentiated.

• Edgeworth expansion may be a solution to reduce the complexity brought by the bootstrap method. In the Edgeworth view, the distribution of a statistic can be expanded as the normal distribution plus an infinite number of Edgeworth series [95]. If the statistic is pivotal, generally a second-order approximation is sufficiently accurate. The main issue is that the polynomials are with coefficients depending on the cumulants of the test statistic, which may be complicated as they are related to the non-Gaussian noise distribution. In practice, the bootstrap method is a way to non-parametrically approximate these polynomials at the expense of computational complexity. However, extra efforts on Edgeworth expansions are worthwhile as they are more efficient to cope with the limited sensing time.

• In Chapter 5, the detection probability of the F-statistic based method in non-Gaussian noise is worth to be further studied. Similar to the MDOF method, one possible way is to approximate the detection probability by a noncentral F-distribution with modified degrees of freedom. Furthermore, it is interesting to investigate the performance loss in detection probability caused by CSI uncertainty.

• In this thesis, we assume there is only one primary signal source as most of spectrum sensing problems consider this case. In practice, all of the proposed methods can be extended to other detection problems with multiple signal sources. Related works on the F-statistic based detector have been discussed in Chapter 5. For the eigenvalue based detector in Chapter 4, sequential detection methods can be considered.

Appendix A
Proof of Property 5.1

Proof. 1. When $\mathcal{H}_0$ holds, $\mathrm{E}\left[\mathbf{y}(l)\right] = \mathbf{0}$ and $\mathrm{Var}\left[\mathbf{y}(l)\right] = \sigma_w^2 \mathbf{I}_M$. Therefore, we have:

$$\mathrm{E}\left[\sum_{l=0}^{L-1} \mathbf{y}\left(l\right)^H \mathbf{P}_k \mathbf{y}\left(l\right) | \mathcal{H}_0\right] = \mathrm{E}\left[\sum_{l=0}^{L-1} \mathbf{w}\left(l\right)^H \mathbf{P}_k \mathbf{w}\left(l\right)\right] = L\sigma_w^2 \mathrm{tr}\left[\mathbf{P}_k\right] = L\sigma_w^2 r_k. \tag{A.1}$$

2. Using Property 5.1.(1), we have:

$$\begin{aligned} &\mathrm{Var}\left[\sum_{l=0}^{L-1} \mathbf{y}(l)^H \mathbf{P}_k \mathbf{y}(l) | \mathcal{H}_0\right] \\ &= \mathrm{E}\left[\left(\sum_{l=0}^{L-1} \mathbf{w}(l)^H \mathbf{P}_k \mathbf{w}(l)\right)^2\right] - \mathrm{E}\left[\sum_{l=0}^{L-1} \mathbf{w}(l)^H \mathbf{P}_k \mathbf{w}(l)\right]^2 \\ &= \mathrm{E}\left[\left(\sum_{l=0}^{L-1} \mathbf{w}(l)^H \mathbf{P}_k \mathbf{w}(l)\right)^2\right] - \sigma_w^4 L^2 r_k^2. \end{aligned} \tag{A.2}$$

Define $\mathbf{R} = [\mathrm{R}_{ij}] = \sum_{l=0}^{L-1} \mathbf{w}(l)\mathbf{w}(l)^H$, P_{ij} as the element of projection matrix $\mathbf{P}_k$ (the subscript k in P_{ij} is omitted for simplicity) and $A_{ij} = \Re(\mathrm{P}_{ij}\mathrm{R}_{ji})$. When $i = j$, both R_{ii} and P_{ii} are real-valued numbers. Note that $\mathbf{R}$ is symmetric and the projection matrix $\mathbf{P}_k$ is idempotent and symmetric. Based on those properties, we have:

$$\begin{aligned} &\mathrm{E}\left[\left(\sum_{l=0}^{L-1} \mathbf{w}(l)^H \mathbf{P}_k \mathbf{w}(l)\right)^2\right] \\ &= \mathrm{E}\left[\left(\mathrm{tr}\left[\mathbf{P}_k \mathbf{R}\right]\right)^2\right] \\ &= \mathrm{E}\left[\left(\sum_i \mathrm{P}_{ii}\mathrm{R}_{ii} + 2\sum_i \sum_{j<i} \Re(\mathrm{P}_{ij}\mathrm{R}_{ji})\right)^2\right] \\ &= \mathrm{E}\left[\left(\sum_i A_{ii}\right)^2 + 4\left(\sum_i \sum_{j<i} A_{ij}\right)^2 + 4\left(\sum_i A_{ii}\right)\left(\sum_i \sum_{j<i} A_{ij}\right)\right]. \end{aligned} \tag{A.3}$$

Since $\mathbf{w}(l)$ is i.i.d, $\mathrm{E}[A_{ij}A_{hm}]$ can be written in case by:

$$\mathrm{E}[A_{ij}A_{hm}] = \begin{cases} \left(L\mu_4 + (L^2-L)\sigma_w^4\right)\mathrm{P}_{ii}^2 & i=j=h=m \\ (L^2\sigma_w^4)\mathrm{P}_{ii}\mathrm{P}_{jj} & i=j,\ h=m \\ L(\sigma_r^4+\sigma_i^4)\Re(\mathrm{P}_{ij})^2 + 2L\sigma_r^2\sigma_i^2\Im(\mathrm{P}_{ij})^2 & i=h,\ j=m \\ 0 & others \end{cases} \tag{A.4}$$

where $\sigma_r^2 \triangleq \mathrm{E}\left[\Re\left(w_i(l)\right)^2\right]$ and $\sigma_i^2 \triangleq \mathrm{E}\left[\Im\left(w_i(l)\right)^2\right]$ denote the variance of the real and imaginary part of noise $w_i(l)$, respectively. Since $w_i(l)$ is assumed to be circularly symmetric distributed, we have:

$$\sigma_r^2 = \sigma_i^2 = \frac{1}{2}\sigma_w^2, \tag{A.5}$$

and

$$\mathrm{E}[A_{ij}A_{hm}] = \frac{L}{2}\sigma_w^4\left|\mathrm{P}_{ij}\right|^2,\ for\, i=h,\ j=m. \tag{A.6}$$

Using the results in (A.4), we have:

$$\begin{aligned} \mathrm{E}\left[\left(\sum_i A_{ii}\right)^2\right] &= \mathrm{E}\left[\sum_i A_{ii}^2 + \sum_i\sum_{j\neq i} A_{ii}A_{jj}\right] \\ &= \left(L\mu_4 + (L^2-L)\sigma_w^4\right)\sum_i \mathrm{P}_{ii}^2 + L^2\sigma_w^4\sum_i\sum_{j\neq i}\mathrm{P}_{ii}\mathrm{P}_{jj} \end{aligned} \tag{A.7}$$

$$\begin{aligned} \mathrm{E}\left[(\sum_i\sum_{j<i} A_{ij})^2\right] &= \mathrm{E}\left[\sum_i\sum_{j<i} A_{ij}A_{ij} + \sum_i\sum_{j<i}\sum_{h\neq i}\sum_{m<h} A_{ij}A_{hm}\right] \\ &= \frac{L}{2}\sigma_w^2\sum_i\sum_{j<i}\left|\mathrm{P}_{ij}\right|^2 \end{aligned} \tag{A.8}$$

$$\mathrm{E}\left[(\sum_i A_{ii})(\sum_i\sum_{j<i} A_{ij})\right] = 0. \tag{A.9}$$

Note that for a projection matrix $\mathbf{P}_k$, we have $\mathrm{tr}\left[\mathbf{P}_k\right] = r_k$ and $\mathbf{P}_k^2 = \mathbf{P}_k$ [88]. Hence,

$(\sum_i \mathrm{P}_{ii})^2 = r_k^2$ and $\sum_i \sum_j |\mathrm{P}_{ij}|^2 = \mathrm{tr}\left[\mathbf{P}_k^2\right] = r_k$. Substituting (A.7-A.9) in (A.3) leads to:

$$\begin{aligned} \mathrm{E}\left[\left(\sum_{l=0}^{L-1} \mathbf{w}(l)^H \mathbf{P}_k \mathbf{w}(l)\right)^2\right] &= \sigma_w^4 \left(L^2 r_k^2 + L r_k + L\frac{\mu_4 - 2\sigma_w^4}{\sigma_w^4} \|\mathbf{p}_k\|^2\right) \\ &= \sigma_w^4 \left(L^2 r_k^2 + L r_k + L\kappa \|\mathbf{p}_k\|^2\right). \end{aligned} \tag{A.10}$$

Finally, substituting (A.10) in (A.2) leads to:

$$\mathrm{Var}\left[\sum_{l=0}^{L-1} \mathbf{y}(l)^H \mathbf{P}_k \mathbf{y}(l) | \mathcal{H}_0\right] = L\sigma_w^4 \left(r_k + \kappa \|\mathbf{p}_k\|^2\right). \tag{A.11}$$

3. Note that $\mathbf{P}_1 + \mathbf{P}_2 = \mathbf{I}_M$ is an orthogonal $M-$dimensional projection and by using (A.11), we have:

$$\begin{aligned} &\mathrm{Var}\left[\sum_{l=0}^{L-1} \mathbf{y}(l)^H \mathbf{P}_1 \mathbf{y}(l) + \sum_{l=0}^{L-1} \mathbf{y}(l)^H \mathbf{P}_2 \mathbf{y}(l) | \mathcal{H}_0\right] \\ &= \mathrm{Var}\left[\sum_{l=0}^{L-1} \mathbf{y}(l)^H (\mathbf{P}_1 + \mathbf{P}_2) \mathbf{y}(l) | \mathcal{H}_0\right] \\ &= L\sigma_w^4 \left(r_1 + r_2 + \kappa \|\mathbf{p}_1 + \mathbf{p}_2\|^2\right) \\ &= L\sigma_w^4 \left(r_1 + r_2 + \kappa \|\mathbf{p}_1\|^2 + \kappa \|\mathbf{p}_2\|^2 + 2\kappa(\mathbf{p}_1' \mathbf{p}_2)\right). \end{aligned} \tag{A.12}$$

Comparing it with the formula of variance decomposition $\mathrm{Var}[a+b] = \mathrm{Var}[a] + \mathrm{Var}[b] + 2\mathrm{Cov}[a,b]$ [107], finally we obtain:

$$\mathrm{Cov}\left[\sum_{l=0}^{L-1} \mathbf{y}(l)^H \mathbf{P}_1 \mathbf{y}(l),\ \sum_{l=0}^{L-1} \mathbf{y}(l)^H \mathbf{P}_2 \mathbf{y}(l) | \mathcal{H}_0\right] = L\sigma_w^4 \kappa \mathbf{p}_1' \mathbf{p}_2. \tag{A.13}$$

□

Appendix B

Proof of Property 5.2

Proof. 1. Taking a Taylor expansion of $\log S_k^2$ about $\log \frac{\sigma_w^2}{2}$, we have:

$$\log S_k^2 = \log \frac{\sigma_w^2}{2} + \frac{S_k^2 - \sigma_w^2/2}{\sigma_w^2/2} - \frac{(S_k^2 - \sigma_w^2/2)^2}{2(\sigma_w^2/2)^2} + O\left(\left(S_k^2 - \sigma_w^2/2\right)^3\right). \tag{B.1}$$

Taking expected value of both sides and using the results in Property 5.1.(2), we have:

$$\begin{aligned} \mathrm{E}\left[\log S_k^2 | \mathcal{H}_0\right] &\sim \log \frac{\sigma_w^2}{2} - \frac{\mathrm{Var}\left[S_k^2 | \mathcal{H}_0\right]}{\sigma_w^4/2} \\ &= \log \frac{\sigma_w^2}{2} - \frac{1}{4L^2 r_k^2} \frac{\mathrm{Var}\left[\sum_{l=0}^{L-1} \mathbf{y}\left(l\right)^H \mathbf{P}_k \mathbf{y}\left(l\right) | \mathcal{H}_0\right]}{\sigma_w^4/2} \\ &= \log \frac{\sigma_w^2}{2} - \frac{r_k^{-1} + r_k^{-2}\kappa \left\|\mathbf{p}_k\right\|^2}{2L}. \end{aligned} \tag{B.2}$$

Substituting in:

$$\mathrm{E}\left[Z\right] = \frac{1}{2}\left(\mathrm{E}[\log S_1^2] - \mathrm{E}[\log S_2^2]\right) \tag{B.3}$$

leads to:

$$\mathrm{E}\left[Z | \mathcal{H}_0\right] \sim \frac{r_2^{-1} + r_2^{-2}\kappa \left\|\mathbf{p}_2\right\|^2 - r_1^{-1} - r_1^{-2}\kappa \left\|\mathbf{p}_1\right\|^2}{4L}. \tag{B.4}$$

2. By ignoring the third term in (B.1), $\log S_k^2$ can be written as:

$$\log S_k^2 = \log \frac{\sigma_w^2}{2} + \frac{S_k^2 - \sigma_w^2/2}{\sigma_w^2/2} + O\left(\left(S_k^2 - \sigma_w^2/2\right)^2\right), \tag{B.5}$$

which leads to:

$$\log S_k^2 - \log \frac{\sigma_w^2}{2} \sim \frac{S_k^2 - \sigma_w^2/2}{\sigma_w^2/2}, \tag{B.6}$$

and

$$\mathrm{E}[\log S_k^2] \sim \log \frac{\sigma_w^2}{2}. \tag{B.7}$$

Using (B.6) and (B.7), we have:

$$\begin{aligned}
\text{Var}\left[\log S_k^2|\mathcal{H}_0\right] &\sim \text{E}\left[\left(\log S_k^2 - \log\frac{\sigma_w^2}{2}\right)^2|\mathcal{H}_0\right] \\
&\sim \text{E}\left[\left(\frac{S_k^2-\sigma_w^2/2}{\sigma_w^2/2}\right)^2|\mathcal{H}_0\right] \\
&= \frac{4}{\sigma_w^4}\text{Var}\left[S_k^2|\mathcal{H}_0\right] \\
&= \frac{1}{L^2 r_k^2\sigma_w^4}\text{Var}\left[\sum_{l=0}^{L-1}\mathbf{y}\left(l\right)^H\mathbf{P}_k\mathbf{y}\left(l\right)|\mathcal{H}_0\right]. \qquad \text{(B.8)}
\end{aligned}$$

Similarly,

$$\begin{aligned}
\text{Cov}\left[\log S_1^2,\log S_2^2|\mathcal{H}_0\right] &\sim \text{E}\left[(\log S_1^2 - \log\frac{\sigma_w^2}{2})(\log S_2^2 - \log\frac{\sigma_w^2}{2})\right] \\
&\sim \frac{\text{E}\left[\left(S_1^2-\frac{\sigma_w^2}{2}\right)\left(S_2^2-\frac{\sigma_w^2}{2}\right)|\mathcal{H}_0\right]}{\sigma_w^4/4} \qquad \text{(B.9)} \\
&= \frac{\text{Cov}\left[\sum_{l=0}^{L-1}\mathbf{y}\left(l\right)^H\mathbf{P}_1\mathbf{y}\left(l\right),\sum_{l=0}^{L-1}\mathbf{y}\left(l\right)^H\mathbf{P}_2\mathbf{y}\left(l\right)|\mathcal{H}_0\right]}{L^2 r_1 r_2\sigma_w^4}.
\end{aligned}$$

Substituting (B.8) and (B.9) in:

$$\text{Var}[Z] = \frac{1}{4}\left[\text{Var}[\log S_1^2] + \text{Var}[\log S_2^2] - 2\text{Cov}[\log S_1^2,\log S_2^2]\right], \qquad \text{(B.10)}$$

and using the results in Property 5.1.(2-3), we have:

$$\text{Var}\left[Z|\mathcal{H}_0\right] \sim \frac{r_1^{-1} + r_1^{-2}\kappa\left\|\mathbf{p}_1\right\|^2 + r_2^{-1} + r_2^{-2}\kappa\left\|\mathbf{p}_2\right\|^2 - 2r_1^{-1}r_2^{-1}\kappa}{4L}. \qquad \text{(B.11)}$$

□

Appendix C
Publications

Journal

• Q. Huang and P.-J. Chung, "An F-test based approach for spectrum sensing in cognitive radio, " *Wireless Communications, IEEE Transactions on*, vol. 12, pp. 4072−4079, Aug.2013.

• Q. Huang, P.-J. Chung, J. Thompson and P. Grant, "An F-statistic Based Detector for Improved Spectrum Sensing in Non-Gaussian Noise ," *IEEE Transactions on Cognitive Communications and Networking*, submitted in Oct. 2015.

Conference

• Q. Huang and P.-J. Chung, "An F-test for multiple antenna spectrum sensing in cognitive radio, " in *Communications (ICC), 2013 IEEE International Conference on*, pp. 4677−4681, Jun. 2013.

• Q. Huang, P.-J. Chung, and J. Thompson, "A nonparametric approach for spectrum sensing using bootstrap techniques," in *Global Communications Conference (GLOBECOM),2014 IEEE*, pp. 851−856, Dec. 2014.

IEEE ICC 2013 - Signal Processing for Communications Symposium

An $F-$test for Multiple Antenna Spectrum Sensing in Cognitive Radio

Qi Huang, Pei-Jung Chung
Institute for Digital Communications
The University of Edinburgh, UK
Q.Huang@ed.ac.uk, P.Chung@ed.ac.uk

***Abstract*—Spectrum sensing is an essential task in cognitive radio technology. Most of current detectors take the noise power as *prior* knowledge which makes the detection performance sensitive to noise uncertainty. In this paper, we propose an $F-$test based detector to overcome this problem. The proposed approach is robust to noise mismatch and requires low computational complexity. Based on the table of $F-$distribution, the exact value for the test threshold and the detection probability are derived, respectively. In addition, we shall show that the false alarm probability of the proposed method is still under control even with channel uncertainty. Simulation results demonstrate that significant performance gain achieved by the proposed approach.**

***Index Terms*—signal detection, $F-$test, spectrum sensing, cognitive radio.**

I. Introduction

Conitive Radio (CR) is proposed by FCC as an intelligent and flexible spectral allocation scheme [1]. The key of cognitive radio is to allow secondary users to operate at the licensed band without causing unacceptable interference to primary users [2], which makes spectrum sensing a fundamental issue: CR users are required to reliably monitor the presence of primary users over a certain spectrum periodically. Many sensing approaches [3]–[8] have been proposed to address this problem. Generally speaking, they fall into the following categories: energy detector, matched-filter detector, feature-based detector and blind detector. Another challenge is that individual CR user may fail to detect the weak primary signal due to the severe fading and hence significantly interferes the licensed user. To improve sensing sensitivity, we investigate the signal detection problem by considering multiple antenna systems in this paper.

Multiple antenna techniques can overcome multipath fading by exploiting the diversity gain without high requirement on overhead to transmit the observation. Recently, it has been applied in spectrum sensing for CR technology. In [9], an optimal detector in the Neyman-Pearson sense is addressed in which all knowledge about the signals, noise and channels are required. The popular energy detector [3] can be applied when noise statistic is available and it can be extended to more complex scenarios [10]. Energy detector is simple and optimal when noise power is the only known information [5]. However, the main drawback is that the sensitivity to noise uncertainty. When the noise mismatch is large, energy detector will become invalid due to high false alarm probability and limitation of signal-to-noise radio (SNR) wall [6]. To overcome this challenge, current research concentrates on blind detection, which exploits the received signal without any knowledge of signal parameters. For example, the eigenvalue-based maximum-minimum eigenvalue (MME) detector is studied in [8] and a generalized maximal likelihood radio test is proposed in [9]. However, they all apply the random matrix theory to decide the test threshold so that a large sample size is required. For blind detectors without the requirement on sample length, such as the multiple antennas assisted and empirical characteristic function (MECF) based detector [11], no closed-form expression for test threshold is available.

In summary, the aforementioned detection methods require noise power or high computational complexity. In this paper, we propose an $F-$test based approach to improve robustness and computational efficiency. Assuming the channel state information (CSI) is known, the proposed method is insensitive to noise uncertainty and achieves a significant performance gain. Furthermore, its computational complexity is comparable with energy detector. Given the table of $F-$distribution, the test threshold and probability of detection can be easily derived. Simulations are carried out to verify the proposed approach.

The rest of the paper is organized as follows. Section II introduces the signal model for multiple antenna sensing and develops the $F-$test based detector. In Section III, we discuss the performance of the proposed detector. Simulation results are presented in Section IV. Section V concludes the paper.

Throughout this paper, boldface letters and boldface capital letters denote vectors and matrices, respectively. $tr(\cdot)$ is the trace operator and $\|\cdot\|$ denotes the Euclidean norm of a vector. $\mathbf{I}_M$ represents the identity matrix of order M.

II. Signal Model and $F-$test Based Detection

Consider a cognitive radio network system with M receiving antennas as shown in Fig.1. We formulate the spectrum sensing problem as a hypothesis test. The null hypothesis $\mathcal{H}_0$ corresponds to an idle spectrum and the alternative hypothesis $\mathcal{H}_1$ corresponds to an occupied spectrum. Then the received signal vector at the CR user can be expressed as

$$\begin{aligned} \mathcal{H}_0 &: \mathbf{y}(l) = \mathbf{w}(l), \\ \mathcal{H}_1 &: \mathbf{y}(l) = \mathbf{h}s(l) + \mathbf{w}(l),\ l = 1, 2...L, \end{aligned} \tag{1}$$

978-1-4673-3122-7/13/$31.00 ©2013 IEEE

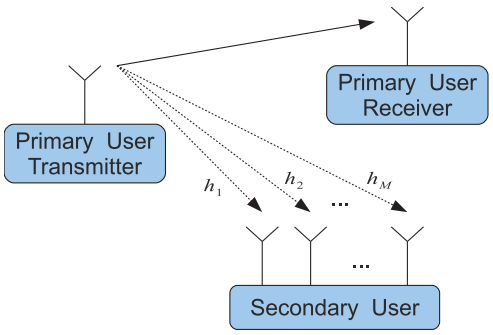

Fig. 1. CR networks with M antenna at the receiver

where $\mathbf{y}(l) \in \mathbb{C}^{M\times 1}$ represents the received signal at time instant l and L is the number of samples. $s(l)$ denotes the primary signal symbol at lth time slot which is assumed to be unknown and deterministic. The primary signal is distorted by the known CSI vector $\mathbf{h} \in \mathbb{C}^{M\times 1}$, which is supposed to stay constant during the sensing period. The noise vector $\mathbf{w}(l) \in \mathbb{C}^{M\times 1}$ consists of i.i.d zero-mean, complex Gaussian distributed elements with unknown variance σ_n^2, i.e., $w_i(l) \sim \mathcal{CN}(0, \sigma_n^2)$, $i = 1, 2 \dots M$. Without loss of generality, we assume the received signal be independent across antennas and time slots.

Note that in a CR network, the learning of CSI is via channel reciprocity. For example, $\mathbf{h}$ can be estimated from the periodically transmitted pilot primary signal [12]–[14].

Based on the linear signal model (1) and Gaussian noise assumption, an $F-$test [15] can be set up to to decide the presence of primary signal. Combining the received data set $\mathbf{Y} = \{\mathbf{y}(l), l = 1, 2 \dots L\}$ and channel information $\mathbf{h}$, the decision rule is given by

$$T \underset{\mathcal{H}_0}{\overset{\mathcal{H}_1}{\gtrless}} \gamma, \tag{2}$$

where γ is the test threshold and the test statistic T is given by

$$T = \frac{n_2}{n_1} \frac{tr(\mathbf{P}\hat{\mathbf{R}}_y)}{tr((\mathbf{I}_M - \mathbf{P})\hat{\mathbf{R}}_y)}. \tag{3}$$

Here $\hat{\mathbf{R}}_y = \frac{1}{L}\sum_{l=1}^{L} \mathbf{y}(l)\mathbf{y}(l)^H$ denotes the sample covariance matrix and $\mathbf{P} = \mathbf{h}(\mathbf{h}^H\mathbf{h})^{-1}\mathbf{h}^H$ represents the projection matrix onto the subspace spanned by $\mathbf{h}$. The test statistic (3) is $F_{n_1,n_2}-$distributed under null hypothesis $\mathcal{H}_0$, with degrees of freedom

$$n_1 = 2L, \tag{4}$$
$$n_2 = 2L(M-1). \tag{5}$$

The test statistic T can be seen as an estimated SNR at the CR receiver. Therefore, the decision rule (2) has the interpretation that we will reject $\mathcal{H}_0$, or declare primary signal to be detected, when the SNR level exceeds a certain threshold γ. In addition, it is worth mentioning that the Gaussian noise assumption implies the equivalence between $F-$test and likelihood radio test [15].

III. Performance Study

In this section, we shall discuss the performance and advantages of the proposed detector. To begin with, the false alarm probability (P_f) and the detection probability (P_d) are defined as follows

$$P_f = \Pr(T > \gamma|\mathcal{H}_0), \tag{6}$$
$$P_d = \Pr(T > \gamma|\mathcal{H}_1). \tag{7}$$

In spectrum sensing for CR networks, a high P_f results in poor spectral efficiency and a high P_d means less interference to primary systems. Therefore, a detector with large P_d and low P_f is desirable in the design of sensing technique.

Depending on the system requirement, one of the two merits can be used to choose the test threshold. However, since the calculation of P_d requires more *prior* information than P_f does, we often decide the test threshold based on false alarm probability.

A. Test threshold and probability of detection

As mentioned above, the test statistic T is $F_{n_1,n_2}-$distributed when the primary user is not active. Let $W_{c,n1,n2}(x)$ be the cumulative distribution function (CDF) of the central $F-$distribution with degrees of freedom n_1 and n_2 [16] (more details are shown in Appendix A). Then the false alarm probability P_f can be expressed as

$$P_f = \Pr(T > \gamma|\mathcal{H}_0) = 1 - W_{c,n1,n2}(\gamma). \tag{8}$$

Given a target false alarm probability α, the test threshold γ can be easily obtained by looking up the table of $W_{c,n1,n2}(x)$, that is

$$\gamma = W^{-1}_{c,n1,n2}(1-\alpha). \tag{9}$$

The probability of detection P_d relies on the distribution of the test statistic under $\mathcal{H}_1$. Due to complicated distributional properties, the exact value of P_d is usually hard to obtain in most designs. However, in the proposed $F-$test based method, the problem can be solved easily. In the presence of the primary user, or $\mathcal{H}_1$ holds, the test statistic (3) is noncentral F-distributed [16], denoted by $F'_{n_1,n_2}(\delta^2)$, where the noncentrality parameter is given by

$$\delta^2 = \frac{2\sum_{l=1}^{L} \|\mathbf{h}s(l)\|^2}{\sigma_n^2}. \tag{10}$$

Let $W_{nc,n1,n2}(x \mid \delta^2)$ denote the CDF of noncentral F-distribution (see Appendix A). Making use of the table for

the noncentral F-distribution, we can obtain the probability of detection as follows

$$P_d = \Pr(T > \gamma | \mathcal{H}_1) = 1 - W_{nc,n1,n2}(\gamma \mid \delta^2). \quad (11)$$

According to [16], P_d is an increasing function of δ^2. Since the noncentrality parameter (10) can be seen as a scaled SNR, we can achieve a better detection probability by increasing sensing samples to improve the SNR level at the receiver.

B. Computational complexity

The computational complexity of the $F-$test based sensing method comes from calculation of the test statistic (3). Because both $\hat{\mathbf{R}}_y$ and $\mathbf{P}$ are Hermitian, the evaluation can be simplified. For example, approximately $LM(M+1)/2$ complex multiplications and $M(M+1)(L-1)/2$ complex additions are needed to compute $\hat{\mathbf{R}}_y$. In Table I, we list the computational complexity of the $F-$test based method, the energy detector and the blind MME detector (with S as the smoothing factor [8]) for comparison.

Among these methods, the MME detector is the most expensive one for its large sample assumption, e.g., L is typically 10^4, and energy detector enjoys the lowest complexity. The computational complexity of the $F-$test based detector increases linearly with the number of samples and is approximately proportional to the squared number of receive antennas. Since L is usually much larger than M, the implementation of $F-$test based detector is inexpensive in practice.

C. Discussion

The proposed method is inspired by linear regression analysis, where the CSI $\mathbf{h}$ acts as the regressor and $\mathbf{y}(l)$ is the response variable. Since no information of noise statistic is needed, the $F-$test based approach is robust against noise uncertainty. Compared with existing detectors suggested in [8], [9], [17], the proposed $F-$test based method is simple to implement and requires only moderate sample size. In addition, CSI is needed to construct $F-$test based sensing. As shown in the simulation, the utilization of of CSI leads to the performance gain and high robustness against noise uncertainty.

IV. Simulation Results

In this section, we shall evaluate the proposed $F-$test based sensing numerically and compare it with other popular detectors, namely the energy detector and the MME detector. To keep consistency with the signal model defined here, we extend the result of MME detector in [8] to the complex value data case. In this circumstance, we use Tracy-Wisdom distribution of order 2 [18] to decide the test threshold and choose the smoothing factor $S = 5$. Specially, the sample length is large so that the MME method can provide reasonable performance. To examine the proposed approach, we consider a 4-antenna ($M = 4$) scenario with Additive white Gaussian noise (AWGN) channel and BPSK modulated primary signal. The known CSI vector is generated by i.i.d zero-mean circularly symmetric complex Gaussian variables with normalized variance. The results are obtained by averaging 5000 Monte Carlo trails. In simulation, we choose the noise power according to the average SNR level defined by

$$\text{SNR} \triangleq \frac{\|\mathbf{h}s(l)\|^2}{M\sigma_n^2}. \quad (12)$$

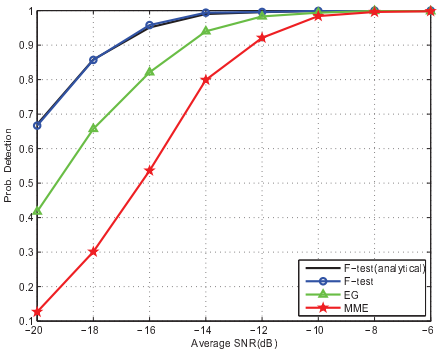

Fig. 2. Probability of detection versus average SNR, for $P_f = 0.05$ and $L = 5000$.

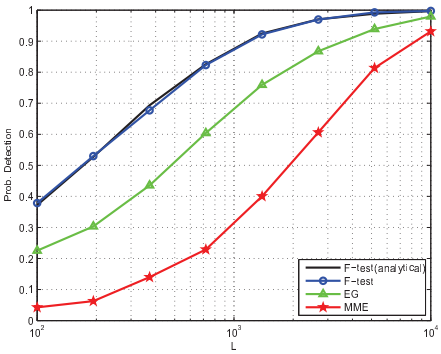

Fig. 3. Probability of detection versus sample length, for $P_f = 0.05$ and average SNR=-14dB.

A. Test performance under perfect parameter estimate

In the first experiment, we assume the parameter estimate is perfect and compare the $F-$test based approach with the energy detector (marked with EG) and MME detector. In Fig.2, we show the P_d against average SNR with a target $P_f = 0.05$ and $L = 5000$. The proposed $F-$test based sensing is shown to achieve the best detection probability among the three, i.e., when the detection probability is 0.9, the SNR gain of the proposed detector is about 2dB and 4.2dB over the energy

TABLE I
COMPLEXITY FOR $F-$TEST BASED METHOD, ENERGY DETECTOR AND MME DETECTOR.

	Complex Multiplications	Complex Additions
$F-$test Based Detector	$M(M+1)(1+L/2)$	$M(M+1)(L-1)/2+2(M-1)$
Energy Detector	ML	$(M-1)(L-1)$
MME Detector	$LM(M+1)/2+\mathcal{O}(M^3)$	$M(M+1)(L-S)(S-1)/2+\mathcal{O}(M^3)$

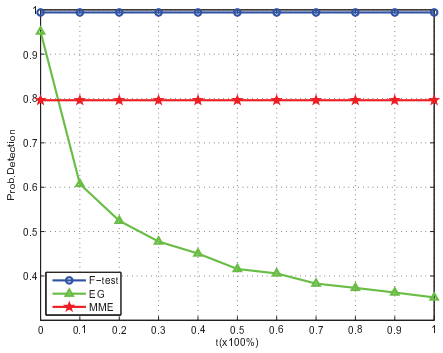

Fig. 4. Probability of detection v.s. noise uncertainty, for desired $P_f = 0.05$, $L = 5000$ and average SNR= -14dB.

detector and the MME method, respectively. In addition, the analytical result for P_d (11) provides an accurate description.

As mentioned above, the MME method needs a long sample length to ensure the selected test statistic be effective in each detection, while the $F-$test based method does not have such limitation. In Fig.3, we plot the impact corresponding to data length for $P_f = 0.05$ and average SNR=-14dB. It can be seen that the MME detector almost fails in the small sample scenario and the proposed detector achieves a much better performance. For example, to obtain a 90% detection probability, the $F-$test based method only needs $1/3$ as many samples as the energy detector and $1/8$ as many samples as the MME detector does, respectively.

B. Test performance under estimate error

In practice, we do not have access to the perfect parameter estimate due to limited feedback or quantization errors. As long as the detector needs *prior* knowledge, the estimation error will degrade detection performance. In the second experiment, we assume $\hat{\mathbf{h}} = \mathbf{h} + \triangle\mathbf{h}$, where $\hat{\mathbf{h}}$ denotes the channel estimate and the error term $\triangle\mathbf{h}$ is i.i.d zero-mean complex Gaussian distributed with covariance matrix $\sigma_e^2\mathbf{I}_M$, e.g., $0 \leq \sigma_e^2 \leq 1$. Since the variance of $\mathbf{h}$ has been normalized, the channel uncertainty can be viewed as from 0% to 100%. For noise mismatch, we assume the imperfect power estimate $\hat{\sigma}_n^2 = \beta\sigma_n^2$ and the factor β is considered as a uniformly distributed random variable in the interval $\left[\frac{1}{1+t}, t+1\right]$, where t denotes the noise uncertainty level from 0% to 100%.

In Fig.4, we plot P_d against noise uncertainty with desired

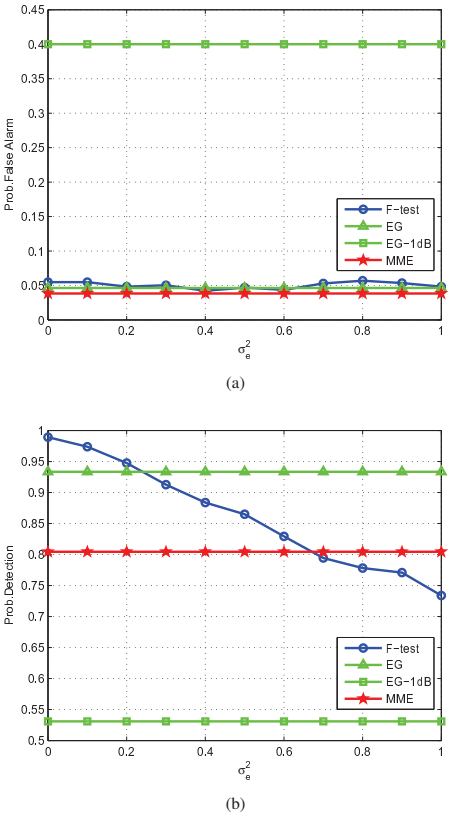

(a)

(b)

Fig. 5. Performance v.s. channel uncertainty σ_e^2. The performance (a):P_f; (b):P_d, for desired $P_f = 0.05$, $L = 5000$ and average SNR= -14dB.

$P_f = 0.05$, $L = 5000$ and average SNR=-14dB. It can be seen that the detection probability of the $F-$test based method and MME detector enjoy robustness against noise mismatch. On the other hand, the probability of detection associated with the energy detector is severely degraded by noise uncertainty.

Based on the same scenario, we show the impact caused by CSI error in Fig.5. Note that the performance of the energy detector with $10\log_{10} t = 1$dB noise uncertainty is a basis for comparison.

The false alarm probability of $F-$test based sensing, as shown in Fig.5(a), is still around the target value even with

channel uncertainty. However, the P_f of energy detector will be out of control with only 1dB noise uncertainty. Fig. 5(b) shows that the detection probability of the proposed approach degrades under channel uncertainty. However, with CSI error up to 23% and 68%, it still outperforms the ideal energy detector and MME detector, respectively. In addition, compared with energy detector with 1dB noise mismatch, the $F-$test based detector has a much higher detection probability over the entire channel uncertainty interval.

In summary, the $F-$test based detector shows the best detection performance at low SNR in the first experiment. It requires much less samples than the energy detector and the MME detector. Furthermore, its performance is not affected by noise uncertainty and has a mild sensitivity to channel uncertainty.

V. Conclusion

In this paper, we propose a novel sensing technique based on $F-$test. The method can be used for multiple antenna CR systems without knowledge of primary signal and noise power. Assuming the CSI is known, the proposed detector is easy to implement and robust to noise uncertainty. The test threshold and detection probability are derived by applying statistical properties of $F-$distribution. Simulation results show that the proposed approach leads to significant performance gain and enhanced robustness against noise uncertainly at low computational complexity. We believe the $F-$test based detector is a promising approach for spectrum sensing.

Appendix A
CDF of the proposed kinds of $F-$distribution

1) The central $F-$distribution

$$W_{c,n1,n2}(x) = \Pr(T < x) = I_k(\frac{1}{2}n_1, \frac{1}{2}n_2), \quad (13)$$

where $k = n_1x/(n_2 + n_1x)$, and I_k is the incomplete beta function. The formula for the incomplete beta function is

$$I_k(x, \frac{1}{2}n_1, \frac{1}{2}n_2) = \frac{\int_0^x t^{\frac{1}{2}n_1-1}(1-t)^{\frac{1}{2}n_2-1}d_t}{B(\frac{1}{2}n_1, \frac{1}{2}n_2)}, \quad (14)$$

where B is the beta function

$$B(\frac{1}{2}n_1, \frac{1}{2}n_2) = \int_0^1 t^{\frac{1}{2}n_1-1}(1-t)^{\frac{1}{2}n_2-1}d_t. \quad (15)$$

2) The noncentral $F-$distribution

$$\begin{aligned} W_{nc,n1,n2}(x \mid \delta^2) &= \Pr(T(\delta^2) < x)) \quad (16)\\ &= \sum_{j=0}^{\infty} w_{j,\delta^2} I_k(\frac{1}{2}n_1 + j, \frac{1}{2}n_2), \end{aligned}$$

where

$$w_{j,\delta^2} = \exp(-\delta^2/2)\frac{(\delta^2/2)^j}{j!}. \quad (17)$$

References

[1] FCC, *Facilitating opportunities for flexible, efficient, and reliable spectrum use employing cognitive radio technologies, notice of proposed rule making and order(ET Docket no.03-322)*, Dec. 2003.

[2] Haykin, "Cognitive radio: brain-empowered wireless communications," *Selected Areas in Communications, IEEE Journal on*, vol. 23, no. 2, pp. 201 – 220, Feb. 2005.

[3] H. Urkowitz, "Energy detection of unknown deterministic signals," *Proceedings of the IEEE*, vol. 55, no. 4, pp. 523 – 531, Apr. 1967.

[4] S. Kapoor, S. Rao, and G. Singh, "Opportunistic spectrum sensing by employing matched filter in cognitive radio network," in *Communication Systems and Network Technologies (CSNT), 2011 International Conference on*, Jun. 2011, pp. 580 –583.

[5] A. Sonnenschein and P. Fishman, "Radiometric detection of spread-spectrum signals in noise of uncertain power," *Aerospace and Electronic Systems, IEEE Transactions on*, vol. 28, no. 3, pp. 654 –660, Jul. 1992.

[6] R. Tandra and A. Sahai, "Fundamental limits on detection in low SNR under noise uncertainty," in *Wireless Networks, Communications and Mobile Computing, 2005 International Conference on*, vol. 1, Jun. 2005, pp. 464 – 469 vol.1.

[7] S. Chaudhari, V. Koivunen, and H. Poor, "Autocorrelation-based decentralized sequential detection of OFDM signals in cognitive radios," *Signal Processing, IEEE Transactions on*, vol. 57, no. 7, pp. 2690 –2700, Jul. 2009.

[8] Y. Zeng and Y.-C. Liang, "Eigenvalue-based spectrum sensing algorithms for cognitive radio," *Communications, IEEE Transactions on*, vol. 57, no. 6, pp. 1784 –1793, Jun. 2009.

[9] A. Taherpour, M. Nasiri-Kenari, and S. Gazor, "Multiple antenna spectrum sensing in cognitive radios," *Wireless Communications, IEEE Transactions on*, vol. 9, no. 2, pp. 814 –823, Feb. 2010.

[10] A. Pandharipande and J.-P. Linnartz, "Performance analysis of primary user detection in a multiple antenna cognitive radio," in *Communications, 2007. ICC '07. IEEE International Conference on*, Jun. 2007, pp. 6482 –6486.

[11] L. Shen, H. Wang, W. Zhang, and Z. Zhao, "Multiple antennas assisted blind spectrum sensing in cognitive radio channels," *Communications Letters, IEEE*, vol. 16, no. 1, pp. 92 –94, Jan. 2012.

[12] Z. Quan, S. Cui, and A. Sayed, "Optimal linear cooperation for spectrum sensing in cognitive radio networks," *Selected Topics in Signal Processing, IEEE Journal of*, vol. 2, no. 1, pp. 28 –40, Feb. 2008.

[13] P. Paysarvi-Hoseini and N. Beaulieu, "Optimal wideband spectrum sensing framework for cognitive radio systems," *Signal Processing, IEEE Transactions on*, vol. 59, no. 3, pp. 1170 –1182, march 2011.

[14] R. Zhang, "On peak versus average interference power constraints for protecting primary users in cognitive radio networks," *Wireless Communications, IEEE Transactions on*, vol. 8, no. 4, pp. 2112 –2120, Apr. 2009.

[15] G. A. F. Seber, *Linear regression analysis / George A.F. Seber, Alan J. Lee.*, ser. Wiley series in probability and statistics. New Jersey : Wiley, c2003., 2003.

[16] N. L. Johnson, S. Kotz, and N. Balakrishnan, *Continuous univariate distributions / Norman L. Johnson, Samuel Kotz, N. Balakrishnan.*, ser. Wiley series in probability and mathematical statistics: Applied probability and statistics. New York ; London : Wiley & Sons, c1994-1995., 1994.

[17] R. Zhang, T. Lim, Y.-C. Liang, and Y. Zeng, "Multi-antenna based spectrum sensing for cognitive radios: A GLRT approach," *Communications, IEEE Transactions on*, vol. 58, no. 1, pp. 84 –88, january 2010.

[18] I. M. Johnstone, "On the distribution of the largest eigenvalue in principal components analysis." *Annals of Statistics*, vol. 29, no. 2, pp. 295 – 327, 2001.

4072 IEEE TRANSACTIONS ON WIRELESS COMMUNICATIONS, VOL. 12, NO. 8, AUGUST 2013

An $F-$Test Based Approach for Spectrum Sensing in Cognitive Radio

Qi Huang and Pei-Jung Chung, *Senior Member, IEEE*

***Abstract*—Spectrum sensing is a key task in cognitive radio networks. Traditional sensing techniques such as energy detector suffer from noise uncertainty problem or require high computational complexity. In this paper, we propose a novel sensing technique using $F-$test by considering a multiple antenna cognitive radio system. This method is insensitive to noise uncertainty and easy to implement. It requires the channel state information (CSI) as *prior* knowledge. Based on statistical properties of $F-$distribution, we shall derive the test threshold and probability of detection, respectively. In addition, the performance of the proposed approach under imperfect channel information will be discussed. Simulation results show that the proposed $F-$test based detector achieves significant performance improvement compared with several popular detectors and offers robustness against noise uncertainty.**

***Index Terms*—Signal detection, multiple antenna, $F-$test, spectrum sensing, cognitive radio.**

I. Introduction

In face of the steadily inceasing demand for high data rates and limited spectral resources, traditional fixed spectrum allocation is no longer efficient. To improve spectrum efficiency, cognitive radio (CR) technology is proposed [1] to open the licensed band by allowing secondary user to utilize the temporally unoccupied spectrum bands. In response to this, IEEE formed the 802.22 working group in 2004 to develop a standard for secondary user access to the idle TV bands [2]. One of the main challenges of CR technology is that secondary user must monitor the presence of primary users over a certain spectrum periodically to avoid interference to primary service [3], which brings spectrum sensing, the fundamental task for CR technology, into account.

Many efficient sensing techniques have been proposed to tackle this challenge [4]–[11]. Among these methods, energy detector [4] is the most popular one due to its simplicity. It has been shown to be optimal only when the noise statistic is available to CR users [5]. However, the central problem of energy detector is its sensitivity to noise mismatch. More seriously, in the presence of large noise uncertainty, the high probability of false alarm and signal-to-noise ratio (SNR) wall phenomenon will make energy detector invalid [6]. Matched filter detector [7] is considered as an optimal method when the full knowledge of the primary signal is known. If CR users have some knowledge about the primary signal features, e.g., modulation type or symbol rate, then feature-based detector can be applied by exploiting the cyclostatio narity embedded in the received signal [8], [9]. But this method needs a long observation time and high computational complexity for implementation. On the other hand, blind detectors are considered when no *prior* information is available [10], [11].

Individual CR users may suffer from a poor sensing sensitivity due to severe fading or low SNRs. In this paper, the spectrum sensing problem in a multiple antenna system is considered. Multiple antenna technique is widely used in wireless communications to overcome multipath fading by exploiting the spatial diversity [12]. Recently, it has been applied in spectrum sensing for CR technology. A Neyman-Pearson sense based optimal detector is proposed in [13], which requires *prior* knowledge about noise power, CSI and primary signals. When noise power is known, the well-known energy detector [4], [5] can be applied and it has been extended to more sophisticated scenarios. For example, the energy-based detector proposed in [14] combines the received signals coherently. As mentioned above, all sensing schemes in this category suffer from the noise mismatch problem. To overcome this difficulty, current research focuses on blind sensing scheme, which exploits the signal structure without any information of signal parameters. Examples are eigenvalue-based detection [10], [15] and generalized likelihood ratio test (GLRT) based detection [13], [16], [17]. However, as shown in [18], the analytical test threshold for those blind detectors requires high computational complexity and the simple asymptotic threshold derived from random matrix theory differs significantly from the exact value in finite sensors and data samples. In addition, all blind detectors suffer from limited detection performance due to the lack of *prior* knowledge.

In summary, most current multiantenna-assisted detectors are sensitive to noise uncertainty or subject to limited sample size and test performance. In this paper, we propose an $F-$test based method to overcome those drawbacks. The proposed approach, in which CSI is required, enjoys high robustness against noise mismatch and moderate computational complexity. Based on statistical properties of $F-$distribution [19], the accurate value for test threshold and detection probability are derived, respectively. In addition, we will investigate the impact of channel uncertainty. The results indicate that when CSI is imperfect, the false alarm probability of the proposed approach is still under control. The detection probability can be calculated using doubly noncentral $F-$distribution in this

Manuscript received October 19, 2012; revised January 30 and May 2, 2013; accepted June 10, 2013. The associate editor coordinating the review of this paper and approving it for publication was L. Geoffrey.

The authors are with the School of Engineering, the University of Edinburgh, Edinburgh, U.K. (e-mail: {q.huang, p.chung}@ed.ac.uk).

Part of this work has been presented at IEEE ICC, Budapest, Hungary, June 2013.

Digital Object Identifier 10.1109/TWC.2013.071613.121633

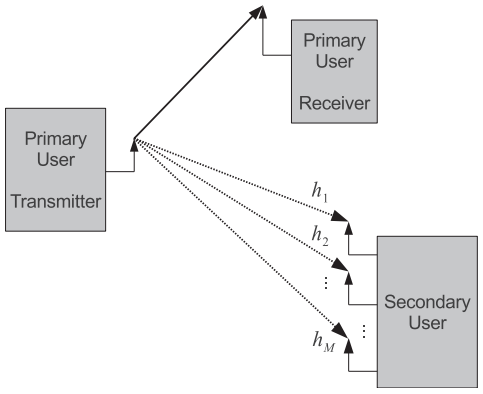

Fig. 1. SIMO CR network.

case and we present a simple approximated value for detection probability to avoid its computational complexity.

It is worth mentioning that an harmonic$-F$ test based method for spectrum sensing was discussed in [20], which is based on multitaper method to estimate the spectrum and the linear model for setting $F-$test is in the frequency domain. It can be seen as a blind wideband sensing and large sample size is required to achieve reasonable performance, i.e., 2200 samples is used in [20]. The proposed $F-$test based method, however, is based on a totally different signal model. It assumes a multiple antenna scenario and CSI is needed to construct the $F-$test. Moreover, to achieve reasonable performance, the required sample size is much smaller.

The remainder of the paper is structured as follows. In Section II, the signal model for multiple antenna sensing is described. In Section III, we propose the $F-$test based detector and derive the test threshold and detection probability. Then Section IV analyses the performance of the proposed approach under channel uncertainty. Comparison with several popular spectrum sensing schemes is discussed in Section V. Simulation results are presented in Section VI. Finally, Section VII concludes the paper.

Throughout this paper, boldface letters and boldface capital letters represent vectors and matrices, respectively. $(\cdot)^H$ denotes conjugate transpose and $(\cdot)^T$ represents transpose. $tr()$ stands for the trace operator and $\|\cdot\|$ represents Euclidean norm of a vector. $\mathbf{I}_M$ denotes the identity matrix of order M.

II. Signal Model

Consider a single-input multiple-output (SIMO) CR network as shown in Fig.1, where there is only one primary user and the secondary user is equipped with M antennas. In spectrum sensing, we aim at finding the idle spectrum band unoccupied by the primary user within the range of secondary users. Here the detection of primary user is formulated as a hypothesis testing problem: the null hypothesis $\mathcal{H}_0$ implies that the primary user is not active; and the alternative $\mathcal{H}_1$ implies that the primary user is active.

Let $\mathbf{y}(l) = [y_1(l), y_2(l), \ldots, y_M(l)]^T$ be the received signal vector at the M antennas, which can be expressed as

$$\begin{aligned} \mathcal{H}_0 &: \quad \mathbf{y}(l) = \mathbf{w}(l), \\ \mathcal{H}_1 &: \quad \mathbf{y}(l) = \mathbf{h}s(l) + \mathbf{w}(l),\ l = 1, 2...L, \end{aligned} \tag{1}$$

where $s(l)$ denotes the transmitted primary signal symbol at time instant l, which is unknown and deterministic. The flat fading channel is represented by the known CSI vector $\mathbf{h} = [h_1, h_2, \ldots, h_M]^T$. We assume that $\mathbf{h}$ is constant during the sensing period. The noise vector $\mathbf{w}(l) = [w_1(l), w_2(l), \ldots, w_M(l)]^T$ is i.i.d zero-mean, complex Gaussian distributed with covariance matrix $\sigma_n^2\mathbf{I}_M$, i.e., $\mathbf{w}(l) \sim \mathcal{CN}(\mathbf{0}, \sigma_n^2\mathbf{I}_M)$, where σ_n^2 is unknown. L is the number of received samples.

Since there is no existing reciprocity standard between primary and secondary systems, the learning of CSI $\mathbf{h}$ is still an open question. One solution to this problem was suggested in [21]–[24]: the knowledge of CSI is acquired from the periodically transmitting pilot [25] when the primary transmitter is known for sure to be active. Moreover, based on this method, the synchronization procedure for acquiring pilot is a challenge in low SNR scenario and certain code properties can be exploited for improving synchronization [26], [27].

III. $F-$test Based Detection

Given the observation $\mathbf{Y} = \{\mathbf{y}(l), l = 1, 2, \ldots, L\}$ and CSI vector $\mathbf{h}$, the problem of central interest is to detect the existence of primary signal. To begin with, we define the probability of false alarm (P_f) and the probability of detection (P_d) as follows

$$P_f = \Pr(T > \gamma | \mathcal{H}_0), \tag{2}$$

$$P_d = \Pr(T > \gamma | \mathcal{H}_1). \tag{3}$$

Where T denotes the test statistic and γ is the test threshold. In the context of cognitive radio, P_f denotes the probability that an idle spectrum is falsely ignored, which leads to a spectral loss. On the other hand, P_d determines the percentage of the occupied spectrum that is truly detected, which avoids the harmful interference to primary system. In the design of spectrum sensing technique, we should keep P_f under a prespecified significance level and make P_d as large as possible.

The linear signal model (1) ensures the applicability of $F-$test [28], which is derived from likelihood ratio principle under Gaussian noise assumption [29] and acts as an efficient tool for hypothesis testing in linear regression analysis. Here, it is applied to test whether there exists linear relationship between the receive data and CSI or not. The decision rule is given by

$$T \underset{\mathcal{H}_0}{\overset{\mathcal{H}_1}{\gtrless}} \gamma, \tag{4}$$

where the test threshold γ is selected to ensure a target probability of false alarm and the test statistic T is

$$T = \frac{n_2}{n_1} \frac{tr(\mathbf{P}\hat{\mathbf{R}}_y)}{tr((\mathbf{I}_M - \mathbf{P})\hat{\mathbf{R}}_y)}. \tag{5}$$

Here $\hat{\mathbf{R}}_y = \frac{1}{L}\sum_{l=1}^{L}\mathbf{y}(l)\mathbf{y}(l)^H$ represents the sample convariance matrix and $\mathbf{P} = \mathbf{h}(\mathbf{h}^H\mathbf{h})^{-1}\mathbf{h}^H$ denotes the projection onto the subspace spanned by $\mathbf{h}$. When $\mathcal{H}_0$ holds, or primary user is not active, the test statistic (5) is $F_{n_1,n_2}-$distributed [19] with degrees of freedom

$$n_1 = 2L, \quad (6)$$

$$n_2 = 2L(M-1). \quad (7)$$

Let $W_{c,n1,n2}(x)$ be the cumulative distribution function (CDF) of the $F-$distribution with degrees of freedom n_1 and n_2 (see Appendix A). Then given a target false alarm probability α, we can obtain the test threshold γ by looking up the existing table of $W_{c,n1,n2}(\gamma)$, that is

$$\gamma = W^{-1}_{c,n1,n2}(1-\alpha). \quad (8)$$

Note that the test statistic (5) can be seen as an SNR estimate for CR users. Therefore, the decision rule (4) implies that we will accept the alternative hypothesis $\mathcal{H}_1$, or declare the existence of primary signal, when SNR is large enough to exceed a given threshold γ.

When primary user is active, the test statistic T is noncentral $F-$distributed [19], i.e., $T \sim F'_{n_1,n_2}(\delta^2)$. The noncentrality parameter δ^2 is given by

$$\delta^2 = \frac{2\sum_{l=1}^{L}\|\mathbf{h}s(l)\|^2}{\sigma_n^2}. \quad (9)$$

The CDF of the noncentral $F-$distribution is defined as $W_{nc,n1,n2}(x \mid \delta^2)$ (see Appendix A). Hence we can obtain the probability of detection as

$$P_d = \Pr(F > \gamma|\mathcal{H}_1) = 1 - W_{nc,n1,n2}(\gamma \mid \delta^2), \quad (10)$$

which is also easy to evaluate by looking up the table. The detection probability P_d is an increasing function of the noncentrality parameter δ^2 [19]. From (9), we can conclude that a higher probability of detection can be obtained by increasing the sample size L.

IV. Impact of Channel Uncertainty

As mentioned above, channel information $\mathbf{h}$ is needed for constructing the $F-$test based method. However, due to estimation or quantization errors, one only has access to the imperfect CSI $\hat{\mathbf{h}} \in \mathbb{C}^{M\times 1}$, which can be modelled as follows:

$$\hat{\mathbf{h}} = \mathbf{h} + \triangle\mathbf{h}, \quad (11)$$

where $\triangle\mathbf{h} = [\triangle h_1, \triangle h_2, \ldots, \triangle h_M]^T$ denotes the error term. Such uncertainty may degrade the performance of the proposed detector. In this section, the impact of channel uncertainty will be discussed.

A. Test threshold and probability of false alarm

The selection of test threshold depends on the target false alarm probability, which is related to the null hypothesis $\mathcal{H}_0$. In this case, the received data only consists of noise because no primary user is active. Note that $\hat{\mathbf{h}}$ is a fixed parameter during a sensing period. Combining (1) and (5), the test statistic under channel uncertainty can be expressed as

$$T(\hat{\mathbf{h}}|\mathcal{H}_0) = \frac{n_2}{n_1}\frac{\sum_{l=1}^{L}\mathbf{w}(l)^H\hat{\mathbf{P}}\mathbf{w}(l)}{\sum_{l=1}^{L}\mathbf{w}(l)^H(\mathbf{I}_M - \hat{\mathbf{P}})\mathbf{w}(l)}, \quad (12)$$

where $\hat{\mathbf{P}} = \hat{\mathbf{h}}(\hat{\mathbf{h}}^H\hat{\mathbf{h}})^{-1}\hat{\mathbf{h}}^H$ denotes the projection matrix onto $\hat{\mathbf{h}}$. Since the noise $\{\mathbf{w}(l); l = 1, 2, \ldots, L\}$ is complex Gaussian distributed, the test statistic under $\mathcal{H}_0$ (12) is F_{n_1,n_2}-distributed, with n_1, n_2 given by (6) and (7). Therefore, given the test threshold γ (8), the false alarm probability is

$$P_f = \Pr(T(\hat{\mathbf{h}}) > \gamma|\mathcal{H}_0) = 1 - W_{c,n1,n2}(\gamma) = \alpha. \quad (13)$$

Hence, in the presence of channel uncertainty, the precomputed threshold γ (8) will still be effective to keep the false alarm probability under the target value.

B. Probability of detection

When the alternative $\mathcal{H}_1$ holds, the received data consists of both signal and noise, implying that the observations will depend on the channel $\mathbf{h}$ and so does the detection probability. Based on (1) and (5), when primary signal exists, the test statistic

$$T(\hat{\mathbf{h}}|\mathcal{H}_1) = \frac{n_2}{n_1}\frac{\sum_{l=1}^{L}(\mathbf{h}s(l)+\mathbf{w}(l))^H\hat{\mathbf{P}}(\mathbf{h}s(l)+\mathbf{w}(l))}{\sum_{l=1}^{L}(\mathbf{h}s(l)+\mathbf{w}(l))^H(\mathbf{I}_M - \hat{\mathbf{P}})(\mathbf{h}s(l)+\mathbf{w}(l))} \quad (14)$$

is doubly noncentral $F-$distribution (DNF) distributed, i.e., $T(\hat{\mathbf{h}}|\mathcal{H}_1) \sim F''_{n_1,n_2}(\delta_1^2, \delta_2^2)$ [19], with the noncentrality parameters

$$\delta_1^2 = \frac{2}{\sigma_n^2}\sum_{l=1}^{L}\left\|\hat{\mathbf{P}}\mathbf{h}s(l)\right\|^2, \quad (15)$$

$$\delta_2^2 = \frac{2}{\sigma_n^2}\sum_{l=1}^{L}\left\|(\mathbf{I}_M - \hat{\mathbf{P}})\mathbf{h}s(l)\right\|^2. \quad (16)$$

We define the CDF of DNF distribution as $W_{dnc,n_1,n_2}(x \mid \delta_1^2, \delta_2^2)$ (see Appendix A). It can be expected that the test power will be maximized when the perfect channel information is available, as shown in the following result.

Lemma 1: Given the degrees of freedom n_1, n_2 and test threshold γ, the detection probability

$$P_d = \Pr(T(\hat{\mathbf{h}}) > \gamma|\mathcal{H}_1) = 1 - W_{dnc,n_1,n_2}(\gamma|\delta_1^2, \delta_2^2) \quad (17)$$

is maximized when $\hat{\mathbf{h}} = \mathbf{h}$.

Proof: Combining (15) and (16), and applying the property of the projection matrix $\hat{\mathbf{P}}$, we have

$$\delta_1^2 + \delta_2^2 = \frac{2}{\sigma_n^2}\left\{\sum_{l=1}^{L}\left\|\hat{\mathbf{P}}\mathbf{h}s(l)\right\|^2 + \sum_{l=1}^{L}\left\|(\mathbf{I}_M - \hat{\mathbf{P}})\mathbf{h}s(l)\right\|^2\right\}$$

$$= \frac{2}{\sigma_n^2}\sum_{l=1}^{L}\|\mathbf{h}s(l)\|^2. \quad (18)$$

It has been shown that the probability of detection P_d given in (17) will rise when δ_1^2 increases or δ_2^2 decreases [30]. Since $\delta_1^2 + \delta_2^2$ is constant and $\delta_2^2 \geqslant 0$, P_d will be maximized when

$$\delta_1^2 = \frac{2}{\sigma_n^2}\sum_{l=1}^{L} \|\mathbf{h}s(l)\|^2, \quad (19)$$

$$\delta_2^2 = 0. \quad (20)$$

Both the equalities hold when and only when $\hat{\mathbf{P}}$ is the projection onto $\mathbf{h}$, which implies that given n_1, n_2 and γ, the test power P_d will reach its maximal at $\hat{\mathbf{h}} = \mathbf{h}$. ■

From *lemma* 1, we conclude that the test performance of the $F-$test based approach under perfect CSI offers a benchmark for comparison.

The closed-form saddlepoint approximation of DNF distribution is presented in [31], which consists of doubly infinite sum of incomplete beta functions. In order to simplify the computation, we apply a simple approach derived from the approximations to noncentral χ^2 distributions [19]. The approximate distribution is given by

$$\frac{1+\delta_1^2 n_1^{-1}}{1+\delta_2^2 n_2^{-1}} F_{v_1,v_2}, \quad (21)$$

with $v_1 = (n_1 + \delta_1^2)^2(n_1 + 2\delta_1^2)^{-1}$ and $v_2 = (n_2 + \delta_2^2)^2(n_2 + 2\delta_2^2)^{-1}$. Therefore, we can ultilize the table of central $F-$distribution to calculate the approximated detection probability under channel uncertainty, that is

$$P_d \approx 1 - W_{c,v_1,v_2}\left(\frac{1+\delta_2^2 n_2^{-1}}{1+\delta_1^2 n_1^{-1}}\gamma\right). \quad (22)$$

V. Implementation

In the previous sections, we derived the test threshold and detection probability of $F-$test based detector, and analysed its performance under imperfect channel information. In this section, the computational complexity and advantages of $F-$test based approach will be discussed.

A. Computational complexity

The computational cost of the proposed detector comes mainly from the computation of test statistic (5). Note that both $\hat{\mathbf{R}}_y$ and $\mathbf{P}$ are Hermitian, hence the evaluation can be simplified. In Table I, we list the complexity of $F-$test based method and compare it with three popular detectors: the energy detector, the blind eigenvalue-based maximun-minimum eigenvalue (MME) detector [10] and the blind GLRT detector [13]. Note that the computation of blind detectors includes both test statistic and test threshold. Because the analytical threshold expression is very complicated [18], we only list the blind detectors' complexity based on asymptotic test threshold.

The energy detector, which enjoys the highest computational efficiency, only requires ML multiplications and $(M-1)(L-1)$ additions. Due to the large sample assumption for asymptotic test threshold, e.g., the typical number of L is 10^4, blind detectors are the most expensive one among these approaches. The complexity of $F-$test based detector grows linearly with the sample size and is approximately proportional to the squared number of antennas. Since L is generally much larger than M, the proposed method has a comparable complexity with energy detector in practice. More importantly, without any assumption on sample size L, its analytical expression for test threshold (8) is simple and accurate.

B. Advantages

Since the test statistic (5) is independent from noise power, the $F-$test based detector offers absolute robustness against noise mismatch. Compared with the traditional robust or blind detectors [8], [10], the proposed detector can be easily constructed and the computational complexity is moderate. The only *prior* information needed is CSI, which can be seen as the price for improved robustness against uncertain noise level and performance gain. In addition, the analysis in Section IV shows that the false alarm probability of the $F-$test based detector is not affected by the channel estimation error.

VI. Simulation Results

In this section, the proposed $F-$test based sensing technique will be evaluated numerically and compared with several popular detectors. To examine the proposed method, each experiment performs 5000 Monte Carlo trials. The channel vector is generated by the i.i.d zero-mean circularly symmetric complex Gaussian random variable with variance normalized to one. We fix the sample size $L = 100$ and require the false alarm probability $P_f \leqslant 0.1$. In each trial, BPSK modulated primary signal and complex Gaussian distributed noise are applied. Simulation results will be obtained using the perfect and imperfect *prior* information, respectively. Note that in order to allow the blind detectors provide a reasonable performance in finite sample size, we shall calculate their test threshold by simulation rather than using the asymptotic formula in [10], [13]. In addition, the SNR is defined as

$$\text{SNR} \triangleq \frac{\|\mathbf{h}s(l)\|^2}{M\sigma_n^2}. \quad (23)$$

A. Performance under Perfect CSI

In the first experiment, we assume perfect channel knowledge $\mathbf{h}$ is available to $F-$test based method and the accurate noise power σ_n^2 is known to energy detector. In Fig.2, we plot the P_d of $F-$test based method, energy detector (marked with EG), MME detector and CLRT detector against average SNR with $M = 4$. We can find that under the same scenario, the proposed method achieves the best detection probability and the analytical formula for P_d, eq (10), gives an accurate description. Due to the lack of *prior* knowledge, the blind GLRT and MME methods have a lower detection probability.

In Fig.3, we draw the Receiver Operating Characteristics (ROC) curve for $M = 4$ and average SNR$= -8$dB. It shows that given a certain false alarm rate, the proposed $F-$test based method achieves a much higher probability of detection than other detectors. For example, when P_f is fixed at 0.01, the detection probability gain of the $F-$test based method is about 36% for the MME and approximately 23% for the energy and GLRT detectors.

TABLE I
COMPUTATIONAL COMPLEXITY FOR $F-$TEST BASED METHOD, ENERGY DETECTOR AND BLIND DETECTORS.

	Complex Multiplications	Complex Additions
$F-$test Based Detector	$M(M+1)(1+L/2)$	$M(M+1)(L-1)/2+2(M-1)$
Energy Detector	ML	$(M-1)(L-1)$
Blind Detector (MME and GLRT)	$LM(M+1)/2+\mathcal{O}(M^3)$	$LM(M+1)/2+\mathcal{O}(M^3)$

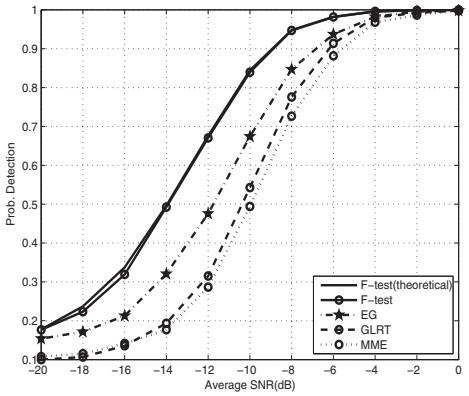

Fig. 2. Probability of detection versus average SNR, for $P_f = 0.1$, $M = 4$ and $L = 100$.

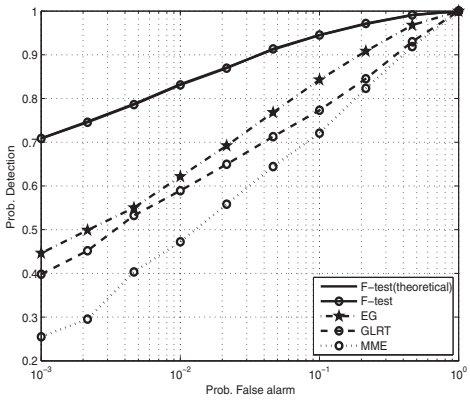

Fig. 3. ROC curve, for $M = 4$, $L = 100$ and average SNR$= -8$dB.

To test the impact of the number of antennas M, we choose the average SNR$=-8$dB and vary the number of antennas from 2 to 8. Fig.4 shows that when $M = 2$, the proposed method has the nearly same test power as energy detector. However, when M increases, the $F-$test based sensing technique has a significant performance improvement. This is due to the linear regression involved in the proposed approach, e.g., it takes the CSI $\mathbf{h}$ as the regressor and $\mathbf{y}(l)$ as the response variable. In other words, $F-$test here compares the similarity between the received signal and CSI. Therefore, a higher test power can be expected when more antennas (larger size of the regressor $\mathbf{h}$) are available.

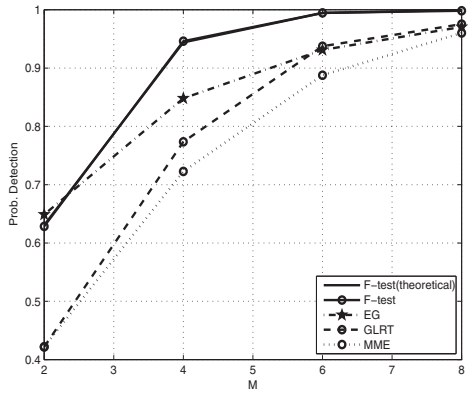

Fig. 4. Probability of detection v.s. number of antennas M, for $P_f = 0.1$, $L = 100$ and average SNR$= -8$dB.

B. Performance under noise uncertainty

As mentioned above, the $F-$test based method enjoys the robustness against noise uncertainty. To validate this property numerically, we assume only the estimated noise power $\hat{\sigma}_n^2 = \eta\sigma_n^2$ is available. The uncertainty $10\log_{10}\eta$ (in dB scale) is considered as a uniformly distributed random variable in the interval $[-E, E]$. Note that the estimated noise power is varied in each realization to a certain degree as mentioned above and is used to decide the test threshold of energy detector.

Fig.5 shows the detection performance against noise mismatch E for $M = 4$ and average SNR$= -8$dB. It can be observed that the performance of energy detector degrades severely under mismatched noise variance. For example, in the typical uncertainty range $E_{dB} \in [1, 2]$ [32], Fig.5(a) indicates that the P_f of energy detector far exceeds the target limit and Fig.5(b) shows that the corresponding P_d is substantially worse than the MME method. On the other hand, the $F-$test based detector, blind GLRT and MME detectors have the favourite noise-robust property as expected.

C. Performance under channel uncertainty

In the following experiments, we consider the scenario with imperfect CSI $\hat{\mathbf{h}}$. In simulation, the error term $\triangle\mathbf{h}$ in (11) varies in each trial, which is generated by i.i.d. zero-mean complex Gaussian distributed variable and the variance of each entry is assumed to be from zero to one, i.e., $0 \leq \sigma_e^2 \leq 1$. Since we have normalized the variance of CSI $\mathbf{h}$, the level of channel uncertainty can be viewed as from 0% to 100%.

Firstly, to get an insight of the impact of channel uncertainty to $F-$test based method, we plot the normalized histogram of

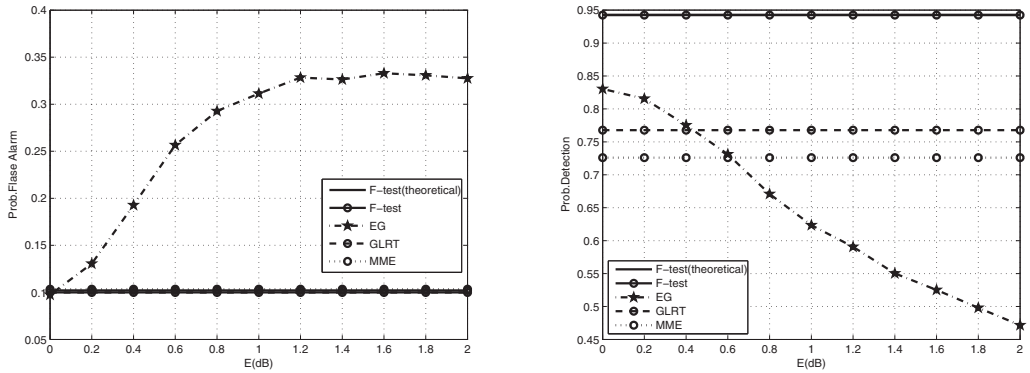

(a) (b)

Fig. 5. Performance v.s. noise uncertainty E. The performance (a):P_f; (b):P_d, for desired $P_f = 0.1$, $L = 100$, $M = 4$ and average SNR= -8dB.

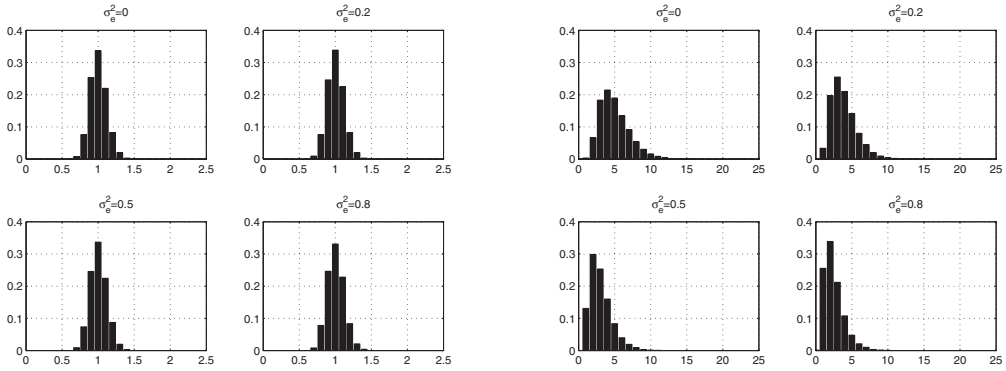

(a) (b)

Fig. 6. Normalized histogram of the test statistic for $F-$test based method under channel uncertainty, (a): $T(\hat{\mathbf{h}}|\mathcal{H}_0)$; (b): $T(\hat{\mathbf{h}}|\mathcal{H}_1)$. The uncertainty level is selected as σ_e^2 =0, 0.2, 0.5 and 0.8, respectively, for $M = 4$, average SNR= 0dB and $L = 100$.

the test statistic in Fig.6 for $M = 4$ and average SNR= 0dB. The error variance σ_e^2 is set as 0, 0.2, 0.5 and 0.8 with the corresponding uncertainty level as 0%, 20%, 50% and 80%, respectively. Fig.6(a) shows that the distribution of $T(\hat{\mathbf{h}}|\mathcal{H}_0)$ does not vary with channel uncertainty, which verifies our analysis in Section IV. While in Fig.6(b), we can find that the histogram of $T(\hat{\mathbf{h}}|\mathcal{H}_1)$ shrinks to a smaller value when σ_e^2 rises, which implies that the probability of detection will decrease with growing channel uncertainty.

Then in Fig.7, the test performance against the channel uncertainty is presented, with average SNR=-8dB and $M = 4$. Note that the line of energy detector with 1dB noise mismatch acts as a basis of comparison. Fig.7(a) shows that unlike the energy detector, the false alarm probability of the $F-$test based method is still around the pre-defined level in the situation with parameter uncertainty. The detection probability of the proposed detector, as shown in Fig.7(b), has a degradation under CSI error. However, with channel uncertainty up to 30%, the $F-$test still outperforms the ideal energy detector. Besides, it performs better than the GLRT detector and the MME detector with channel uncertainty up to 50% and 65%, respectively. Moreover, compared with energy detector with 1dB noise mismatch, the $F-$test has a better performance over the entire interval of CSI error. In addition, the approximated value for P_d (22) is quite accurate.

In Fig.8, we increase the number of antennas to 8. It can be observed that the performance loss of $F-$test based approach caused by channel uncertainty becomes insignificant. For instance, Fig.8(b) shows that the detection probability only has an up to 11% degradation over the whole uncertainty interval.

In summary, the $F-$test based detector shows the best detection performance at perfect channel estimate and performs reasonably well for moderate channel uncertainty. Compared

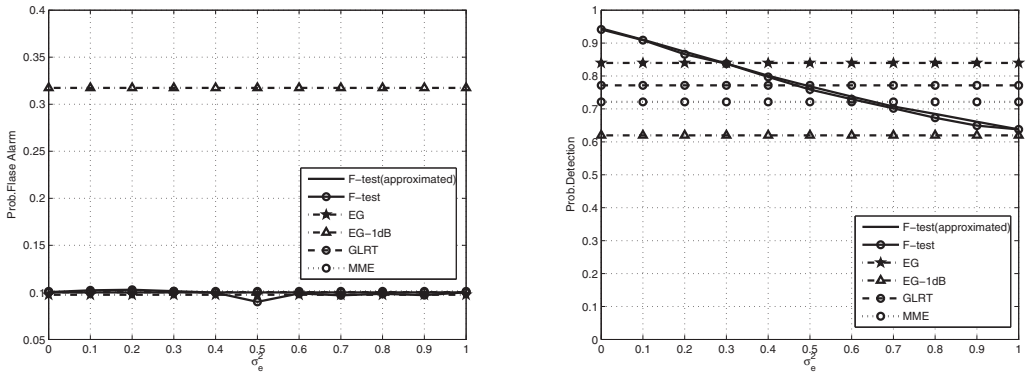

(a) (b)

Fig. 7. Performance v.s. channel uncertainty σ_e^2. The performance (a):P_f; (b):P_d, for desired $P_f = 0.1$, $L = 100$, average SNR=-8dB and $M = 4$.

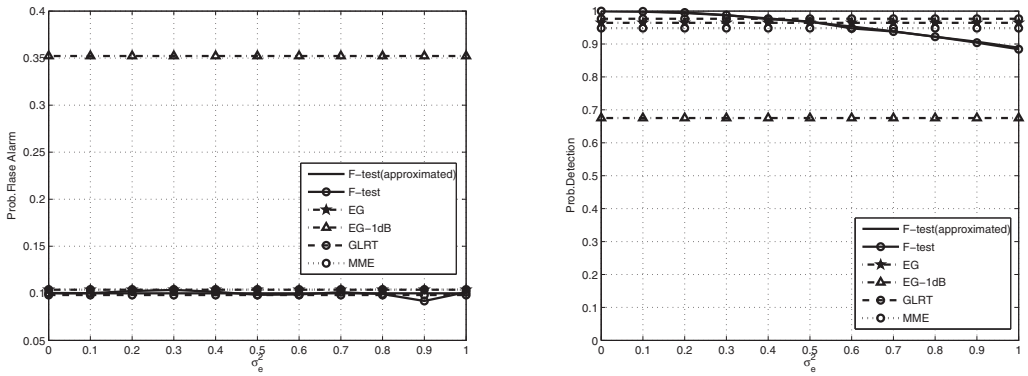

(a) (b)

Fig. 8. Performance v.s. channel uncertainty σ_e^2. The performance (a):P_f; (b):P_d, for desired $P_f = 0.1$, $L = 100$, average SNR=-8dB and $M = 8$.

with energy detector, its performance is insensitive to noise mismatch.

VII. Conclusion

In this paper, we propose a spectrum sensing method based on the $F-$test. The method can be applied for multiple antenna CR systems without the knowledge of primary signal and noise statistic. The proposed approach is simple to implement, enjoys high robustness against uncertain noise level and achieves significant performance gain. Statistical properties of $F-$distribution are applied to derive the test threshold and evaluate the detection probability. When perfect channel information is not available, the $F-$test based detector suffers a mild performance loss in probability of detection and its false alarm probability remains unchanged. Simulations have been carried out to verify the proposed method. Given its superior performance and moderate computational complexity, $F-$test based approach is an attractive approach for spectrum sensing.

Appendix A
CDF of $F-$distributions

1) The central $F-$distribution

$$W_{c,n1,n2}(x) = \Pr(T < x) = I_k(\frac{1}{2}n_1, \frac{1}{2}n_2), \quad (24)$$

where $k_1 x/(n_2 + n_1 x)$, and I_k is the incomplete beta function. The formula for the incomplete beta function is

$$I_k(x, \frac{1}{2}n_1, \frac{1}{2}n_2) = \frac{\int_0^x t^{\frac{1}{2}n_1 - 1}(1-t)^{\frac{1}{2}n_2 - 1}dt}{B(\frac{1}{2}n_1, \frac{1}{2}n_2)}, \quad (25)$$

where B is the beta function

$$B(\frac{1}{2}n_1, \frac{1}{2}n_2) = \int_0^1 t^{\frac{1}{2}n_1 - 1}(1-t)^{\frac{1}{2}n_2 - 1}dt. \quad (26)$$

2) The noncentral central $F-$distribution

$$W_{nc,n1,n2}(x \mid \delta^2) = \Pr(T(\delta^2) < x)) \quad (27)$$
$$= \sum_{j=0}^{\infty} w_{j,\delta^2} I_k(\frac{1}{2}n_1 + j, \frac{1}{2}n_2),$$

where

$$w_{j,\delta^2} = \exp(-\delta^2/2)\frac{(\delta^2/2)^j}{j!}. \quad (28)$$

3) The doubly noncentral central $F-$distribution

$$W_{dnc,n1,n2}(x \mid \delta_1^2, \delta_2^2) = \Pr(T(\delta_1^2, \delta_2^2) < x))$$
$$= \sum_{k=0}^{\infty} w_{k,\delta_2^2} \sum_{j=0}^{\infty} w_{j,\delta_1^2} I_k(\frac{1}{2}n_1 + j, \frac{1}{2}n_2 + k). \quad (29)$$

ACKNOWLEDGMENT

The authors would like to thank the editor for the speedy coordination of the review process and all the reviewers for their valuable comments that significantly improved the manuscript.

REFERENCES

[1] FCC, Facilitating opportunities for flexible, efficient, and reliable spectrum use employing cognitive radio technologies, notice of proposed rule making and order(ET Docket no.03-322), Dec. 2003.
[2] I. Mitola and J. Maguire, "Cognitive radio: making software radios more personal," *IEEE Personal Commun.*, vol. 6, no. 4, pp. 13–18, Aug. 1999.
[3] Haykin, "Cognitive radio: brain-empowered wireless communications," *IEEE J. Sel. Areas Commun.*, vol. 23, no. 2, pp. 201–220, Feb. 2005.
[4] H. Urkowitz, "Energy detection of unknown deterministic signals," *Proc. IEEE*, vol. 55, no. 4, pp. 523–531, Apr. 1967.
[5] A. Sonnenschein and P. Fishman, "Radiometric detection of spread-spectrum signals in noise of uncertain power," *IEEE Trans. Aerospace Electron. Syst.*, vol. 28, no. 3, pp. 654–660, July 1992.
[6] R. Tandra and A. Sahai, "Fundamental limits on detection in low SNR under noise uncertainty," in *Proc. 2005 International Conf. Wireless Netw., Commun. Mobile Comput.*, vol. 1, pp. 464–469.
[7] D. Cabric, A. Tkachenko, and R. Brodersen, "Spectrum sensing measurements of pilot, energy, and collaborative detection," in *Proc. 2006 IEEE Military Commun. Conf.*, pp. 1–7.
[8] S. Chaudhari, V. Koivunen, and H. Poor, "Autocorrelation-based decentralized sequential detection of OFDM signals in cognitive radios," *IEEE Trans. Signal Process.*, vol. 57, no. 7, pp. 2690–2700, July 2009.
[9] Z. Chen, T. Luan, and X.-D. Zhang, "Sensing orthogonal frequency division multiplexing systems for cognitive radio with cyclic prefix and pilot tones," *IET Commun.*, vol. 6, no. 1, pp. 97–106, 2012.
[10] Y. Zeng and Y.-C. Liang, "Eigenvalue-based spectrum sensing algorithms for cognitive radio," *IEEE Trans. Commun.*, vol. 57, no. 6, pp. 1784–1793, June 2009.
[11] P. Bianchi, M. Debbah, M. Maida, and J. Najim, "Performance of statistical tests for single-source detection using random matrix theory," *IEEE Trans. Inf. Theory*, vol. 57, no. 4, pp. 2400–2419, Apr. 2011.
[12] A. Goldsmith, *Wireless Communications*. Cambridge University Press, 2005.
[13] A. Taherpour, M. Nasiri-Kenari, and S. Gazor, "Multiple antenna spectrum sensing in cognitive radios," *IEEE Trans. Wireless Commun.*, vol. 9, no. 2, pp. 814–823, Feb. 2010.
[14] A. Pandharipande and J.-P. Linnartz, "Performance analysis of primary user detection in a multiple antenna cognitive radio," in *Proc. 2007 IEEE International Conf. Commun.*, pp. 6482–6486.
[15] A. Kortun, T. Ratnarajah, M. Sellathurai, and C. Zhong, "On the performance of eigenvalue-based spectrum sensing for cognitive radio," in *Proc. 2010 IEEE Symp. New Frontiers Dynamic Spectrum*, pp. 1–6.
[16] T. J. Lim, R. Zhang, Y. C. Liang, and Y. Zeng, "GLRT-based spectrum sensing for cognitive radio," in *Proc. 2008 IEEE Global Telecommun. Conf.*, pp. 1–5.
[17] R. Zhang, T. Lim, Y.-C. Liang, and Y. Zeng, "Multi-antenna based spectrum sensing for cognitive radios: a GLRT approach," *IEEE Trans. Commun.*, vol. 58, no. 1, pp. 84–88, Jan. 2010.
[18] A. Kortun, M. Sellathurai, T. Ratnarajah, and C. Zhong, "Distribution of the ratio of the largest eigenvalue to the trace of complex wishart matrices," *IEEE Trans. Signal Process.*, vol. 60, no. 10, pp. 5527–5532, Oct. 2012.
[19] N. L. Johnson, S. Kotz, and N. Balakrishnan, *Continuous Univariate Distributions*, N. L. Johnson, S. Kotz, and N. Balakrishnan, ser. Wiley Series in Probability and Mathematical Statistics: Applied Probability and Statistics. Wiley & Sons, 1994.
[20] S. Haykin, D. Thomson, and J. Reed, "Spectrum sensing for cognitive radio." *Proc. IEEE*, vol. 97, no. 5, pp. 849–877, May 2009.
[21] Z. Quan, S. Cui, and A. Sayed, "Optimal linear cooperation for spectrum sensing in cognitive radio networks," *IEEE J. Sel. Topics Signal Process.*, vol. 2, no. 1, pp. 28–40, Feb. 2008.
[22] Z. Quan, S. Cui, A. Sayed, and H. Poor, "Optimal multiband joint detection for spectrum sensing in cognitive radio networks," *IEEE Trans. Signal Process.*, vol. 57, no. 3, pp. 1128–1140, 2009.
[23] J. Ma, G. Zhao, and Y. Li, "Soft combination and detection for cooperative spectrum sensing in cognitive radio networks," *IEEE Trans. Wireless Commun.*, vol. 7, no. 11, pp. 4502–4507, 2008.
[24] P. Paysarvi-Hoseini and N. Beaulieu, "Optimal wideband spectrum sensing framework for cognitive radio systems," *IEEE Trans. Signal Process.*, vol. 59, no. 3, pp. 1170–1182, Mar. 2011.
[25] L. Tong, B. Sadler, and M. Dong, "Pilot-assisted wireless transmissions: general model, design criteria, and signal processing," *IEEE Signal Process. Mag.*, vol. 21, no. 6, pp. 12–25, Nov. 2004.
[26] H. Wymeersch, N. Noels, H. Steendam, and M. Moeneclaey, "Synchronization at low SNR: performance bounds and algorithms," in *2004 Invited Presentation Commun. Theory Workshop*.
[27] C. Wang, X. Wang, H. Lin, and J.-Y. Chouinard, "Low SNR timing and frequency synchronization for PIP-OFDM system," in *Proc. 2010 IEEE Veh. Technol. Conf. – Spring*, pp. 1–5.
[28] G. A. F. Seber, *Linear Regression Analysis*, G. A. F. Seber, A. J. Lee, ser. Wiley series in probability and statistics. Wiley, 2003.
[29] R. H. Shumway, "Replicated time-series regression: an approach to signal estimation and detection," pp. 383–408, 1983.
[30] H. Scheff, *The Analysis of Variance*, H. Scheff, ser. Wiley Publications in Mathematical Statistics. Wiley & Sons, 1959.
[31] R. W. Butler and M. S. Paolella, "Calculating the density and distribution function for the singly and doubly noncentral F," *Statistics Comput.*, vol. 12, no. 1, pp. 9–16, Jan. 2002.
[32] A. Sahai and D. Cabric, "Spectrum sensing: fundamental limits and practical challenges," in *2005 IEEE International Symp. New Frontiers Dynamic Spectrum Access Netw.*

Qi Huang received the B.E. degree in electrical engineering and automation from Beihang University, Beijing, China, and the M.Sc. degree with distinction in signal processing and communications from the University of Edinburgh, UK. She is currently pursuing the Ph.D. degree at the Institute for Digital Communications, University of Edinburgh, UK. Her current research interests include cognitive radio network and statistical signal processing.

Pei-Jung Chung received Dr.-Ing. in 2002 from Ruhr-Universität Bochum, Germany with distinction. From 2002 to 2004 she held a post-doctoral position at Carnegie Mellon University and University of Michigan, Ann Arbor, USA, respectively. From 2004 to 2006 she was Assistant Professor with National Chiao Tung University, Hsin Chu, Taiwan. In 2006 she joined the Institute for Digital Communications, School of Engineering, the University of Edinburgh, UK as Lecturer. Currently, she is Associate Member of IEEE Signal Processing Society Sensor Array Multichannel Technical Committee and serves for IEEE Communications Society, Multimedia Communications Technical Committee as Vice Chair of Interest Group on Acoustic and Speech Processing for Communications. Her research interests include array processing, statistical signal processing, wireless MIMO communications and distributed processing in wireless sensor networks.

Globecom 2014 - Cognitive Radio and Networks Symposium

A Nonparametric Approach for Spectrum Sensing Using Bootstrap Techniques

Qi Huang * , Pei-Jung Chung † and John Thompson *
* Institute for Digital Communications, The University of Edinburgh, UK
Email: * Q.Huang@ed.ac.uk, John.Thompson@ed.ac.uk
† Delta Electronics, Inc. Taipei, Taiwan Email: † peijung.chung@gmail.com

***Abstract*—This paper deals with the blind spectrum sensing problem for arbitrary noise. The majority of current methods consider the Gaussian noise. However, this assumption cannot model the impulsive noise due to the artificial source. In this paper, we remove the requirement on Gaussianity and propose a detection method based on the bootstrap technique. By using multiple receiving antennas, the proposed detector exploits the eigenstructure of sample covariance matrix. Since there is no closed-form expression for the joint distribution of eigenvalues, the nonparametric bootstrap resampling is applied to estimate the null distribution of the test statistic. Simulation results show that the proposed detector performs well in different noise types and a performance gain can be expected when the noise is non-Gaussian.**

***Index Terms*—signal detection, bootstrap, non-Gaussian noise, spectrum sensing, cognitive radio.**

I. Introduction

Cognitive radio (CR) is a flexible spectral allocation scheme that opens the licensed band to the secondary user [1]. In order to avoid harmful interference to the primary user, CR user must perform spectrum sensing first to detect the presence of primary signal. Based on different operational requirements, traditional methods fall into the following categories: energy detector [2], cyclostationarity-based detector [3], eigenvalue-based detector [4] and generalized likelihood ratio test (GLRT) based detection [5]. Most of them are derived from Gaussian noise. Or, the test threshold and test performance are studied based on Gaussianity. For the noise due to the natural sources, such as the thermal noise, the Gaussian model is justified. However, there still exist man-made noise in CR scenario [6], which makes the whole noise heavy-tailed or impulsive. Under such non-Gaussianity, the test performance of aforementioned methods becomes uncertain.

Only several detection methods have been proposed to deal with the non-Gaussian noise [7]–[10]. A detector based on Kolmogorov-Smirnov test is proposed in [7], which requires a sequence of noise samples in advance. In [8], a GLRT-based detector is proposed based on the assumption that the noise is Generalized Gaussian distributed. When the power of channel gain and noise moments are known, the optimal and sub-optimal L_p-norm detectors can be applied in low signal-to-noise ratio (SNR) regime [9]. In [10], the polarity-coincidence-array based approach is proposed which is suitable to the real-valued signal.

In this paper, a bootstrap-based detector is proposed with minimal requirements on noise. That is, no assumptions are made on noise power and noise types. By using multiple antennas at the CR sensor, the proposed method is fundamentally a binary hypothesis test for the difference between sample eigenvalues. We assume that when primary signal exists, the difference between eigenvalues will be relatively larger than the noise only case. Inspired by [11], bootstrap resampling is applied to estimate the null distribution of the test statistic. Note that the bootstrap technique works in arbitrary noise and does not require large samples. However, when the sample size is small, as it is in this paper, the bias in sample eigenvalues is significant and may degrade the test performance. Therefore, a blindly bootstrap bias correction step is also proposed.

The rest of the paper is organized as follows. The data model is described in Section II before discussing the hypothesis test in Section III. In Section IV, the detection procedure using bootstrap is proposed, including the approximation of null distribution and bias correction. A brief discussion is highlighted in Section V and Simulation results are shown in Section VI. Finally, Section VII concludes the paper.

In this paper, boldface letters and boldface capital letters represent vectors and matrices, respectively. $(\cdot)^H$ is conjugate transpose and $(\cdot)^T$ indicates transpose. $\mathbf{I}_M$ is the identity matrix of order M. $\mathrm{E}[\cdot]$ denotes the statistical expectation. $|\cdot|$ and $\|\cdot\|$ stands for Euclidean norm of a scalar and vector, respectively.

II. Data Model

Consider a single-input multiple-output (SIMO) CR network where the secondary receiver is equipped with M antennas. Based on the received signal $\mathbf{y}(t) = [y_1(t), y_2(t), \ldots, y_M(t)]^T$, the problem of central interest is to decide whether the primary signal exists or not, which can be formulated as a hypothesis test:

$$\begin{aligned} \mathcal{H}_0 &: \mathbf{y}(t) = \mathbf{n}(t), \\ \mathcal{H}_1 &: \mathbf{y}(t) = \mathbf{h}s(t) + \mathbf{n}(t),\ t = 1, 2, ..., L, \end{aligned} \quad (1)$$

where $s(t)$ is the zero-mean complex primary signal to be detected and we assume its power is σ_s^2. The flat fading channel is represented by $\mathbf{h} = [h_1, h_2, \ldots, h_M]^T$, which is unknown and assumed to be a constant during the sensing interval. $\mathbf{n}(t) = [n_1(t), n_2(t), \ldots, n_M(t)]^T$ represents the complex noise vector with zero mean and covariance $\sigma_n^2\mathbf{I}_M$.

978-1-4799-3512-3/14/$31.00 ©2014 IEEE

L is the sample size. Note that both σ_s^2 and σ_n^2 are unknown. Besides, no assumption is made on the distribution of noise or signal.

Based on the above signal model, the received data $\mathbf{y}(t)$ can be seen as independent and identically distributed (i.i.d.) with zero mean and covariance matrix:

$$\begin{aligned} \mathcal{H}_0 &: \quad \mathbf{R}_y = \sigma_n^2 \mathbf{I}_M, \\ \mathcal{H}_1 &: \quad \mathbf{R}_y = \sigma_s^2 \mathbf{h}\mathbf{h}^H + \sigma_n^2 \mathbf{I}_M. \end{aligned} \tag{2}$$

The corresponding eigenvalues [12] λ_i, $i = 1, 2, ..., M$ are

$$\begin{aligned} \mathcal{H}_0 &: \quad \lambda_1 = \lambda_2 = \ldots = \lambda_M = \sigma_n^2, \\ \mathcal{H}_1 &: \quad \lambda_1 > \lambda_2 = \ldots = \lambda_M = \sigma_n^2. \end{aligned} \tag{3}$$

The eq (3) has an interpretation that, when $\mathcal{H}_0$ holds, all the eigenvalues are contributed by the noise only. However, when $\mathcal{H}_1$ is true, the largest eigenvalue $\lambda_1 = \mathbf{h}^H \mathbf{h} \sigma_s^2 + \sigma_n^2$ is contributed by both the primary signal and noise.

Based on our assumption, the covariance $\mathbf{R}_y$ is unknown. The one we can obtain is the sample covariance matrix

$$\hat{\mathbf{R}}_y = \frac{1}{L-1} \sum_{t=1}^{L} \mathbf{y}(t) \mathbf{y}(t)^H. \tag{4}$$

When the sample size L is finite, the sample eigenvalue β_i, $i = 1, 2, ..., M$ obtained from $\hat{\mathbf{R}}_y$ are definitely distinct [12] under both $\mathcal{H}_0$ and $\mathcal{H}_1$:

$$\beta_1 > \beta_2 > \ldots > \beta_M. \tag{5}$$

III. Hypothesis testing

By employing the difference of eigenvalues, the hypothesis test (3) can be converted to

$$\begin{aligned} \mathcal{H}_0 &: \quad \lambda_1 - \frac{1}{M-1} \sum_{i=2}^{M} \lambda_i = 0, \\ \mathcal{H}_1 &: \quad \lambda_1 - \frac{1}{M-1} \sum_{i=2}^{M} \lambda_i > 0. \end{aligned} \tag{6}$$

Considering that we can only obtain the sample eigenvalues, the test statistic is given as follows

$$\hat{T} = \beta_1 - \frac{1}{M-1} \sum_{i=2}^{M} \beta_i. \tag{7}$$

Since the sample eigenvalues β_i, $i = 1, 2, ..., M$ are distinct from each other with probability one, the test statistic $\hat{T}$ will be nonzero under both $\mathcal{H}_0$ and $\mathcal{H}_1$. However, a reasonable assumption can be made that $\hat{T}$ will be large when primary signal exists but relatively small in the noise only case. Therefore, the hypothesis testing problem (6) can be converted to the following decision rule

$$\hat{T} \underset{\mathcal{H}_0}{\overset{\mathcal{H}_1}{\gtrless}} \gamma, \tag{8}$$

where γ is the test threshold to ensure a target false alarm probability defined as follows

$$P_f = \Pr(\hat{T} > \gamma | \mathcal{H}_0). \tag{9}$$

Note that the evaluation of γ needs the null distribution of the test statistic $\hat{T}$. To the best of our knowledge, there are no existing results on the joint distribution of eigenvalues without additional assumption on the Gaussianity. In this paper, we shall apply a bootstrap procedure [13] to overcome this difficulty.

IV. Bootstrap-based method

The bootstrap technique is an attractive tool for estimating parameter or testing hypothesis when conventional methods are no longer valid. For example, the asymptotic results, e.g., distributions of eigenvalues derived from random matrix theory [4], [5], make assumptions on Gaussianity and large sample size, which are inapplicable to our case. The bootstrap method, however, is distribution-free and works in small samples. The principle is that, rather than repeating the experiment, one creates the bootstrap data sets via randomly resampling the original sample set with replacement. In this section, we shall start with a general bootstrap procedure and then apply it to the proposed detection problem.

A. General concept

Let $\chi = [x_1, x_2, \ldots, x_L]$ be an i.i.d sample set from an unknown distribution F and θ denotes an unknown characteristic (e.g., mean or variance of F) estimated by $\hat{\theta}$. The problem of interest is to find the distribution of $\hat{\theta}$ or measure its estimate accuracy, such as the bias or standard error of $\hat{\theta}$. Generally, one approximates those properties of $\hat{\theta}$ by repeating the experiment for a sufficient number of times. The bootstrap method, however, treats the original data χ as an empirical estimate of the true distribution and resamples χ directly [14]. A general bootstrap principle is outlined in Table I.

TABLE I
The Bootstrap Principle

1) Given an i.i.d data set $\chi = [x_1, x_2, \ldots, x_L]$.
2) Draw a bootstrap sample set $\chi^* = [x_1^*, x_2^*, \ldots, x_L^*]$ via resampling χ with replacement. An example can be : $\chi^* = [x_1, x_1, \ldots, x_8]$.
3) Compute the bootstrap statistic $\hat{\theta}^*$ from χ^*.
4) Repeat 2) and 3) B times to obtain a set of bootstrap statistic $\{\hat{\theta}^*(b), b = 1, 2, \ldots, B\}$.
5) Estimate the statistical properties of $\hat{\theta}$ from $\hat{\theta}^*(b)$.

As an extension of the distribution estimate, the bootstrap method can also be applied to the hypothesis testing problem. For a hypothesis testing problem: $\mathcal{H}_0 : \vartheta \leq \vartheta_0$ against $\mathcal{H}_1 : \vartheta > \vartheta_0$, the test statistic is defined as

$$\hat{T}_b = \hat{\vartheta} - \vartheta_0. \tag{10}$$

The null distribution of $\hat{T}_b$ can be approximated by the bootstrap statistics $\{\hat{\vartheta}^*(b) - \hat{\vartheta}\}$ [15]. Given a significance value (false alarm probability in spectrum sensing) α, one can compute the test threshold γ_b through the following relation

$$\alpha = \frac{1}{B}\sum_{b=1}^{B} I[(\hat{\vartheta}^*(b) - \hat{\vartheta}) > \gamma_b], \tag{11}$$

where $I[\cdot]$ denotes the indicator function.

B. Application to the proposed detector

The hypothesis testing problem (6) can be reformulated as

$$\begin{aligned} \mathcal{H}_0 &: \quad T = 0, \\ \mathcal{H}_1 &: \quad T > 0, \end{aligned} \tag{12}$$

where $T = \lambda_1 - \frac{1}{M-1}\sum_{i=2}^{M}\lambda_i$ with $\hat{T}$ (7) as the estimator. By definition, T and $\hat{T}$ are non-negative. As discussed above, the null distribution of $\hat{T}$ can be approximated by $\{\hat{T}^*(b) - \hat{T}\}$ and one can compute the test threshold γ based on those bootstrap estimates. We summarize the detection procedure in Table II, where the included eigenvalue bias correction step will be discussed later.

TABLE II
DETECTION PROCEDURE USING BOOTSTRAP

Input: $\mathbf{Y} = [\mathbf{y}(1), \mathbf{y}(2), \ldots, \mathbf{y}(L)]$.
Target false alarm probability α.
1) Compute the bias corrected sample eigenvalues using Table III and obtain the test statistic
$\hat{T} = \hat{\beta}_1 - \frac{1}{M-1}\sum_{i=2}^{M}\hat{\beta}_i$.
2) Draw a bootstrap sample set $\mathbf{Y}^*$ from $\mathbf{Y}$.
3) Compute the bias corrected bootstrap test statistic
$\hat{T}^* = \hat{\beta}_1^* - \frac{1}{M-1}\sum_{i=2}^{M}\hat{\beta}_i^*$.
4) Repeat 2) and 3) B times. Ranking the bootstrap statistics as
$(\hat{T}^*(1) - \hat{T}) \leq \ldots \leq (\hat{T}^*(k) - \hat{T}) \leq \ldots \leq (\hat{T}^*(B) - \hat{T})$
5) From the ordered statistics, choose the index k by $\alpha = 1 - k/B$. The test threshold is obtained as $\gamma = \hat{T}^*(k) - \hat{T}$.
Output: Hypothesis testing $\hat{T} \underset{\mathcal{H}_0}{\overset{\mathcal{H}_1}{\gtrless}} \gamma$.

As mentioned above, the test statistic $\hat{T}$ (7) is constructed by the sample eigenvalues. However, as discussed in [11], [12], the sample eigenvalue contributed by the primary signal is asymptotically unbiased, whereas the one contributed by the noise only is asymptotically biased. When the sample size is limited, the bias becomes quite significant, e.g., $\hat{T}$ may be large even if no primary signal exists. Note that in this paper, we do not make assumption on large data size. Therefore, a bias reduction is necessary to ensure accuracy of sample eigenvalues.

Define the bias of sample eigenvalue β_i as the difference between the expectation of β_i and the exact eigenvalue λ_i, that is

$$Bias(\beta_i) = E(\beta_i) - \lambda_i,\ i = 1, 2, \ldots, M. \tag{13}$$

Since no assumption is made on the distribution of signal and noise, we apply the distribution-free bootstrap method [13] to estimate the bias $Bias(\beta_i)$. That is

$$\hat{Bias}(\beta_i) = \frac{1}{B_1}\sum_{b=1}^{B_1}\beta_i^*(b) - \beta_i,\ i = 1, 2, \ldots, M, \tag{14}$$

where B_1 is the bootstrap replications and empirically, $B_1 = 30$ gives quite satisfactory results. The corrected sample eigenvalue is given by

$$\begin{aligned} \hat{\beta}_i &= \beta_i - \hat{Bias}(\beta_i) \\ &= 2\beta_i - \frac{1}{B_1}\sum_{b=1}^{B_1}\beta_i^*(b),\ i = 1, 2, \ldots, M. \end{aligned} \tag{15}$$

The bootstrap bias correction procedure is outlined in Table III. Note that it should be applied to both the test statistic $\hat{T}$ and bootstrap statistic $\hat{T}^*$.

TABLE III
BOOTSTRAP BIAS CORRECTION

Input: $\mathbf{Y} = [\mathbf{y}(1), \mathbf{y}(2), \ldots, \mathbf{y}(L)]$.
1) Compute the sample eigenvalues $\beta_i,\ i = 1, 2, \ldots M$.
2) Draw a bootstrap sample set $\mathbf{Y}^*$ from $\mathbf{Y}$.
3) Compute the bootstrapped sample eigenvalues: $\beta_i^*,\ i = 1, 2, \ldots M$.
4) Repeat 2) and 3) B_1 times to obtain
$Bias(\beta_i) = \frac{1}{B_1}\sum_{b=1}^{B_1}\beta_i^*(b) - \beta_i,\ i = 1, 2, \ldots, M.$
5) Compute the bias reduced sample eigenvalue $\hat{\beta}_i = \beta_i - Bias(\beta_i),\ i = 1, 2, \ldots, M$.
Output: The ordered bias reduced sample eigenvalue $\hat{\beta}_1 > \hat{\beta}_2 > \ldots > \hat{\beta}_M$.

V. DISCUSSION

Since both the eigenstructure property ((3) and (5)) and bootstrap method hold for arbitrary noise, the proposed approach is nonparametric and enjoys the distribution-free property. As shown in Section VI, under non-Gaussianity, several popular detectors derived in Gaussian become invalid due to the high false alarm probability. The proposed detector, however, works for a broad class of noise types and offers an overall better test performance.

The main issue is the computational complexity, which grows linearly with $B_1 B$. Simulation results show that $B_1 B$ in the order of 10^4 gives sufficiently accurate results. When the sample size is moderate, such complexity is compatible with the computer power today. Moreover, it is comparable to other popular blind detectors. Take the GLRT-based detector [5] as an example. To obtain an accurate test threshold in Gaussian, the analytical expression is complex [16] and the method using Monte Carlo simulations usually requires 10^5 trials [5].

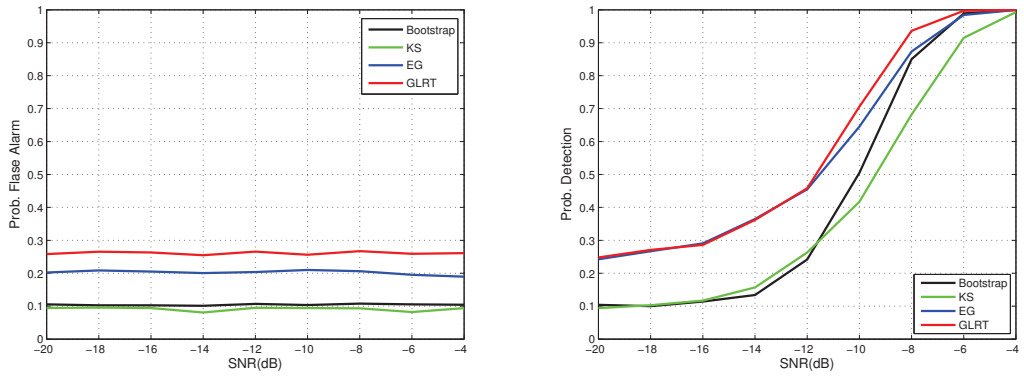

(a) (b)

Fig. 1. Performance under Laplacian noise, for (a): Probability of false alarm versus SNR; (b): Probability of detection versus SNR.

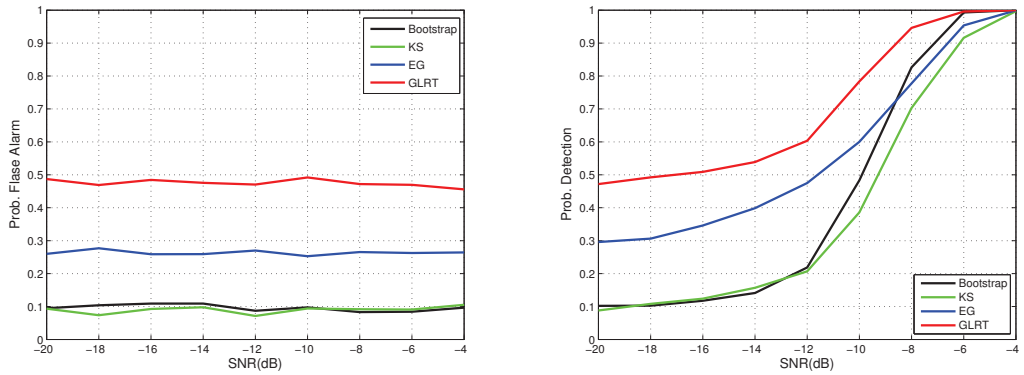

(a) (b)

Fig. 2. Performance under Gaussian Mixture noise, for (a): Probability of false alarm versus SNR; (b): Probability of detection versus SNR.

It is worth mentioning that when the noise is Gaussian distributed, the optimal test is the GLRT-based detection [5] . In this paper, the GLRT statistic (constructed by the ratio of sample eigenvalues) is not applied due to the bias issue, as even the use of bias correction procedure cannot make the sample eigenvalue be completely equal to the true eigenvalue. Such bias will have an effect on the accuracy of bootstrap estimate $\{\hat{\vartheta}^*(b) - \hat{\vartheta}\}$. The test statistic $\hat{T}$ (7) in this paper is applied since the bias can be further offset in $\{\hat{T}^*(b) - \hat{T}\}$ by employing the difference between sample eigenvalues.

VI. Simulation Results

In this section, we shall present the test performance of the proposed method by numerical experiments. For comparison, the popular energy detector (marked with EG) [2], GLRT-based detector [5] and Kolmogorov-Smirnov based detector (marked with KS) [7] are also evaluated. Since the noise type is unknown, to have a fare comparison, the test thresholds for energy and GLRT-based detector are calculated using the results derived in Gaussian [2], [16]. The KS based detector, which requires a sequence of noise only samples, is another distribution-free approach and can be applied to any noise types.

In the following simulations, we assume $M = 4$ and a Rayleigh fading channel is considered. Primary signal is modelled as Gaussian distributed and the sample size is fixed at $L = 100$. The target false alarm probability α is 10%. The bootstrap parameter B_1 and B are set as 30 and 300, respectively. To test the distribution-free property of the proposed detectors, we consider the following noise types that

are relevant in the context of CR:

1) Generalized Gaussian Model (GGM): GGM is a broad family which adds a shape parameter to the Gaussian distribution [17]. It is widely used to model the non-Gaussian noise such as heavy-tailed and impulsive noise [18]. The probability density function (pdf) of GGM with a variance σ_n^2 and shape parameter ρ is given by

$$P_n(n) = \frac{\rho\Gamma(4/\rho)}{2\pi\sigma_n^2(\Gamma(4/\rho))^2}\exp(-\frac{1}{c}(\frac{|n|}{\sigma_n})^\rho), \qquad (16)$$

where $c \triangleq (\Gamma(2/\rho)\Gamma(4/\rho))^{\rho/2}$ and $\Gamma(\rho) = \int_0^\infty x^{\rho-1}e^{-x}dx$.
The GGM is short-tailed when $\rho > 2$ and heavy-tailed when $0 < \rho < 2$. The Gaussian ($\rho = 2$) and Laplacian ($\rho = 1$) distribution are special cases of GGM. In this paper, the heavy-tailed Laplacian noise is applied.

2) Gaussian Mixture Model (GMM): GMM is another popular model to characterize the impulsive noise [19]. The corresponding pdf is

$$P_n(n) = \sum_{i=1}^{I}\frac{c_i}{\pi\sigma_i^2}\exp(-\frac{|n|^2}{\sigma_i^2}), \qquad (17)$$

where $c_i, \sigma_i^2 > 0$, $\sum_{i=1}^I c_i = 1$ and $\sum_{i=1}^I c_i\sigma_i^2 = \sigma_n^2$. A special case is ε-mixture model, where $I = 2$, $c_1 = 1-\epsilon$ and $\sigma_1^2 = \sigma_n^2/(1-\epsilon+\kappa\epsilon)$. Here, we choose $\epsilon = 0.06$ and $\kappa = 10$ to model the impulsive man-made noise.

Note that all the results are obtained by averaging 2000 Monte Carlo trails. In addition, the SNR is defined as

$$\text{SNR} \triangleq \frac{\sigma_s^2\|\mathbf{h}\|^2}{M\sigma_n^2}. \qquad (18)$$

The probability of false alarm under Laplacian and Gaussian Mixture noise are evaluated in Fig.1(a) and Fig.2(a). On one hand, both the two distribution-free detectors (e.g., bootstrap-based and KS-based detector) meet the target false alarm rate and the accuracy of bootstrap method is verified. On the other hand, the energy detector and GLRT based detector fail in such non-Gaussianity as their false alarm probability far exceed the target limit. For instance, given 10% as the target value, the P_f of energy and GLRT-based detector are near 50% and 27% under Gaussian Mixture noise, respectively. The reason is that their test thresholds are only known under Gaussian noise.

The detection probability against SNR is described in Fig.1(b) and Fig.2(b). Note that the performance of energy and GLRT detector are ignored since the are impaired by the high false alarm probability. For the rest two detectors, results show that the proposed bootstrap method offers a better test performance. For example, as shown in Fig.1(b), to achieve a 90% detection probability, the bootstrap method has a 1.3dB SNR gain compared with KS detector. In addition, the KS-based method needs a sequence of noise samples in advance while the bootstrap method does not.

VII. Conclusion

In this paper, we study the blind spectrum sensing problem in the situation of unknown noise type. The proposed detector is based on the fact that, the eigenvalue corresponds to the primary signal is larger than the rest of eigenvalues correspond to the noise only. The test statistic is derived from the difference between eigenvalues and its null distribution is estimated by the bootstrap resampling. When the data length is small, the bias in sample eigenvalue may make the test statistic under null and alternative hypothesis not well separated. To improve the accuracy of test statistic, we also propose a bootstrap bias correction procedure. Simulation results show that the proposed bootstrap detection is valid in a variety of noise types and demonstrate its superiority when the noise is non-Gaussian.

In addition, several interesting topics are worth to be considered further. For example, the signal structure can be applied to achieve a better detection performance, and we can extend the bootstrap-based sensing by considering the case of multiple primary transmitters.

References

[1] Haykin, "Cognitive radio: brain-empowered wireless communications," *Selected Areas in Communications, IEEE Journal on*, vol. 23, no. 2, pp. 201 – 220, Feb. 2005.

[2] H. Urkowitz, "Energy detection of unknown deterministic signals," *Proceedings of the IEEE*, vol. 55, no. 4, pp. 523 – 531, Apr. 1967.

[3] Z. Chen, T. Luan, and X.-D. Zhang, "Sensing orthogonal frequency division multiplexing systems for cognitive radio with cyclic prefix and pilot tones," *Communications, IET*, vol. 6, no. 1, pp. 97 –106, 4 2012.

[4] Y. Zeng and Y.-C. Liang, "Eigenvalue-based spectrum sensing algorithms for cognitive radio," *Communications, IEEE Transactions on*, vol. 57, no. 6, pp. 1784 –1793, Jun. 2009.

[5] A. Taherpour, M. Nasiri-Kenari, and S. Gazor, "Multiple antenna spectrum sensing in cognitive radios," *Wireless Communications, IEEE Transactions on*, vol. 9, no. 2, pp. 814 –823, Feb. 2010.

[6] S. Haykin, D. Thomson, and J. Reed, "Spectrum sensing for cognitive radio." *Proceedings of the IEEE*, vol. 97, no. 5, pp. 849 – 877, May. 2009.

[7] G. Zhang, X. Wang, Y.-C. Liang, and J. Liu, "Fast and robust spectrum sensing via kolmogorov-smirnov test," *Communications, IEEE Transactions on*, vol. 58, no. 12, pp. 3410–3416, 2010.

[8] S. Zahabi and A.-A. Tadaion, "Local spectrum sensing in non-gaussian noise," in *Telecommunications (ICT), 2010 IEEE 17th International Conference on*, 2010, pp. 843–847.

[9] F. Moghimi, A. Nasri, and R. Schober, "Lp-norm spectrum sensing for cognitive radio networks impaired by non-gaussian noise," in *Global Telecommunications Conference, IEEE*, 2009, pp. 1–6.

[10] T. Wimalajeewa and P. Varshney, "Polarity-coincidence-array based spectrum sensing for multiple antenna cognitive radios in the presence of non-gaussian noise," *Wireless Communications, IEEE Transactions on*, vol. 10, no. 7, pp. 2362–2371, 2011.

[11] R. F. Brcich, A. Zoubir, and P. Pelin, "Detection of sources using bootstrap techniques," *Signal Processing, IEEE Transactions on*, vol. 50, no. 2, pp. 206–215, 2002.

[12] A. C. Rencher and W. F. Christensen, *Methods of multivariate analysis.*, ser. Wiley series in probability and mathematical statistics. Hoboken, N.J. : Wiley., 2012.

[13] B. Efron and R. Tibshirani, *An introduction to the bootstrap / Bradley Efron and Robert J. Tibshirani.*, ser. Monographs on statistics and applied probability: 57. New York ; London ,1993., 1993.

[14] A. Zoubir and B. Boashash, "The bootstrap and its application in signal processing," *Signal Processing Magazine, IEEE*, vol. 15, no. 1, pp. 56–76, 1998.

[15] P. Hall and S. R. Wilson, "Two guidelines for bootstrap hypothesis testing," *Biometrics*, no. 2, p. 757, 1991.

References

[1] A. Khattab, M. A. Bayoumi, and D. Perkins, *Cognitive radio networks: from theory to practice.* Analog circuits and signal processing, New York, Springer, 2013.

[2] E. Biglieri, A. J. Goldsmith, L. J. Greenstein, N. Mandayam, and H. V. Poor, *Principles of Cognitive Radio.* Cambridge University Press, 2012.

[3] M. A. McHenry, P. A. Tenhula, D. McCloskey, D. A. Roberson, and C. S. Hood, "Chicago spectrum occupancy measurements and analysis and a long-term studies proposal," in *Proceedings of the first international workshop on Technology and policy for accessing spectrum*, ACM, 2006.

[4] M. A. McHenry, D. McCloskey, and G. Lane-Roberts, "Spectrum occupancy measurements, location 4 of 6: Republican national convention, new york city, new york, august 30, 2004-september 3, 2004, revision 2," *Shared Spectrum Company Report*, 2005.

[5] FCC, "Spectrum policy task force(et docket no 02-155)," 2002.

[6] "General survey of radio frequency bands 30 MHz to 3GHz." `http://www.sharedspectrum.com/wp-content/uploads/2010_0923%20General%20Band%20Survey%20-%2030MHz-to-3GHz.pdf`.

[7] S. Haykin, "Cognitive radio: brain-empowered wireless communications," *Selected Areas in Communications, IEEE Journal on*, vol. 23, pp. 201 – 220, Feb. 2005.

[8] H. Urkowitz, "Energy detection of unknown deterministic signals," *Proceedings of the IEEE*, vol. 55, pp. 523 – 531, Apr. 1967.

[9] D. Cabric, S. Mishra, and R. Brodersen, "Implementation issues in spectrum sensing for cognitive radios," in *Signals, Systems and Computers, 2004. Conference Record of the Thirty-Eighth Asilomar Conference on*, vol. 1, pp. 772–776 Vol.1, Nov. 2004.

[10] Z. Quan, S. Cui, and A. Sayed, "Optimal linear cooperation for spectrum sensing in cognitive radio networks," *Selected Topics in Signal Processing, IEEE Journal of*, vol. 2, pp. 28 –40, Feb. 2008.

[11] Z. Quan, S. Cui, A. Sayed, and H. Poor, "Optimal multiband joint detection for spectrum sensing in cognitive radio networks," *Signal Processing, IEEE Transactions on*, vol. 57, no. 3, pp. 1128–1140, 2009.

[12] R. Tandra and A. Sahai, "Wireless networks, communications and mobile computing, international conference on," in *Fundamental limits on detection in low SNR under noise uncertainty*, vol. 1, pp. 464–469, Jun. 2005.

[13] Y. Zeng and Y.-C. Liang, "Eigenvalue-based spectrum sensing algorithms for cognitive radio," *Communications, IEEE Transactions on*, vol. 57, pp. 1784 –1793, Jun. 2009.

[14] A. Kortun, T. Ratnarajah, M. Sellathurai, and C. Zhong, "On the performance of eigenvalue-based spectrum sensing for cognitive radio," in *New Frontiers in Dynamic Spectrum, IEEE Symposium on*, pp. 1 –6, Apr. 2010.

[15] A. Taherpour, M. Nasiri-Kenari, and S. Gazor, "Multiple antenna spectrum sensing in cognitive radios," *Wireless Communications, IEEE Transactions on*, vol. 9, pp. 814 – 823, Feb. 2010.

[16] T. J. Lim, R. Zhang, Y. C. Liang, and Y. Zeng, "GLRT-based spectrum sensing for cognitive radio," in *Global Telecommunications Conference IEEE.*, pp. 1 –5, Dec. 2008.

[17] R. Zhang, T. Lim, Y.-C. Liang, and Y. Zeng, "Multi-antenna based spectrum sensing for cognitive radios: A GLRT approach," *Communications, IEEE Transactions on*, vol. 58, pp. 84–88, Jan. 2010.

[18] S. Chaudhari, V. Koivunen, and H. Poor, "Autocorrelation-based decentralized sequential detection of OFDM signals in cognitive radios," *Signal Processing, IEEE Transactions on*, vol. 57, pp. 2690–2700, Jul. 2009.

[19] E. Axell and E. Larsson, "Optimal and sub-optimal spectrum sensing of OFDM signals in known and unknown noise variance," *Selected Areas in Communications, IEEE Journal on*, vol. 29, pp. 290–304, Feb. 2011.

[20] P. Urriza, E. Rebeiz, and D. Cabric, "Multiple antenna cyclostationary spectrum sensing based on the cyclic correlation significance test," *Selected Areas in Communications, IEEE Journal on*, vol. 31, pp. 2185–2195, Nov. 2013.

[21] G. Huang and J. Tugnait, "On cyclostationarity based spectrum sensing under uncertain gaussian noise," *Signal Processing, IEEE Transactions on*, vol. 61, pp. 2042–2054, Apr. 2013.

[22] S. Haykin, D. Thomson, and J. Reed, "Spectrum sensing for cognitive radio," *Proceedings of the IEEE*, vol. 97, pp. 849–877, May. 2009.

[23] M. Sanchez, L. de Haro, M. Ramon, A. Mansilla, C. Ortega, and D. Oliver, "Impulsive noise measurements and characterization in a UHF digital TV channel," *Electromagnetic Compatibility, IEEE Transactions on*, vol. 41, pp. 124–136, May. 1999.

[24] K. Blackard, T. Rappaport, and C. Bostian, "Measurements and models of radio frequency impulsive noise for indoor wireless communications," *Selected Areas in Communications, IEEE Journal on*, vol. 11, pp. 991–1001, Sep. 1993.

[25] W. Lauber and J. Bertrand, "Statistics of motor vehicle ignition noise at VHF/UHF," *Electromagnetic Compatibility, IEEE Transactions on*, vol. 41, pp. 257–259, Aug 1999.

[26] T. Blankenship and T. Rappaport, "Characteristics of impulsive noise in the 450-mhz band in hospitals and clinics," *Antennas and Propagation, IEEE Transactions on*, vol. 46, pp. 194–203, Feb 1998.

[27] H. Bogucka, P. Kryszkiewicz, and A. Kliks, "Dynamic spectrum aggregation for future 5G communications," *Communications Magazine, IEEE*, vol. 53, pp. 35–43, May 2015.

[28] T. Doumi, "Spectrum considerations for public safety in the united states," *Communications Magazine, IEEE*, vol. 44, pp. 30–37, Jan. 2006.

[29] K. Hassan, R. Gautier, I. Dayoub, M. Berbineau, and E. Radoi, "Multiple-antenna-based blind spectrum sensing in the presence of impulsive noise," *Vehicular Technology, IEEE Transactions on*, vol. 63, pp. 2248–2257, Jun. 2014.

[30] F. Moghimi, A. Nasri, and R. Schober, "Lp-norm spectrum sensing for cognitive radio networks impaired by non-gaussian noise," in *Global Telecommunications Conference, IEEE*, pp. 1–6, 2009.

[31] M. Bkassiny and S. Jayaweera, "Robust, non-gaussian wideband spectrum sensing in cognitive radios," *Wireless Communications, IEEE Transactions on*, vol. 13, pp. 6410–6421, Nov. 2014.

[32] G. Zhang, X. Wang, Y.-C. Liang, and J. Liu, "Fast and robust spectrum sensing via kolmogorov-smirnov test," *Communications, IEEE Transactions on*, vol. 58, no. 12, pp. 3410–3416, 2010.

[33] J. Lunden, S. Kassam, and V. Koivunen, "Robust nonparametric cyclic correlation-based spectrum sensing for cognitive radio," *Signal Processing, IEEE Transactions on*, vol. 58, no. 1, pp. 38–52, 2010.

[34] T. Wimalajeewa and P. Varshney, "Polarity-coincidence-array based spectrum sensing for multiple antenna cognitive radios in the presence of non-gaussian noise," *Wireless Communications, IEEE Transactions on*, vol. 10, no. 7, pp. 2362–2371, 2011.

[35] K. Arshad and K. Moessner, "Robust spectrum sensing based on statistical tests," *Communications, IET*, vol. 7, no. 9, 2013.

[36] R. Y. Rubinstein and D. P. Kroese, *Simulation and the Monte Carlo method*, vol. 707. John Wiley Sons, 2011.

[37] S. Howison, *Practical applied mathematics: modelling, analysis, approximation*. No. 38, Cambridge University Press, 2005.

[38] Q. Huang and P.-J. Chung, "An F-test for multiple antenna spectrum sensing in cognitive radio," in *Communications (ICC), 2013 IEEE International Conference on*, pp. 4677–4681, Jun. 2013.

[39] Q. Huang and P.-J. Chung, "An F-test based approach for spectrum sensing in cognitive radio," *Wireless Communications, IEEE Transactions on*, vol. 12, pp. 4072–4079, Aug. 2013.

[40] Q. Huang, P.-J. Chung, and J. Thompson, "A nonparametric approach for spectrum sensing using bootstrap techniques," in *Global Communications Conference (GLOBECOM), 2014 IEEE*, pp. 851–856, Dec. 2014.

[41] J. Mitola, *Cognitive Radio: An Integrated Agent Architecture for Software Defined Radio*. PhD thesis, KTH Royal Institute of Technology, 2000.

[42] FCC, "Unlicensed operations in the tv broadcast bands, second memorandum opinion and order," pp. 10–174, Sep. 2010.

[43] "Ofcom implementing TV white spaces." `http://stakeholders.ofcom.org.uk/consultations/white-space-coexistence/statement`.

[44] J. Ma, G. Li, and B. H. Juang, "Signal processing in cognitive radio," *Proceedings of the IEEE*, vol. 97, pp. 805–823, May. 2009.

[45] J. Lu and I.-T. Lu, "Propagation based spectrum sensing: A novel beamforming detection method," in *Cognitive Radio Oriented Wireless Networks and Communications (CROWNCOM), 2011 Sixth International ICST Conference on*, pp. 11–15, Jun. 2011.

[46] M. C. Won-Yeol Lee, Vuran and S. Mohanty, "A survey on spectrum management in cognitive radio networks," *Communications Magazine, IEEE*, vol. 46, pp. 40–48, Apr. 2008.

[47] Z. Chen, T. Luan, and X.-D. Zhang, "Sensing orthogonal frequency division multiplexing systems for cognitive radio with cyclic prefix and pilot tones," *Communications, IET*, vol. 6, pp. 97 –106, Apr. 2012.

[48] L. T. Sorensen, K. E. Skouby, D. Dietterle, A. Jhunjhunwala, X. Fu, and X. Wang, "User scenarios 2020: a worldwide wireless future," *WWRF Outlook*, no. 4, 2009.

[49] A. Aijaz and A. Aghvami, "Cognitive machine-to-machine communications for internet-of-things: A protocol stack perspective," *Internet of Things Journal, IEEE*, vol. 2, pp. 103–112, Apr. 2015.

[50] "IEEE802.22 working group on wireless regional area networks." `http://www.ieee802.org/22/`.

[51] FCC, "Facilitating opportunities for flexible, efficient, and reliable spectrum use employing cognitive radio technologies, notice of proposed rule making and order(et docket no. 03-322)," Dec. 2003.

[52] "IEEE 802.11af standard for information technology." `https://standards.ieee.org/findstds/standard/802.11af-2013.html`.

[53] "IEEE dynamic spectrum access network DySPAN standards committee." `http://grouper.ieee.org/groups/dyspan/`.

[54] "Technical and operational requirements for the possible operation of cognitive radio systems in the white spaces of the frequency band 470-790 mhz." `http://www.erodocdb.dk/Docs/doc98/official/pdf/ECCREP159.PDF`.

[55] "Complementary report to ECC report 159 further definition of technical and operational requirements for the operation of white space devices in the band 470-790 mhz." `http://www.erodocdb.dk/Docs/doc98/official/pdf/ECCREP185.PDF`.

[56] L. L. Scharf and C. Demeure, *Statistical signal processing : detection, estimation, and time series analysis*. Addison-Wesley, 1991.

[57] S. M. Kay, *Fundamentals of statistical signal processing.* Prentice-Hall signal processing series, Prentice-Hall., 1993.

[58] P. Schreier and L. L. Scharf, *Statistical signal processing of complex-valued data : the theory of improper and noncircular signals.* Cambridge University Press, 2010.

[59] A. Sonnenschein and P. Fishman, "Radiometric detection of spread-spectrum signals in noise of uncertain power," *Aerospace and Electronic Systems, IEEE Transactions on*, vol. 28, pp. 654–660, Jul. 1992.

[60] D. Ramirez, G. Vazquez-Vilar, R. Lopez-Valcarce, J. Via, and I. Santamaria, "Detection of rank-p signals in cognitive radio networks with uncalibrated multiple antennas," *Signal Processing, IEEE Transactions on*, vol. 59, pp. 3764–3774, Aug. 2011.

[61] J. Tugnait, "On multiple antenna spectrum sensing under noise variance uncertainty and flat fading," *Signal Processing, IEEE Transactions on*, vol. 60, pp. 1823–1832, Apr. 2012.

[62] L. Wei, O. Tirkkonen, P. Dharmawansa, and M. McKay, "On the exact distribution of the scaled largest eigenvalue," in *Communications (ICC), 2012 IEEE International Conference on*, pp. 2422–2426, Jun. 2012.

[63] A. Kortun, M. Sellathurai, T. Ratnarajah, and C. Zhong, "Distribution of the ratio of the largest eigenvalue to the trace of complex wishart matrices," *Signal Processing, IEEE Transactions on*, vol. 60, pp. 5527 –5532, Oct. 2012.

[64] H.-S. Chen, W. Gao, and D. Daut, "Spectrum sensing for OFDM systems employing pilot tones," *Wireless Communications, IEEE Transactions on*, vol. 8, pp. 5862–5870, Dec. 2009.

[65] Y. Zeng, Y.-C. Liang, and T.-H. Pham, "Spectrum sensing for ofdm signals using pilot induced auto-correlations," *Selected Areas in Communications, IEEE Journal on*, vol. 31, pp. 353–363, Mar. 2013.

[66] Q. Zhang, O. Dobre, S. Rajan, and R. Inkol, "Cyclostationarity approach to joint blind estimation of CP-SCLD block transmission parameters for cognitive radio," in *New Frontiers in Dynamic Spectrum, 2010 IEEE Symposium on*, pp. 1–5, Apr. 2010.

[67] J. Lunden, V. Koivunen, A. Huttunen, and H. Poor, "Collaborative cyclostationary spectrum sensing for cognitive radio systems," *Signal Processing, IEEE Transactions on*, vol. 57, pp. 4182–4195, Nov. 2009.

[68] M. Kim, P. Kimtho, and J.-i. Takada, "Performance enhancement of cyclostationarity detector by utilizing multiple cyclic frequencies of OFDM signals," in *New Frontiers in Dynamic Spectrum, 2010 IEEE Symposium on*, pp. 1–8, Apr. 2010.

[69] Z. Lei and F. Chin, "Sensing ofdm systems under frequency-selective fading channels," *Vehicular Technology, IEEE Transactions on*, vol. 59, pp. 1960–1968, May. 2010.

[70] L. Tong, B. Sadler, and M. Dong, "Pilot-assisted wireless transmissions: general model, design criteria, and signal processing," *Signal Processing Magazine, IEEE*, vol. 21, pp. 12–25, Nov. 2004.

[71] T. Yucek and H. Arslan, "A survey of spectrum sensing algorithms for cognitive radio applications," *Communications Surveys Tutorials, IEEE*, vol. 11, pp. 116–130, Jan. 2009.

[72] B. Farhang-Boroujeny, "Filter bank spectrum sensing for cognitive radios," *Signal Processing, IEEE Transactions on*, vol. 56, pp. 1801–1811, May. 2008.

[73] E. Candes and M. Wakin, "An introduction to compressive sampling," *Signal Processing Magazine, IEEE*, vol. 25, pp. 21–30, Mar. 2008.

[74] H. Sun, A. Nallanathan, C.-X. Wang, and Y. Chen, "Wideband spectrum sensing for cognitive radio networks: a survey," *Wireless Communications, IEEE*, vol. 20, pp. 74–81, Apr. 2013.

[75] J. Ma, G. Zhao, and Y. Li, "Soft combination and detection for cooperative spectrum sensing in cognitive radio networks," *Wireless Communications, IEEE Transactions on*, vol. 7, no. 11, pp. 4502–4507, 2008.

[76] W. Zhang, R. Mallik, and K. Letaief, "Optimization of cooperative spectrum sensing with energy detection in cognitive radio networks," *Wireless Communications, IEEE Transactions on*, vol. 8, pp. 5761–5766, Dec. 2009.

[77] Y. Liu, S. Xie, R. Yu, Y. Zhang, and C. Yuen, "An efficient mac protocol with selective grouping and cooperative sensing in cognitive radio networks," *Vehicular Technology, IEEE Transactions on*, vol. 62, pp. 3928–3941, Oct. 2013.

[78] T. Cui, F. Gao, and A. Nallanathan, "Optimization of cooperative spectrum sensing in cognitive radio," *Vehicular Technology, IEEE Transactions on*, vol. 60, pp. 1578–1589, May. 2011.

[79] V. Rakovic, D. Denkovski, V. Atanasovski, P. Mahonen, and L. Gavrilovska, "Capacity-aware cooperative spectrum sensing based on noise power estimation," *Communications, IEEE Transactions on*, vol. 63, pp. 2428–2441, Jul. 2015.

[80] R. Tandra and A. Sahai, "Snr walls for signal detection," *Selected Topics in Signal Processing, IEEE Journal of*, vol. 2, pp. 4–17, Feb. 2008.

[81] D. Middleton, *Statistical-physical models of man-made and natural radio noise.* Institute for Telecommunication Sciences, U.S., 1974.

[82] F. Moghimi, A. Nasri, and R. Schober, "Adaptive lp norm spectrum sensing for cognitive radio networks," *Communications, IEEE Transactions on*, vol. 59, no. 7, pp. 1934–1945, 2011.

[83] P. Paysarvi-Hoseini and N. Beaulieu, "Optimal wideband spectrum sensing framework for cognitive radio systems," *Signal Processing, IEEE Transactions on*, vol. 59, pp. 1170 –1182, Mar. 2011.

[84] Y. Yilmaz, Z. Guo, and X. Wang, "Sequential joint spectrum sensing and channel estimation for dynamic spectrum access," *Selected Areas in Communications, IEEE Journal on*, vol. 32, pp. 2000–2012, Nov. 2014.

[85] B. Li, C. Zhao, M. Sun, Z. Zhou, and A. Nallanathan, "Spectrum sensing for cognitive radios in time-variant flat-fading channels: A joint estimation approach," *Communications, IEEE Transactions on*, vol. 62, pp. 2665–2680, Aug. 2014.

[86] B. Li, S. Li, A. Nallanathan, Y. Nan, C. Zhao, and Z. Zhou, "Deep sensing for next-generation dynamic spectrum sharing: More than detecting the occupancy state of primary spectrum," *Communications, IEEE Transactions on*, vol. 63, pp. 2442–2457, Jul. 2015.

[87] N. L. Johnson, S. Kotz, and N. Balakrishnan, *Continuous univariate distributions.* Wiley and Sons, 1994.

[88] G. A. F. Seber, *Linear regression analysis.* Wiley and Sons, 2003.

[89] P.-J. Chung, J. F. Bahme, C. Mecklenbrauker, and A. Hero, "Detection of the number of signals using the benjamini-hochberg procedure," *Signal Processing, IEEE Transactions on*, vol. 55, pp. 2497–2508, Jun. 2007.

[90] A. Drosopoulos and S. Haykin, "Angle-of-arrival estimation in presence of multipath," *Electronics Letters*, vol. 27, pp. 2273–2274, Nov. 1991.

[91] H. Scheffe, *The analysis of variance.* Wiley and Sons, 1959.

[92] S. Shellhammer, *Numerical Spectrum Sensing Requirements*. IEEE 802.22-06/0088r0, Jun.

[93] A. Zoubir and B. Boashash, "The bootstrap and its application in signal processing," *Signal Processing Magazine, IEEE*, vol. 15, no. 1, pp. 56–76, 1998.

[94] B. Efron and R. Tibshirani, *An introduction to the bootstrap.* Chapman Hall, 1993.

[95] P. Hall, *The bootstrap and Edgeworth expansion.* Springer-Verlag., 1992.

[96] P. Hall and S. R. Wilson, "Two guidelines for bootstrap hypothesis testing," *Biometrics*, no. 2, p. 757, 1991.

[97] S. Jun and T. Dongsheng, *The jackknife and bootstrap*. Springer, 1995.

[98] R. F. Brcich, A. Zoubir, and P. Pelin, "Detection of sources using bootstrap techniques," *Signal Processing, IEEE Transactions on*, vol. 50, no. 2, pp. 206–215, 2002.

[99] A. C. Rencher and W. F. Christensen, *Methods of multivariate analysis.* Wiley and Sons, 2012.

[100] A. M and D. R. Iskander, *Bootstrap Techniques for Signal Processing.* Cambridge University Press, 2004.

[101] N. H. Lu and B. Eisenstein, "Weak signal detection in non-gaussian noise of unknown level," *Aerospace and Electronic Systems, IEEE Transactions on*, vol. AES-20, no. 6, pp. 830–834, 1984.

[102] G. Gonzalez-Farias, J. Molina, and R. Rodriguez-Dagnino, "Efficiency of the approximated shape parameter estimator in the generalized gaussian distribution," *Vehicular Technology, IEEE Transactions on*, vol. 58, no. 8, pp. 4214–4223, 2009.

[103] F. N. David and N. L. Johnson, "A method of investigating the effect of nonnormality and heterogeneity of variance on tests of the general linear hypothesis," *The Annals of Mathematical Statistics*, vol. 22, pp. 382–392, Sep.

[104] F. N. David and N. L. Johnson, "The effect of non-normality on the power function of the F-test in the analysis of variance," *Biometrika*, vol. 38, no. 1/2, pp. 43–57.

[105] G. E. P. Box and G. S. Watson, "Robustness to non-normality of regression tests," *Biometrika*, vol. 49, pp. 93–106, Jun.

[106] R. L. Prentice, "Degrees-of-freedom modifications for F- tests based on nonnormal errors.," *Biometrika*, vol. 61, no. 3, p. 559, 1974.

[107] Y. Dodge, *The Oxford dictionary of statistical terms*. Oxford University Press, 2003.

[108] A. F. Molisch, *Wireless communications*. Wiley and Sons, 2006.

[109] A. L. Edwards, *Statistical analysis*. Rinehart and Winston, 1969.

[110] E. Paparoditis and D. N. Politis, "Bootstrap hypothesis testing in regression models," *Statistics and probability letters*, vol. 74, no. 4, pp. 356–365, 2005.